INSTITUTUL DE GEOLOGIE ŞI GEOFIZICĂ

STUDII TEHNICE ŞI ECONOMICE

SERIA I | *Mineralogie-Petrografie* | Nr. 14

A DOUA CONFERINŢĂ NAŢIONALĂ PENTRU ARGILE BUCUREŞTI — APRILIE 1975

BUCUREŞTI
1978

Responsability of the paper content gets exclusively over the author

INSTITUTE OF GEOLOGY AND GEOPHYSICS

TECHNICAL AND ECONOMICAL STUDIES

I SERIES *Mineralogy—Petrography* No. 14

THE SECOND NATIONAL CLAY CONFERENCE BUCHAREST—APRIL 1975

BUCHAREST
1978

INSTITUTUL DE GEOLOGIE ŞI GEOFIZICĂ

STUDII TEHNICE ŞI ECONOMICE

SERIA I *Mineralogie—Petrografie* Nr. 14

A DOUA CONFERINŢĂ NAŢIONALĂ PENTRU ARGILE BUCUREŞTI—APRILIE 1975

BUCUREŞTI
1978

CONTENTS

LA TRANSFORMATION CHIMIQUE ET MINÉRALOGIQUE DE L'ARGILE DES SOLS LESSIVÉS GLOSSIQUES — CARACTERISTIQUES, DÉVELOPPÉS SUR LIMONS QUATERNAIRES [1]

PAR

H. ASVADUROV[2], MARIA CONSTANTINESCU[2], GHEORGHE GÂȚĂ[2], GHEORGHE NEACȘU[3], VASILICA NEACȘU[4], CATRINEL PAPADOPOL[4]

Abstract

Chemical and Mineralogical Clay Transformation of Some Glossudalfs and Glossaqualfs Developed on Quaternary Loams. The genesis of two soil profiles located in a forest is studied, and the following three soil-forming processes are identified; clay illuviation, secondary gleyzation and clay weathering. The latter was demonstrated by: (1) strong depletion of bases and of iron oxides (prof. 2) and occurrence of chloritization in the eluvial horizon; (2) free circulation and accumulation of iron oxides in the illuvial horizon; (3) migration of clay (and some amorphous compounds) accompanied by (a) the increase of illite content in the clayey tongues,and (b) the transformation of the chlorite lattice into an aluminium-iron chlorite in the soil matrix (by blocking the interlayer iron) in the illuvial horizon of the Glossaqualf.

Introduction

Les études concernant la transformation chimique et minéralogique de l'argile de quelques sols lessivés ont montré la nature des processus de lessivage décrits sous le nom de „podzolisation secondaire" (Cernescu, 1945), de „lessivage argilo-ferri-illuvial" (Asvadurov et

[1] Communiqué à la deuxième Conférence Nationale des Argiles, 11—12 Avril, 1975, Bucarest.

[2] Institutul de cercetări pedologice și agrochimice, Bd. Ion Ionescu de la Brad 4, București.

[3] Intreprinderea geologică de prospecțiuni pentru substanțe minerale solide, str. Caransebeș 1, București.

[4] Institutul de geologie și geofizică, str. Caransebeș 1, București.

al., 1972 a) et les principaux aspects qui caractérisent la formation des sols lessivés à pseudogley (C e r n e s c u et al., 1973).

Généralement les sols lessivés glossiques les plus caractéristiques se sont développés en Roumanie sur des dépôts quaternaires qui couvrent le relief plat des sommets, des terrasses ou des piémonts de la zone forestière. Les profils présentent un horizon éluvial désaturé (*A2*) de 35—50 cm épaisseur et une différentiation importante en ce qui concerne la composition granulométrique (indice d'entraînement de l'argile — Idt. >2), une transition en langues vers l'horizon illuvial dont la partie supérieure est morcellée. Souvent, en section horizontale, l'horizon *Bt* montre un réseau réticulé, dû à la présence des accumulations d'argile gris-claire à revêtements rougeâtres formés par la ségrégation des oxydes de fer. La partie inférieure est développée sur des horizons anciens ou sur des roches, en general, non calcaires.

Dans cette étude les auteurs présentent les résultats des recherches concernant l'intensité et la dynamique de l'altération de l'argile d'un sol lessivé glossique à faible pseudogley et d'un sol glossique (acide) à fort pseudogley („pseudogley glossiques"). On a analysé séparément le matériau albique des langues, le matériau des accumulations argileuses et celui de la matrice de l'horizon *Bt*, du deuxième profil.

La présence d'une hydrolise intense des alumino-silicates dans les horizons de surface, met en évidence les processus qui caractérisent l'altération de l'argile dans l'horizon diagnostique (*A2*) de ces sols. L'étude des profils formés sur des dépôts homogènes, en ce qui concerne leur composition granulométrique, donne des renseignements sur la direction d'évolution de l'argile de ces sols.

Matériaux et méthodes analytiques utilisés

Les profils etudiés sont les suivants :

—profil no. 1 — sol glossique à faible pseudogley, caractérisé par une „marmorisation réticulée" au sein de transition $(A2 + B)g$;

— profil no. 2 — sol glossique à fort pseudogley (pseudogley secondaire glossique) caracterisé par une „marmorisation réticulée" au sein de l'horizon *Btg*.

Description du profil no. 1

Milieu pédogénétique :

Position : fôret de Mănăstirea à 4 km SE de la ville de Dej (vallée du Someş).
Relief : sommet, terrain plat.
Matériau originel : limon loessique.
Drainage naturel : imparfait, à hydromorphie temporaire.
Végétation naturelle : fôret à *Quercus petraea* et *Carpinus betulus* ; pré à *Agrostis tenuis, Festuca rubra* et *Poa nemoralis*.

Données climatologiques : Tm = 8,2°C ; Pm = 660 mm ; $\frac{P}{T+10} = 36,2$.

Description du profil :

A1 0—10 cm ; limon fin, brun-jaunâtre et brun-gris vers la partie supérieure (10YR 6/2-3 — humide), gris clair vers brun très pâle (10YR 7/2-3 — sec) ; structure granulaire avec tendance à structure feuilletée ; transition graduelle.

A2 10—30 cm ; limon fin, brun pâle (10YR 6/3 — humide), brun-gris vers brun très pâle (10YR 7/2,5 — sec) ; polyédrique subangulaire avec tendance à structure feuilletée ; transition graduelle.

A2g 30—45 cm (y compris la partie supérieure de l'horizon *Btg* à structure dégradée) ; limon fin, brun-jaunâtre (10YR 5/5 — humide), brun très pâle (10YR 7,5/3 — sec) ; polyédrique angulaire ; caractères de fragipan ; par endroits des revêtements d'argile gris-blanc appauvris en fer ; petites concrétions mangano-ferrugineuses ; transition graduelle.

(A2 + B)g 45—55 cm ; limon argileux fin, brun-jaunâtre et gris clair (10YR 5/4 et 7/2 — humide) ; brun-jaunâtre et blanc (10YR 6/6 et 8/2 — sec) surtout dans les langues verticales ; polyédrique subangulaire vers une structure prismatique moyenne ; caractères de fragipan ; réaction positive à NaF — n/1 ; transition en langues.

Bt 55—105 cm ; argile-limoneuse, brun-jaunâtre foncé et brun-jaunâtre (10YR 4/4 et 5/4 — humide), brun-jaunâtre (10YR 5/4 — sec) ; structure prismatique ; massif ; taches et petites concrétions mangano-ferrugineuses rares ; transition graduelle vers un sol enterré.

IIABx 105—135 cm ; limon argileux fin, brun-jaunâtre et brun pâle (10YR 5/6 et 6/3 — humide), brun-jaunâtre et brun très pâle (10YR 6/6 et 7/3 — sec) ; caractères morphologiques d'un horizon éluvial à fragipan enterré masqués par l'accumulation de l'argile de l'horizon *Bt* supérieur ; massif ; taches et concrétions mangano-ferrugineuses et manganeuses ; transition graduelle.

IIBtg 135—165 cm ; argile limoneuse, brun-jaunâtre à taches gris clair (10YR 5/8 et 7/8 — humide) et brun-jaunâtre et blanc (10YR 5/8 et 8/2 — sec) ; caractères morphologiques d'un horizon illuvial à pseudogley plus riche en revêtements argileux que l'horizon *Bt* supérieur ; massif ; extrêmement dur à l'état sec.

Description du profil no. 2

Milieu pédogénétique :

Position : à 1 km N du village Rus, SE Ileanda (vallée du Someş).

Relief : terrain plan d'une terrasse supérieure.

Matériau originel : limon loessique.

Drainage naturel : imparfait, à hydromorphie temporaire.

Végétation naturelle : forêt „Refeni" à *Quercus robur* et *Fagus silvatica* ; pré à *Agrostis canina* et *A. tenuis*.

Données climatologiques : Tm = 8°C ; Pm = 800 mm ; $\frac{P}{T+10} = 45$.

Description du profil :

A1 0—8 cm ; limon fin, gris vers gris clair (10YR 6,5/1 — humide), gris clair (10YR 7/1 — sec) ; structure granulaire fine, modérément développée ; friable ; transition graduelle.

A2g 8—35 cm ; limon fin, brun très pâle (10YR 7/3 — humide), blanc (10YR 8/1 — sec) ; massif, avec tendance à structure feuilletée ; petites concrétions mangano-ferrugineuses rares ; transition graduelle.

(A2 + B)g 35—55 cm ; limon argileux fin, jaune-brunâtre et brun-jaunâtre (10YR 6/6 et 6/4 — humide), blanc et jaune-brunâtre (10YR 8/1 + 6/8 — sec) ; langues verticales blanchâtres (albiques) limoneuses (*L*) ; massif ; caractères de fragipan ; séparations mangano-ferrugineuses sous forme de taches diffuses ; réaction positive claire au test à NaF — n/1 ; transition en langue.

Bt21g 55—90 cm ; limon argileux fin, brun-jaunâtre et brun pâle (10YR 5/6 et 6/3-humide), brun très pâle (10YR 7/4—sec) avec des taches blanches et jaune-brunâtre (10 YR 7,5/1 et 6/8—sec) ; langues verticales argileuses (*T1*) à réaction positive au test à NaF—n/1 ; à l'état sec, on remarque l'apparition des fissures verticales dans ces langues argileuses ; structure prismatique très ferme ; la matrice présente de nombreuses concrétions et taches mangano-ferrugineuses avec des bandes de rouille qui bordent les langues argileuses ; rares racines fines pénètrent à l'intérieur des langues argileuses ; transition graduelle.

Bt22g 90—120 cm ; limon argileux fin, brun-jaunâtre et brun très pâle (10YR 5/4-8 et 6/3—humide), brun-jaunâtre (10YR 5/8 et 7,5/1—sec) ; structure prismatique ; très ferme ; les langues argileuses (*T2*) bordées par des bandes de rouille ; concentrations des concrétions mangano-ferrugineuses surtout à 100—115 cm de profondeur ; transition graduelle.

IIBt23g 120—165 cm ; argile limoneuse, brun vif avec des taches gris à gris clair (7,5YR 5/6 avec 6,5/1—humide), brun-jaunâtre avec des taches gris clair (10YR 5/8 avec 7/1—sec) ; structure prismatique ferme ; taches d'oxydes de fer, concrétions mangano-ferrugineuses rares.

Méthodes analytiques utilisées

On a effectué : l'analyse granulométrique[5] par pipette et tamissage après la destruction de la matière organique, par H_2O_2 ; le pH dans l'eau potentiométrique à l'électrode de verre, la matière organique par la méthode Walkley — Black complétée par Gogoaşă (1959) ; l'azote total d'après Kyeldahl ; la capacité d'échange et les cations échangeables par la méthode Schollenberger ; les sesquioxydes libres d'après Mehra — Jackson et l'Al d'échange d'après Berg par déplacement au moyen d'une solution normale de KCl et le dosage gravimétrique.

La fraction argileuse (< 0,002 mm) a été obtenue par décantation, après la destruction de la matière organique, la percolation à l'acide acétique et la dispersion à l'aide du NaOH. On a fait l'analyse chimique par voie classique (fusion avec Na_2CO_3 et dosage des oxydes et fusion à $HF + H_2SO_4$ et dosage du K_2O et du Na_2O) ; l'extraction des sesqui-

[5] Sous la direction de P. Vasilescu, I.C.P.A., Bucarest.

oxydes libres d'après Mehra — Jackson. Pour le profil no. 1, les diffractogrammes de l'argile sont obtenus en utilisant des lames orientées avec un diffractomètre Tur-M 61 dans les conditions suivantes : radiation Kα, filtre de Ni, 30 wK., 25 mA ; on a estimé la composition semi-quantitative par le mesurage des pics caractéristiques (une corrélation avec le contenu en K de l'argile a été faite).

Pour le profil no. 2, la détermination du quartz et de la silice amorphe a été fait par absorbtion en infrarouge, la composition minéralogique à été déterminée quantitativement d'après la méthode de Gâţă (1973)[6] et le degré d'alteration de l'illite d'après White.

Résultats et discussions

Analyses granulométriques

Matériau originel des profils. La composition granulométrique des profils est prédominante limoneuse („silteuse") (tab. 1A, 2A ; fig. 1, 2). Les horizons *IIABx* et *IIBtg* (prof. 1) ou *Bt22g* et *IIBt23* (prof. 2) sont formés aux dépens d'anciens horizons d'un sol lessivé enterré (le *IIABx* et respectivement *Bt22g* sur l'horizon éluvial et le *IIBtg* et respectivement *IIBt23* sur l'horizon illuvial de ce sol) ; le changement dû au développement polyphasique du profil et mis en évidence morphologiquement et par voie analytique surtout à 50 cm et 105 cm (prof. 1) ou 35—60 cm et 100—140 cm de profondeur (prof. 2).

La composition granulométrique assez homogène et le caractère loessique du matériau originel (tab. 1A, 2A ; fig. 1B et 2B) sont témoignés par :

a) le rapport assez constant (1,1—1,3) tout le long du profil, entre les fractions moyennes (0,002—0,02 mm) et les fractions grossières (0,02—0,2 mm) ;

b) la prédominance des fractions à 0,01—0,05 mm ∅ et l'absence des fractions grossières (> 2 mm ∅) et même du sable grossier (les 1—5% particules de 0,2—2 mm ∅ indiquées dans le tableau, représentent la teneur en concrétions ferri-manganésifères) ;

c) la similitude qui existe entre les compositions granulométriques du sol étudié et des autres sols lessivés évolués sur des dépôts loessiques dans d'autres régions du pays (Asvadurov, Vasilescu, 1968).

Le développement du profil n'a pas été influencé par l'érosion, l'épaisseur (40—50 cm) de l'horizon éluvial étant similaire à celle des horizons éluviaux des sols de même type, dans les profils desquels on trouve à 100—140 cm de profondeur des roches dures ou des horizons

[6] L'Arch. de l'Inst. Polyt. de Bucarest.

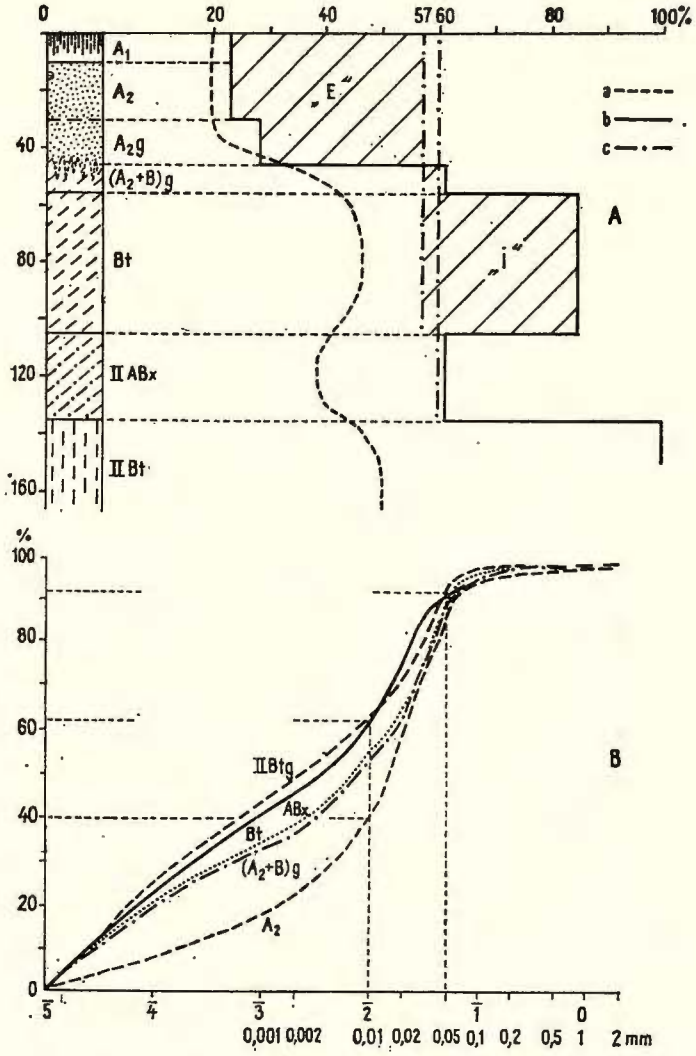

Fig. 1. — A) La teneur en argile (< 0,002 mm) au long du profil (a); le rapport $\frac{Sa}{Sq} \cdot 100$ (b); les moyennes pondérées (0—105 et 0—135 cm profondeur) des rapports $\frac{Sa}{Sq} \cdot 100$ (c).

B) Courbes cumulatives de la composition granulométrique des horizons diagnostiques du profil no.1.

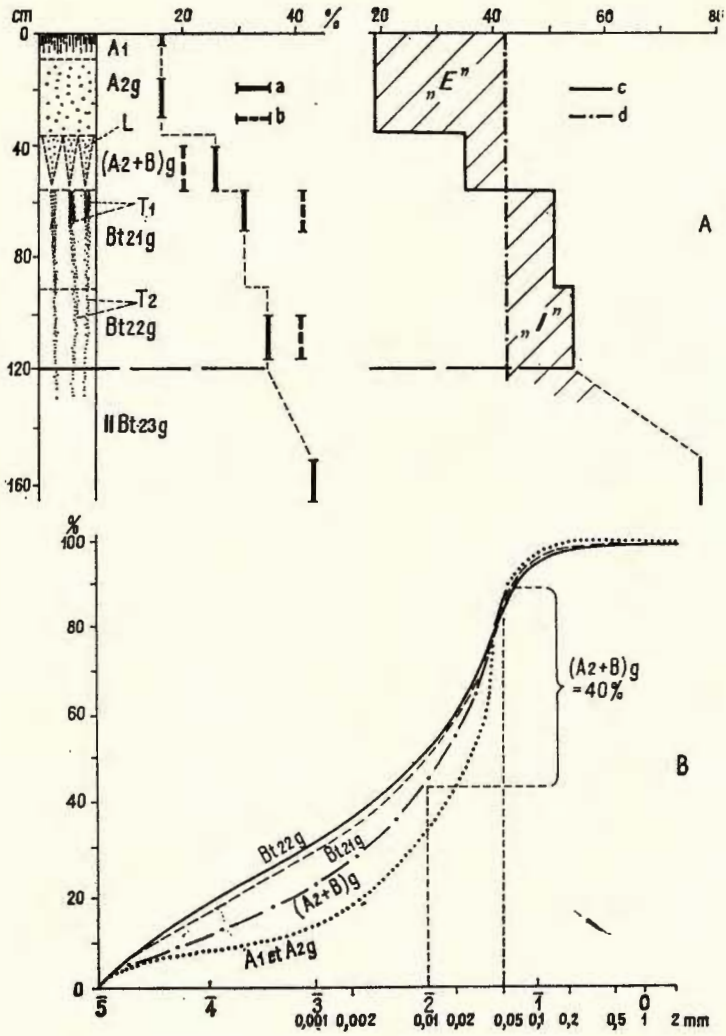

Fig. 2. — A) La teneur en argile (< 0,002 mm) du matériau de la matrice (a) et des langues (b); le rapport $\frac{Sa}{Sq} \cdot 100$ (c); la moyenne pondérée (0—120 cm profondeur) du rapport $\frac{Sa}{Sq} \cdot 100$ (d).

B) Courbes cumulatives de la composition granulométrique de quelques horizons diagnostiques du profil no. 2.

TABLEAU 1

A) Profil no. 1 — Analyse granulométrique, teneur en humus, en azote total et en oxydes libres du sol (à 105°C)

Horizon	Profondeur cm	Fractions granulométriques (mm) %							Humidité %	Mat. org. %	N %	Oxydes libres			Argile * %	$Fe_2O_3 \times 100$ / Argile*
		2—0,2	0,2—0,05	0,05—0,02	0,02—0,002	< 0,002	< 0,001	< 0,01				Fe_2O_3 %	MnO %	R_2O_3 %		
A1	0— 10	2,6	6,8	28,0	42,0	19,2	13,0	39,9	1.71	4,3	0,18	1,11	0,06	1,70	18,0	6,1
A2	10— 30	2,9	6,6	26,4	43,8	19,4	14,7	40,5	1,32	1,6	0,07	1,06	0,07	1,78	18,9	5,6
A2g	30— 45	4,9	6,6	25,5	39,8	22,4	17,3	41,6	1,42	0,6	0,03	1,18	0,04	1,91	21,9	5,4
(A2+B)g	45— 55	3,7	5,8	18,1	32,8	38,3	34,2	56,6	2,90	0,5	—	1,35	0,02	2,21	37,0	3,6
Bt	55— 70	2,3	4,9	13,5	32,7	46,0	41,1	63,9	4,25	0,6	—	1,51	0,03	2,45	43,7	3,4
IIABx	105—120	4,1	5,4	18,5	32,8	38,4	34,3	55,4	3,10	0,4	—	1,67	0,08	2,50	37,0	4,5
IIBtg	145—160	1,4	4,1	17,3	26,7	49,6	45,6	64,6	4,41	0,2	—	2,03	0,09	2,77	47,3	4,3

* Argile < 0,002 mm (+ matière organique et H_2O).

B) Cations échangeables

Horizon	Profondeur cm	méq./100 g sol						% ((T = 100)					V %	Al méq.	pH (H_2O)	K_2O mg %
		Ca^{2+}	Mg^{2+}	K^+	Na^+	H^+	T	Ca^{2+}	Mg^{2+}	K^+	Na^+	H^+				
A1	0— 10	1,15	0,85	0,07	0,12	11,96	14,15	8,1	6,0	0,5	0,9	84,5	15,5	3,86	4,8	7,0
A2	10— 30	1,04	0,21	0,02	0,09	8,33	9,67	10,7	2,2	0,2	0,8	86,0	14,0	3,74	4,8	4,0
A2g	30— 45	1,45	0,48	0,03	0,09	7,96	10,01	14,5	4,8	0,3	0,9	79,5	20,5	3,25	4,9	4,0
(A2+B)g	45— 55	6,99	2,56	0,15	0,27	8,90	18,87	37,0	13,6	0,8	1,4	47,2	52,8	3,66	5,2	12,0
Bt	55— 70	13,05	3,21	0,23	0,44	9,46	26,39	49,5	12,2	0,9	1,6	35,8	64,2	3,25	5,3	—
IIABx	105—120	15,22	5,04	0,13	0,48	2,73	22,60	67,3	17,9	0,6	2,1	12,1	87,9	—	6,4	—
IIBtg	145—160	21,60	5,66	0,25	0,58	2,36	30,45	70,9	18,6	0,8	1,9	7,8	92,2	—	7,2	—

C) Analyse totale de l'argile et des oxydes libres (g/100 g séché à 105 °C)

Horizon	Profondeur cm	SiO_2	Al_2O_3	Fe_2O_3	TiO_2	MnO	P_2O_5	CaO	MgO	K_2O	Na_2O	Perte au feu	Total	H_2O (−)
A2	10— 30	48,90	23,60	8,30	1,26	0,12	0,46	1,21	1,93	2,30	0,20	12,58	100,84	3,90
A2g	30— 45	48,89	24,52	8,85	1,24	0,08	0,34	1,69	2,32	2,60	0,20	9,85	100,58	4,06
(A2+B)g	45— 55	48,10	24,99	9,35	0,96	0,00	0,19	1,48	2,37	2,60	0,16	9,76	99,96	4,61
Bt	55— 70	48,58	25,78	8,88	0,71	0,05	0,13	1,66	2,17	2,10	0,10	9,52	99,68	5,61
IIABx	105—120	49,11	25,60	8,73	0,79	0,13	0,10	1,83	1,79	1,95	0,15	9,47	99,65	6,19
IIBtg	145—160	49,87	25,21	8,85	0,71	0,07	0,06	1,73	1,72	1,80	0,10	9,44	99,59	7,30

Horizon	Profondeur cm	Rapports moléculaires (Al_2O_3 = 1)					$\frac{SiO_2}{R_2O_3}$	Oxydes libres			$(Fe_2O_3)La$	$\frac{(Fe_2O_3)la \times 100}{(Fe_2O_3)ta}$	$\frac{(Fe_2O_3)la \times 100}{(Fe_2O_3)La}$
		SiO_2	Fe_2O_3	CaO	MgO	K_2O		Fe_2O_3 %	MnO %	R_2O_3 %			
A2	10— 30	3,52	0,22	0,09	0,21	0,10	2,81	3,82	0,06	6,29	4,48	43	85
A2g	30— 45	3,39	0,23	0,12	0,24	0,11	2,69	3,60	0,06	5,68	5,25	41	67
(A2+B)g	45— 55	3,27	0,23	0,10	0,24	0,10	2,61	2,98	0,00	5,60	6,37	32	46
Bt	55— 70	3,20	0,22	0,12	0,21	0,09	2,62	2,73	0,03	6,36	6,15	31	44
IIABx	105—120	3,26	0,22	0,13	0,18	0,08	2,67	3,32	0,08	5,43	5,41	38	61
IIBtg	145—160	3,36	0,22	0,13	0,17	0,08	2,75	3,14	0,05	5,39	5,71	35	54

$(Fe_2O_3)La = (Fe_2O_3)$ lié à l'argile $= (Fe_2O_3)ta - (Fe_2O_3)la$;
$(Fe_2O_3)la = (Fe_2O_3)$ libre de l'argile ;
$(Fe_2O_3)ta = (Fe_2O_3)$ total de l'argile.

TABLEAU 2

A) Profil no. 2 — Analyse granulométrique, teneur en humus, en azote total et en oxydes libres du sol (à 105°C)

Horizon	Profondeur cm	Fractions granulométriques (mm) %						Humidité %	Mat. org. %	N %	Oxydes libres			Argile * %	$Fe_2O_3 \times 100$ / Argile *
		2—0,2	0,2—0,02	0,02—0,002	<0,002	<0,001	<0,01				Fe_2O_3 %	Mn %	R_2O_3 %		
A1	0— 5	1,4	44,4	37,8	16,4	11,6	34,6	1,81	6,0	0,20	1,10	0,09	1,21	15,4	7,1
A2g	15— 30	5,8	41,4	36,3	16,5	11,9	33,7	1,01	1,0	0,04	0,71	0,01	0,74	16,3	4,3
L	40— 45	1,3	40,5	37,7	20,5	16,0	35,2	1,24	0,6	—	1,05	0,02	1,21	20,0	5,2
(A2+B)g	40— 55	1,4	37,4	35,2	26,0	20,9	44,7	1,60	0,5	—	2,03	0,02	2,31	26,0	7,8
Bt21g	55— 70	1,6	33,5	33,4	31,5	27,5	50,3	2,69	0,2	—	2,33	0,03	2,79	31,7	7,3
T1	55— 70	0,4	32,4	25,7	41,5	37,2	53,1	3,44	—	—	0,91	0	1,11	41,6	2,2
Bt22g	100—115	2,2	32,2	29,6	35,0	31,3	51,1	3,02	—	—	2,87	0,02	3,23	34,8	8,2
IIBt23g	150—165	0,7	28,7	27,6	43,0	39,6	57,3	4,81	—	—	3,13	0,02	3,66	42,9	7,3

* Argile < 0,002 mm (+ matière organique et H_2O).

B) Cations échangeables

Horizon	Profondeur cm	méq./100 g sol						% (T = 100)					V %	Al méq.	pH (H_2O)
		Ca^{2+}	Mg^{2+}	K^+	Na^+	H^+	T	Ca^{2+}	Mg^{2+}	K^+	Na^+	H^+			
A1	0— 45	1,23	0,57	0,31	0,07	10,41	12,59	9,8	4,5	2,5	0,5	82,7	17,3	3,15	4,1
A2g	15— 30	1,05	0,26	0,03	0,06	5,19	6,59	15,9	3,9	0,5	0,9	78,8	21,2	2,57	4,5
L	40— 55	1,40	0,54	0,10	0,07	7,39	9,5	14,8	5,7	1,0	0,7	77,8	22,2	3,10	4,8
(A2+B)g	40— 55	2,73	1,41	0,12	0,25	7,57	12,08	22,6	11,7	1,0	2,0	62,7	37,3	5,04	5,0
Bt21g	55— 70	4,27	2,11	0,14	0,21	9,67	16,40	26,0	12,9	0,8	1,3	59,0	41,0	6,32	5,1
T1	55— 70	8,38	4,42	0,28	0,68	10,75	24,52	34,2	20,9	1,2	2,8	43,9	56,1	7,66	5,2
Bt22g	100—115	7,83	4,40	0,18	0,62	8,02	21,05	37,2	20,9	0,9	2,9	38,1	61,9	4,63	5,3
IIBt23g	150—165	15,62	6,82	0,33	1,02	4,92	28,71	54,4	23,7	1,1	3,5	17,3	82,7	—	5,4

C) Analyse totale de l'argile et des oxydes libres (g/100 g séché à 105°C)

Horizon	Profondeur cm	SiO_2	Al_2O_3	Fe_2O_3	TiO_2	MnO	CaO	MgO	K_2O	Na_2O	Perte au feu	H_2O (−)
A1	0— 5	51,40	22,05	4,95	0,73	0,06	0,54	1,39	2,31	0,51	15,76	2,37
A2g	15— 30	52,80	22,85	5,36	1,08	0,08	0,72	1,44	2,43	0,46	9,71	2,26
L	40— 55	53,65	24,90	7,01	0,90	traces	0,62	1,79	2,63	0,47	8,84	2,29
(A2+B)g	40— 55	50,48	24,99	9,26	0,97	,,	0,65	1,84	2,51	0,30	9,14	2,92
Bt21g	55— 70	49,62	24,99	9,76	0,83	,,	0,80	1,96	2,28	0,62	9,11	2,67
T1	55— 70	52,58	25,90	6,79	0,63	,,	0,70	1,73	2,79	0,42	9,60	4,04
Bt22g	100—115	50,91	24,59	9,33	0,68	0,01	0,67	1,86	2,31	0,45	9,17	4,02
T2	100—115	52,44	26,57	6,21	0,64	traces	0,83	1,78	2,39	0,27	9,13	4,35

Horizon	Profondeur cm	Rapports moléculaires ($Al_2O_3 = 1$)						$\frac{SiO_2}{R_2O_3}$	Oxydes libres			(Fe_2O_3) La	$\frac{(Fe_2O_3)la \times 100}{(Fe_2O_3)\ ta}$	$\frac{(Fe_2O_3)la\ 100}{(Fe_2O_3)\ La}$
		SiO_2	Fe_2O_3	CaO	MgO	K_2O	Na_2O		Fe_2O_3 %	MnO %	R_2O_3 %			
A1	0— 5	4,03	0,14	0,04	0,16	0,11	0,04	2,96	—	—	—	—	—	—
A2g	15— 30	3,46	0,13	0,05	0,14	0,10	0,03	2,57	1,65	0,03	3,02	3,71	31	44
L	40— 55	3,65	0,18	0,04	0,18	0,11	0,03	2,38	1,91	0,00	3,04	5,10	27	37
(A2+B)g	40— 55	3,43	0,28	0,05	0,18	0,11	0,02	2,43	3,06	0,00	4,09	6,20	33	49
Bt21g	55— 70	3,44	0,25	0,06	0,18	0,10	0,04	2,14	5,10	0,00	7,39	4,66	53	109
T1	55— 70	3,44	0,18	0,05	0,17	0,11	0,03	2,25	2,09	0,00	3,91	2,88	31	72
Bt22g	100—115	3,36	0,24	0,05	0,19	0,10	0,03	2,48	—	—	—	—	—	—
T2	100—115	3,35	0,22	0,06	0,17	0,10	0,02	2,45	—	—	—	—	—	—

L = langue albique ; *T1* et *T2* = langues argileuses.
$(Fe_2O_3)La = (Fe_2O_3)$ lié à l'argile $= (Fe_2O_3)ta - (F_2O_3)\ la$;
$(Fe_2O_3)la = (Fe_2O_3)$ libre de l'argile ;
$(Fe_2O_3)ta = (Fe_2O_3)$ total de l'argile.

pédogénétiques anciens (fig. 3)[7]. Dans ces conditions, les valeurs du rapport argile (< 0,002 mm) / „microsquelette" (2—0,002 mm), décrit par Orleanu, Dulvara (1970), sont significatives.

Profil no. 1. On obtient pour l'épaisseur de 0 à 105 ou 135 cm une moyenne pondérée du rapport $\frac{Sa}{Sq} \cdot 100$ (Sa — teneur en argile, Sq — teneur en „microsquelette") de 57, respectivement 60%, représentant la valeur du rapport caractéristique pour le materiau originel

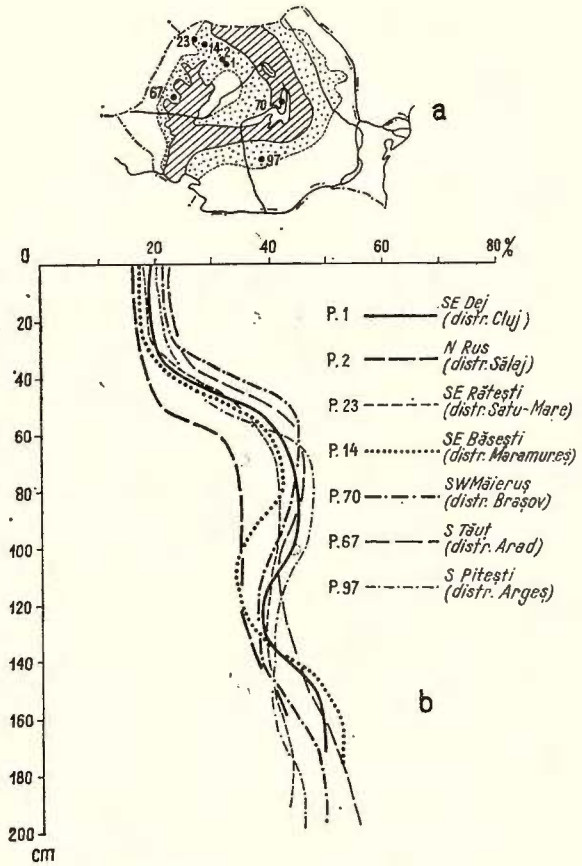

Fig. 3. — Location de quelques profils de sols lessivés (a) et variation de la teneur en argile (< 0,002 mm ∅) qui met en évidence, à 100—140 cm, des stratifications anciennes litho- ou pédogénétiques (b).

[7] D'après les données de l'auteur et les bulletins d'analyses de l'archive de l'I.C.P.A., Bucarest.

(fig. 1A). Les valeurs obtenues sont très proches de la valeur $\frac{Sa}{Sq} \cdot 100$ de l'horizon $(A2 + B)g$ et $IIABx$ (60%). Par conséquence, on peut supposer que la composition granulométrique du matériau originel est similaire à celle de ces horizons. En utilisant les courbes cumulatives, on peut estimer à environ 40% le contenu de la fraction loessique (0,01—0,05 mm ∅) dans le matériau originel (fig. 1B.) Ces valeurs indiquent une teneur en argile illuvionnée (I) presque égale à celle en argile éluvionnée (E) dans le profil actuel (fig. 1A).

Profil no. 2. On obtient pour l'épaisseur de 0 à 120 cm une moyenne pondérée du rapport $\frac{Sa}{Sq} \cdot 100$ (Sa — teneur en argile, Sq — teneur en microsquelette) de 42%, représentant la valeur du rapport caractéristique pour le matériau originel (fig. 2A). Mais cette valeur doit être moindre parce qu'on n'a pas inclus dans le calcul la teneur en argile des langues et l'argile migrée au dessous de 120 cm de profondeur. On peut estimer qu'elle dépasse un peu 35%, étant très proche de la valeur $\frac{Sa}{Sq} \cdot 100$ de l'horizon $(A2 + B)g$. Par conséquence, on peut supposer que la composition granulométrique du materiau originel était similaire à celle de cet horizon. En utilisant les courbes cumulatives, on peut estimer à environ 40% le contenu de la fraction loessique (0,01—0,05 mm ∅) dans le matériau originel (fig. 2B).

L'accumulation marquée de l'argile dans l'horizon Bt des profils a créé des conditions de plus en plus favorables à l'engorgement de l'eau dans l'horizon éluvial et, par conséquence, à la pseudogléyfication du sol et à la redistribution du fer indépendamment de l'argile (tab. 1, 2 ; planche).

Analyse chimique et minéralogique

Profil no. 1. La désaturation accentuée de l'horizon éluvial (V = = 14 — 20% ; pH = 4,8—4,9) du profil no. 1 et la présence de l'aluminium échangeable (3,8 méq.) classifient ce sol parmi les sols lessivés typiques à pseudogley, transition vers les sols lessivés acides (tab. 1B).

Les données de l'analyse globale n'indiquent pas un changement essentiel de l'argile (< 0,002 mm) au long du profil ; le rapport $SiO_2 : R_2O_3$ varie entre 2,7—2,8 en $A2$ et 2,6 en Bt (tab. 1C). La valeur un peu plus élevée du rapport $SiO_2 : R_2O_3$ dans l'horizon éluvial ($A2$) est dûe au décroissement relatif en Fe_2O_3 et Al_2O_3. Un léger décroissement du rapport $SiO_2 : R_2O_3$ dans la partie supérieure de Bt est dû à la concentration relative en Fe_2O_3 en $(A2 + B)g$ et Al_2O_3 en Bt. La quantité réduite en MnO s'explique par la résistance à l'oxydation du Mn (par rapport au Fe^{2+}), qui est entraîné en profondeur par l'eau de percolation. Le TiO_2 s'accumule résiduellement d'une façon relative dans la partie supérieure de l'horizon éluvial grâce à sa résistance chimique.

Dans les conditions de pseudogléyfication secondaire (après la formation de l'horizon *Bt* à perméabilité réduite) la solubilité du fer se réalise et sa distribution locale est évidente. Les teneurs en Fe_2O_3-total et Fe_2O_3-lié à l'argile, plus élevées dans $(A2 + B)g$ et *Bt*, que dans les horizons $A1 + A2$, indiquent la présence d'une argile plus riche en oxydes de fer dans ces horizons. Par contre les rapports Fe_2O_3-libre du sol/argile et Fe_2O_3-libre de l'argile/Fe_2O_3-lié à l'argile montrent une accumulation des oxydes de fer dans les horizons *A1* et *A2*. Des microzones où le fer est précipité à l'état ferrique (sous formes de taches et de concrétions) surtout en *A2g* et $(A2 + B)g$ correspondent au niveau où l'argile de l'horizon $(A2 + B)g$ et de *Bt* est appauvrie en fer libre.

La détermination des minéraux argileux (argile$<$0,002 mm ∅) a été effectuée aux rayons *X* (fig. 4).

Dans l'horizon illuvial (*Bt*), qui dans le profil étudié reflète la composition du matériau originel, prédominent l'illite (27—33%) et les minéraux interstratifiés (10—14 Å) illite-vermiculite (52—64%). Dans l'horizon éluvial (*A2*) on trouve comme minéraux dominants l'illite (30—41%), la vermiculite (32—40%) reconnue comme vermiculite alumineuse (reflexe 060 à 1,49 Å) et la chlorite (3—5%); les minéraux interstratifiés illite-vermiculite, absents dans l'horizon *A2*, se retrouvent dans l'horizon de transition $(A2 + B)g$ (tab. 3A).

On constate, dans l'horizon éluvial acide, l'évolution de l'illite et de l'illite-vermiculite vers la vermiculite alumineuse et même la formation de la chlorite secondaire (par addition d'aluminium provenant de la solution du sol). L'accumulation relative de kaolinite, en rapport avec le décroissement des autres minéraux, peut être attribuée à la transformation des minéraux interstratifiés dans un milieu acide et aéré, à sa faible possibilité de lessivage.

L'aplatissement des pics des interstratifications illite-vermiculite et la présence du matériau amorphe (réaction positive à NaF—n/1) indiquent un processus actif d'altération de l'argile dans le sous horizon $(A2 + B)g$ occupé par la nappe fréatique en saison humide.

Profil no. 2. La désaturation accentuée de l'horizon éluvial (V = = 17—22%; pH = 4,1—4,8) et même de l'horizon illuvial *Bt21g* (V = = 37%; pH = 5,0) et la présence de l'aluminium échangeable (2,5—7,7 méq.) classifient ce sol parmi les sols lessivés acides. En comparant les données chimiques obtenues pour le matériau qui constitue la matrice de l'horizon *Bt* et pour celui des langues argileuses présentes dans le même horizon, on constate dans le matériau de ces dernières l'acroissement des contenus d'argile, des cations et d'aluminium échangeables et le décroissement du fer (tab. 2B).

Les données de l'analyse globale n'indiquent pas un changement essentiel de la composition chimique de l'argile le long du profil (tab. 2C). La valeur un peu plus élevée du rapport $SiO_2 : R_2O_3$ dans l'horizon éluvial est dûe au décroissement relatif en Fe_2O_3 et Al_2O_3 dans cet horizon et le minimum enregistré dans la partie supérieure de l'horizon *Bt* à la concentration rélative en Fe_2O_3. La quantité réduite de MnO s'ex-

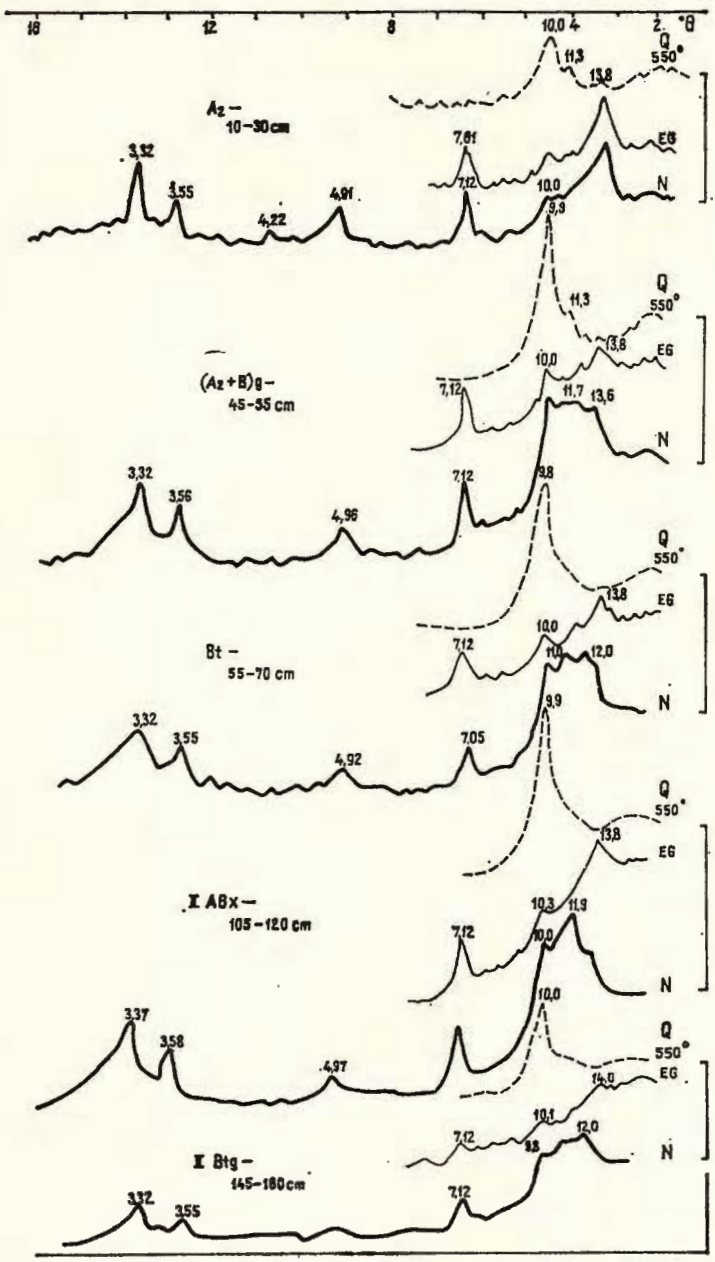

Fig. 4. — Les diffractogrammes des échatillons d'argile (< 0,002 mm) : Q — chauffage à 550°C ; EG — saturation en éthylèneglycol ; N — normale, après l'extraction des oxydes de fer ; S — l'échelle en grades représente l'angle °θ. Les chiffres placés aux sommets des pics expriment les équidistances (d/n) évaluées en angströms.

plique par la résistance à l'oxydation du Mn (par rapport au Fe^{2+}), qui est entraîné en profondeur par l'eau de percolation. Les basses valeurs pour CaO et MgO, surtout dans l'horizon éluvial, sont en concordance avec l'appauvrissement en calcium et magnésium d'échange. Le TiO_2 s'accumule résiduellement d'une façon relative dans la partie supérieure de l'horizon éluvial grâce à sa résistance chimique.

Les teneurs en Fe_2O_3 — total et Fe_2O_3 — lié à l'argile, plus élevées dans l'horizon *Bt22g* que dans l'horizon *A2g*, indiquent la présence d'une argile plus riche en oxydes de fer dans le premier horizon. Les rapports Fe_2O_3 — libre du sol / argile et Fe_2O_3 libre de l'argile / Fe_2O_3 — lié à l'argile montrent une accumulation des oxydes de fer dans l'horizon *Bt21*. Il y a donc une migration descendante du fer. En même temps on constate, dans les conditions de pseudogléyfication, un déplacement latéral des oxydes de fer dont le résultat est l'enrobement des langues argileuses (*T1* et *T2*) par des revêtements de rouille et la concentration des concrétions ferri-manganésifères dans certains horizons.

Dans les diagrammes au rayons *X* on ne distingue pas des minéraux argileux très bien définis à l'exception de la kaolinite. Il y a une réflexion très large entre 9,7 et 15,2 Å caractéristique pour les minéraux interstratifiés chlorite-illite où l'on peut identifier un composant chlorite (13,8—15,2 Å) à coté d'un composant illite (9,7—10,3 Å); la kaolinite (7,10—7,15 Å), le quartz (3,34 Å), la silice amorphe et les sesquioxydes sont en quantités réduites. Vue la quantité des principaux minéraux argileux, l'horizon *Bt22g* (100—115 cm) apparait différent de *Bt21g*; le premier conserve la composition minéralogique resultée d'une altération antérieure qui n'a pas été changée par un processus de pédogénèse ultérieur, ce qui atteste la stratification déjà mentionnée (tab. 2A).

Le processus actuel conduit à une altération intense en *A2g* où on remarque une accumulation résiduelle du quartz, de la silice amorphe et de la kaolinite, qui diminuent dans *Bt21*. L'illite apparaît sans variations significatives le long du profil. Pourtant le degré d'altération [le rapport des intensités des lignes de difraction (001) à (002) pour illite] = 1,07 et la valeur 6,51% K_2O pour le potassium en structure micacée, montrent une „dégradation" accentuée de l'argile dans *A2g* et *L* (tab. 3B). De même on remarque surtout l'augmentation de la teneur en chlorite qui atteint 41%, probablement à cause des changements des équilibres des minéraux intérstratifiés illite-chlorite, dûs au déplacement du potassium de l'espace interfoliaire suivi immédiatement de son remplacement par des „îlots" d'aluminium (qui est devenu plus mobile au niveau bas du pH du sol); la teneur réduite des minéraux interstratifiés et la rigidité du réseau chloritique représentent, une fois de plus, un argument pour la présence d'un processus d'altération intense (fig. 5).

En comparaison avec le matériau des horizons dans lesquels on le trouve, le matériau des langues est en général plus riche en illite; par contre il contient des quantités réduites de sesquioxydes libres, de kaolinite et de chlorite.

Mais le matériau des langues situées dans un horizon sous-jacent est similaire au matériau de l'horizon immédiatement sur-jacent, c'est à dire que le matériau de *L* provient de l'horizon *A2g*, celui de *T1* de (*A2* + *B*)*g* et *T2* de *Bt21g*. Cette affirmation est confirmée par :

1. La ressemblance des valeurs en pourcents de quartz et de silice amorphe.

2. La ressemblance de la teneur en chlorite, minéraux interstratifiés et illite.

3. La correspondance des paramètres basaux de la chlorite, correspondance qui a également été remarquée pour les fractions saturées en ethylenglycol des horizons *Bt21g* et *T2* (ou le blocage de Fe^{2+} dans l'espace interfoliaire augmente la valeur du paramètre de la chlorite de 14,2 Å à 15,2 Å dans les deux échantillons).

Le déplacement mécanique de l'argile (et de certains matériaux amorphes) est accompagné d'un enrichissement en potassium de l'espace interfoliaire dû à une circulation plus accentuée du potassium. Il en resulte dans les langues une augmentation en illite sur le compte de la

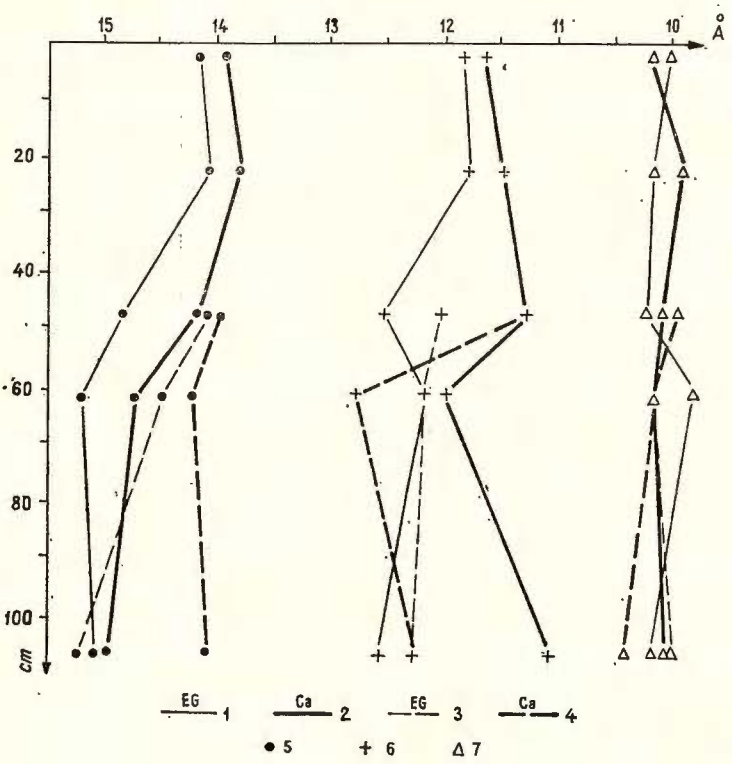

Fig. 5. — La variation des paramètres basaux des fractions coloydales saturées en ethylenglycol (EG) et calcium (Ca) — de la matrice du sol (1, 2) et des langues argileuses (3, 4); chlorite (5); minéraux interstratifiés (6); illite (7).

TABLEAU 3

A) Profil no. 1 — La composition minéralogique de la fraction argileuse (< 0,002 mm).

Horizon Profondeur cm	Traitements	Illite	Kaolinite	Vermiculite alumineuse	Chlorite alumineuse	Quartz	Minéraux interstratifiés	
							35 % chlorite — 65 % vermiculite	50 % illite — 50 % vermiculite
A2	550°	30—36 % 10 Å	15—19 %	32—40 % 10 Å	3—5 % 13,8 Å	1—3 %	7—9 % 11,3 Å	
	EG	10 Å	7,01 Å	13,8 Å	13,8 Å	4,22 Å; 3,32Å	13,8 Å	
(10—30)	N	10 Å	7,12; 3,55 Å	13,8 Å	13,8 Å		13,8 Å	
(A2+B)g	550°	33—41 % 9,9 Å	10—12 %	6—8 % 9,9 Å		2—4 %	7—9 % 11,3 Å	32—40 % 9,9 Å
	EG	10 Å	7,12 Å	13,8 Å			13,8 Å	13,8 Å
(45—55)	N	10 Å	7,12; 3,56 Å	13,6 Å		3,32 Å	13,6 Å	11,7 Å
Bt1	550°	27—33 % 9,8 Å	8—10 %			2—4 %		52—64 % 9,8 Å
	EG	10 Å	7,12 Å					13,8 Å
(55—70)	N	10 Å	7,05; 3,55 Å			3,32 Å		12,8 Å
IIABx	550°	25—31 % 9,9 Å	10—12 %			2—4 %		52—64 % 9,9 Å
	EG	10,3 Å	7,12 Å					13,8 Å
(105—120)	N	10 Å	7,12; 3,58 Å			3,37 Å		11,9 Å
IIBtg	550°	23—29 % 10 Å	10—12 %			2—4 %		54—66 % 10,0 Å
	EG	10,1 Å	7,12 Å					14,0 Å
(145—160)	N	9,8 Å	7,12; 3,55 Å			3,32 Å		12,0 Å

B) Profil no 2 — Composition minéralogique de la fraction argileuse (<0,002 mm).*

Horizon	Profondeur cm	Chlorite	Minéraux interstratifiés	Illite	Kaolinite	Quartz	Silice amorphe	Fe_2O_3 libres	Al_2O_3 libres	Degré d'altération d'illite	K_2O à structure micacée
		%	%	%	%	%	%	%	%		
A1	0—5	39	21	20	9	—	—	—	—	1,55	6,28
A2g	15—30	41	17	25	8	5	1	2	1	1,07	6,51
L	40—55	40	19	25	7	5	1	2	1	1,13	6,73
(A2+B)g	40—55	36	21	26	8	4	1	3	1	1,13	6,04
Bt21g	55—70	36	22	25	6	3	1	5	2	1,83	5,60
T1	55—70	30	24	31	7	3	1	2	2	1,64	6,45
Bt22g	100—115	41	17	22	9	—	—	—	—	0,60	6,89
T2	110—115	29	25	30	6	3	1	—	—	1,76	5,72

* Échantillons non analysés.

chlorite (29—30% chlorite dans *T1* et *T2* par rapport à 35—36% chlorite dans le matériau des horizons sur-jacents).

Considérations générales

Pour les sols lessivés évolués sur des dépôts loessiques, la sédimentation-solidification würmienne a continué pendant l'Holocène, le résultat de la sédimentation étant le dépôt du matériau de l'actuel horizon éluvial (Asvadurov et al., 1972 b). Cette évolution polycyclique du sol sur les dépôts loessiques est comparable à celle de „lessivage sur des limons anciens (antéwürmiens) acides et mal aérés" décrits par Duchaufour (1968).

Dans la fraction argileuse des sols lessivés à horizon *Bt* saturé en bases ($V > 55\%$) sont prédominants des minéraux de type illite ou illite-chlorite, caractéristiques des sols évolués en milieu faiblement acide et biologiquement actif d'un climat tempéré. Dès que les sols lessivés sont profondément désaturés ($V < 55\%$), par ex. les sols lessivés acides, à fragipan, à podzolique etc., la teneur en chlorite, en vermiculite dioctaèdrique et en kaolinite augmente. La variation en pourcents des composants minéralogiques montre les différants stades de transformation pour les minéraux argileux dioctaédriques interstratifiés de type illite-chlorite, conditionnée par l'évolution pédogénetique polyphasique de ces sols.

L'étude des profils glossiques caractéristiques a montré la présence d'un processus de lessivage, d'une pseudogléyfication secondaire et le développement d'un processus lent de podzolisation. Cette évolution caractérise surtout les sols lessivés développés sur des dépôts loessiques anciens. Les processus mentionnés ci-dessus sont temoignés par :

1. La présence d'un horizon argillique bien développé, dû au déplacement mécanique de l'argile, qui conserve sa composition minéralogique originelle.
2. La ségrégation du fer dans les horizons du profil, accompagnée d'une migration latérale surtout dans la partie supérieure de l'horizon illuvial.
3. La désaturation accentuée, l'appauvrissement en oxydes de fer et l'apparition de vermiculite alumineuse (prof. 1) et de chlorite secondaire (prof. 1 et 2) dans l'horizon éluvial.
4. Le processus initial de lessivage du fer lié à l'argile et remplacé par la rédistribution indépendante des deux composants (prof. 1), ou par la migration indépendante et l'accumulation marquée des oxydes de fer dans l'horizon illuvial (prof. 2).
5. La migration de l'argile (et de certains composants amorphes), accompagnée, dans le cas des sols à forte pseudogléyfication, par une transformation :

— du réseau des minéraux de type 2 : 1, conduisant à l'augmentation de la teneur en illite — dans les langues argileuses ;

— du réseau de la chlorite par le blocage du Fe^{2+} conduisant à la formation de la chlorite alumino-ferrique — dans la matrice du sol.

La connaissance du caractère hydromorphe (par nappe durable d'eau acide et réductrice), de la composition et de l'évolution des argiles des sols pareils est importante pour la pratique. En connaissant ces caractères, les améliorateurs peuvent prendre des mesures pour assurer le drainage et la fértilisation de ces sols. C'est à cause de la présence d'une quantité assez grande de vermiculite alumineuse ou de chlorite dioctaèdrique que les engrais potassiques n'augmentent pas suffisamment la mobilité du potassium — dûe à la concurrence de l'aluminium ; par contre, il est possible de diminuer la mobilité du magnésium. En utilisant la dolomitisation accompagnée d'engrais potassiques on peut éviter l'accroissement du raport K/Mg et en même temps on peut probablement créer des conditions d'un espace interfoliaire plus mobile.

BIBLIOGRAPHIE

Asvadurov H., Vasilescu P. (1968) Asupra originii materialului parental al orizonturilor eluviale la unele soluri silvestre podzolice din România. *Ştiinţa Solului*, 6, 1, Bucureşti.

— Atanasescu Ruxandra, Conescu Adriana, Gâţă Elena (1972a) Contribuţii la cunoaşterea unor soluri podzolice din depresiunea Oaş. *Stud. tehn. econ.*, C, 19, Bucureşti.

— Bitiri Maria, Vasilescu, P. (1972b) Poziţia gravitianului final în profilul unor soluri argiloiluviale podzolice din România. *Stud. cerc. ist. veche.* Edit. Acad. R.S.R., 3, 23, Bucureşti.

Cernescu N. (1945) Contribuţii la cunoaşterea chimismului genetic al solurilor zonale cu orizont de acumulare a argilei, II. Podzolul de depresiune. *Bul. Fac. de Agronomie din Bucureşti*, 3, Bucureşti.

— Atanasescu Ruxandra, Cicotti M., Conescu, Adriana, Gâţă Elena, Giuşcă R. (1973) Solul silvestru podzolic pseudogleic, N. C. Cernescu — Opere alese, Edit. Acad. R.S.R., Bucureşti.

Duchaufour Ph. (1968) L'évolution des sols. Masson et Cie Editeurs, Paris.

Gogoaşă T. (1959) Dozarea titrimetrică a humusului din sol. *D.S. Com. Geol.* XLII (1954—1955), Bucureşti.

Orleanu C., Dulvara Eufrosina (1970) Contributions à l'interprétation des données sur la composition mécanique des sols lessivés. *Inst. Geol. Stud. tehn. econ.*, C, 18, Bucureşti.

EXPLICATION DE LA PLANCHE

PLANCHE

Fig. 1. — Fragments d'argillanes le long d'un canal d'une microzone appauvrie en oxydes de l'horizon *A2g* du profil no. 2 (× 25); a — N ||, b — N + (d'après M. O p r i ş).

Fig. 2. — Argillanes (avec une faible teneur en oxydes de fer) le long d'un canal situé dans une microzone appauvrie en oxydes de l'horizon *Bi21g + T1* du profil no. 2 (× 70); a — N ||, b — N + (d'après M. O p r i ş).

H. ASVADUROV et al. La transformation de l'argile des sols lessivés glossiques. Pl.

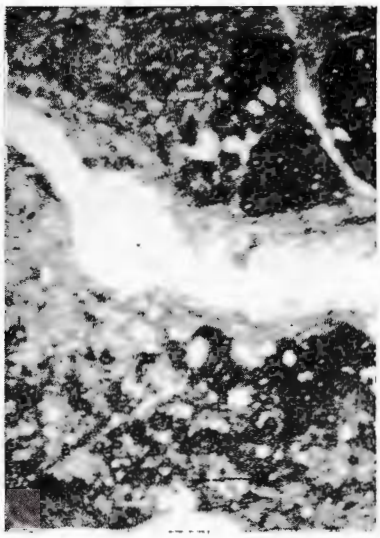

1 a

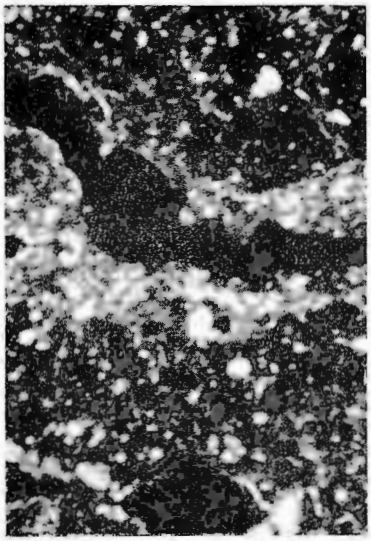

1 b

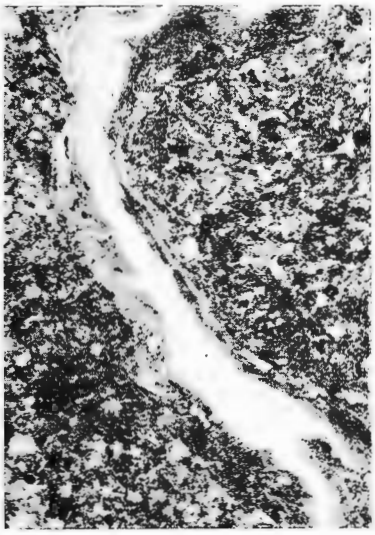

2 a

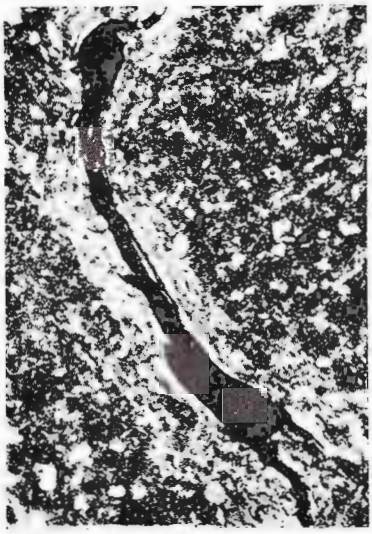

2 b

ARGILLIC ALTERATION OF TERTIARY VOLCANITES FROM THE VOIA REGION (THE METALIFERI MOUNTAINS) AND ITS RELATIONSHIP WITH THE OTHER TYPES OF HYDROTHERMAL ALTERATION [1]

BY

ION BERBELEAC[2], GHEORGHE NEACȘU[3], TIBERIU URCAN[3]

Sommaire

Altération argilique des volcanites tertiaires de la région de Voia (Monts Métallifères) et ses relations avec d'autres types d'altération hydrothermale. L'activité volcanique tertiaire correspondant à la 2-ème et 3-ème phase du second cycle d'éruption (Badénien supérieur-Pliocène?) est associée d'une série de processus hydrométasomatiques et métallogéniques déployés durant deux phases à plusieurs étapes. Au cours de ces deux phases cinq associations différentes de néominéraux apparaissent : propylitique, argilique intermédiaire, argilique avancée, séricitique et K-silicatée. Ces associations présentent une nette zonalité en sens vertical et horizontal. Ainsi l'altération de type argilique est localisée dans la partie supérieure de l'auréole hydrométasomatique caractérisée par une circulation intense. Elle comporte des associations minérales où prédominent l'illite, la kaolinite et le quartz alors que la dyckite et la pyrophyllite apparaissent sporadiquement. Les minéraux métalliques associés à ce type d'altération sont représentés tout spécialement par la pyrite et la marcassite ; les sulfures polymétalliques constituent des apparitions locales insignifiantes au point de vue économique.

The pointing out of some deep-seated mineralizations differing from the surface ones — an imperious necessity of modern times — requires a complex research with applicative character which may supply efficient indicators for the prospecting and exploration activity. Such indicators of increasing importance are defined by the presence of neomineral assemblages within hydrothermally metamorphosed areas, evidencing

[1] Paper presented at the 2nd National Clay Conference, April 11—12, 1975, Bucharest.

[2] Institutul de geologie și geofizică, str. Caransebeș 1, București.

[3] Intreprinderea geologică de prospecțiuni pentru substanțe minerale solide, str. Caransebeș, 1, București.

the genetic connection among the magmatism, magmatic metamorphism and metallogenesis processes.

The data which are to be presented refer to the results obtained by the investigation of an intensely hydrothermalized region located within the central-eastern part of the Brad-Săcărîmb Basin — the upper course of the Voia Valley (Fig. 1). Here the observations carried out by one of the authors (Berbeleac, 1970, 1973[4], 1975) as well as the data yielded by this paper complete those published by other authors who dealt generally or especially with hydrothermal alterations (Ghiţulescu, Socolescu, 1941; Rădulescu, 1953; Rădulescu, Borcoş, 1968; Borcoş, Stanciu, 1963; Stanciu et al., 1967; Giuşcă et al., 1965; Ianovici et al., 1969) within the Metaliferi Mts.

The geological framework

The upper basin of the Voia Valley represents an area located within the zone of two volcano-tectonic alignments trending NW—SE; Săcărîmb-Măcriş-Cordurea and Băiaga Geamăna-Moneasa-Zimbriţa-Stirba (Berbeleac, 1975).

The Tertiary volcanic activity as well as the metamorphic and the metallogenetic ones from this region had manifested within the mentioned alignments and belong exclusively to the 2nd cycle (Upper Badenian-Pliocene?); the 2nd and 3rd eruption phases of the quartziferous andesites display Barza, Săcărîmb and Cetraş petrotypes. Among the latter there is noted a great petrologic variation (partially marked in Fig. 1), and determined in different proportions of quartz and femic minerals.

The main volcanoes of polygenous type (Cetraş), either composed (Măcriş, Coasta Mare) or simple (Buha, Moneasa, Paua), released important quantities of lavas which cover the largest part of the perimeter, where there are also present quartziferous andesites with hornblende ± ± biotite (Barza), volcano-sedimentary rocks, probably Pliocene and Badenian-Sarmatian, or sedimentary rocks of Upper Helvetian-Badenian age.

The attempt to correlate the hydrometasomatic transformations with the volcanic and metallogenetic activity points out the association of hydrothermal and metallogenous processes with two phases, the 2nd and the 3rd ones corresponding to the Barza, Săcărîmb and Cetraş quartziferous andesite eruptions. The maximum intensity of these processes occurred during the 2nd eruption phase (Barza and Săcărîmb andesites); the alterations and metallogenesis affiliated with the 3rd phase (Cetraş andesite) are less representative.

Control factors of the hydrometasomatic processes

The distinct structural and paragenesis characters of the hydrothermalized deposits as well as the metalliferous ones from the region

[4] I.G.P.S.M.S. archives.

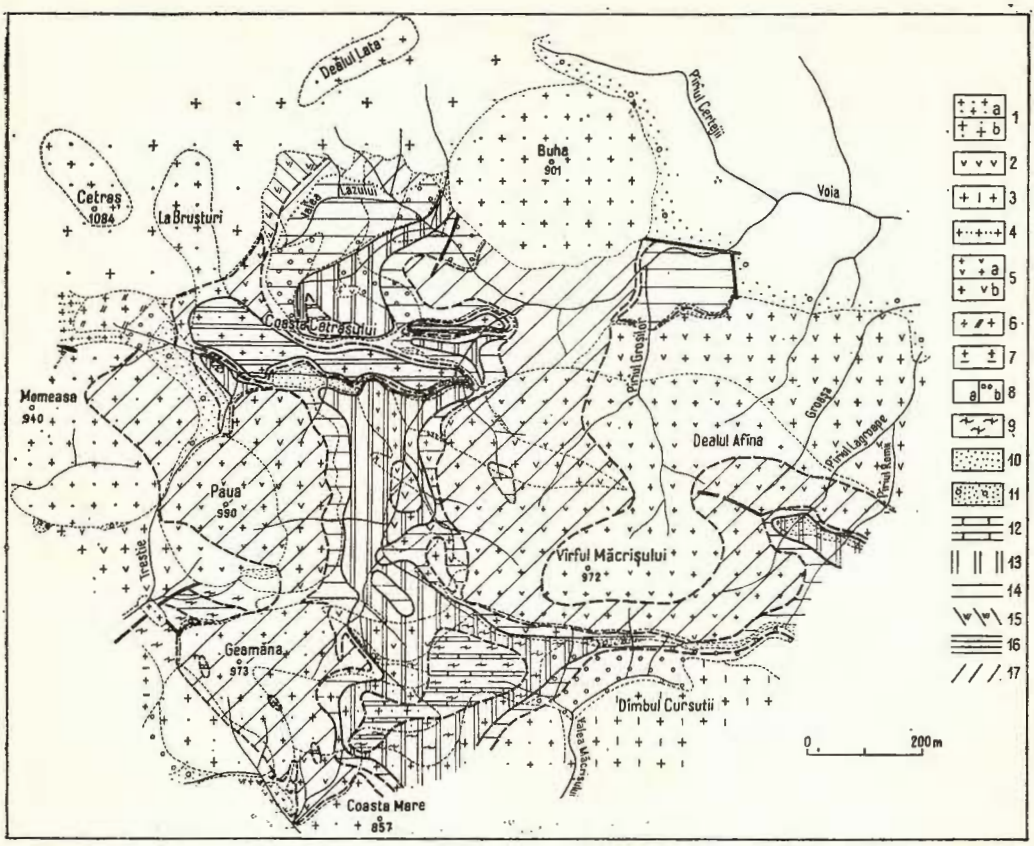

Fig. 1. — Geological Map and Neomineral Assemblages within Tertiary Volcanites and Sediments from the Voia Region (the Metaliferi Mountains).

A) Eruptive rocks (Cycle II, Upper Badenian-Sarmatian-Pliocene?) : 1, quartziferous andesite with hornblende and biotite ± pyroxenes (Cetraș); 2, quartziferous andesite with biotite and hornblende ± pyroxenes (rooting); 3, quartziferous andesite with biotite and hornblende (lavas); 4, quartziferous andesite bearing hornblende and pyroxenes ± biotite (rooting); 5, quartziferous andesite with hornblende and biotite ± pyroxenes (Săcărîmb): *a*, rooting, *b*, lavas; 6, hornblende-bearing quartziferous andesite; 7, quartziferous andesite with hornblende (lavas); 8, amphibolite-bearing quartziferous andesite ± biotite: *a*, flows, *b*, agglomerates, breccias and tuffs.

B) Sedimentary deposits: 9, volcano-sedimentary complex (Badenian-Sarmatian); 10, conglomerates, clays and sandstones (Badenian); 11, conglomerates, clays, sandstones and limestones (Upper Helvetian? — Lower Badenian).

C) Neomineral assemblages: 12, quartz-alunitic ± pyrite and marcasite; 13, advanced argillic with about 3—15 % pyrite, marcasite and about 0—2 % polymetallic sulphides; 14, intermediate argillic with about 1—5 % pyrite and marcasite and about 0—5 % polymetallic sulphides; 15, biotitic with argillaceous minerals, sericite, quartz and about 2—5 % pyrite; 16, propylitic with epidote, albite, carbonates, argillaceous minerals and about 0—3 % pyrite; 17, propylitic with chlorite, carbonates ± argillaceous minerals and about 0—1 % pyrite.

under study were determined by the geotectonical and petrochemical conditions specifical to the 2nd and 3rd eruption phases of the quartziferous andesites. These conditions imprinted specific characters to the volcanic structures and determined the selective extinction and arrangement on direction and vertical extent of the neomineral assemblages. Their distribution was also controlled by the character and thermodynamic conditions of the solutions and the lithology of the formations subjected to transformations.

The circulation of hydrothermal solutions in this region had unfolded during two phases with a few sequences characterized by a wide range of neominerals. The first phase is represented by two sequences intimately associated with the eruptions of the quartziferous andesite bearing hornblende ± biotite (Barza) and quartziferous andesite bearing hornblende + biotite (Săcărîmb). The maximum intensity of hydrothermal processes seems to be associated with the first sequence (Barza andesite) as the field data reveal a marked hydrometasomatosis of the products generated by the eruptions of the Barza andesite.

As regards the 3rd hydrothermal phase the non-essential alterations displayed in the structure of the Coasta Mare Hill are to be noticed.

The neoproducts made up during the two phases within the Tertiary volcanites were integrated into five assemblages : propylitic, intermediate argillic, advanced argillic, alunitic and sericitic for which the diagrams *ACF-AKF* (Fig. 2) were carried out. The biotite assemblage mentioned in Figure 1 was included in the intermediate argillic type considering it as representing a subtype of the latter.

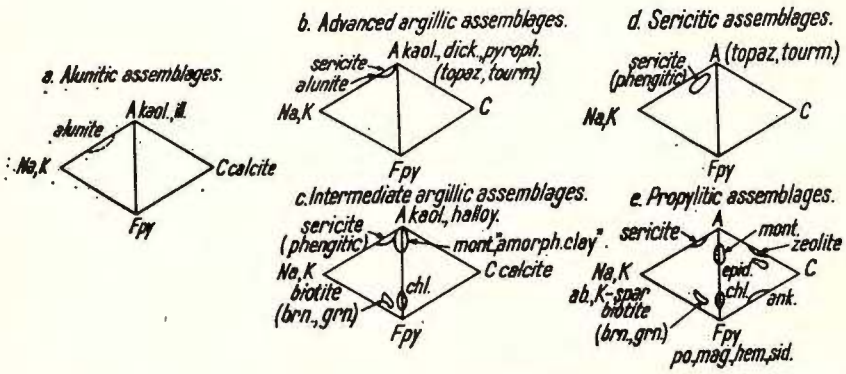

Fig. 2. — Mineral assemblages in major types of wall rock alteration (*b* — e according to Meyer and Hemley, 1967): kaol. — kaolinite; ill. — illite; dick. — dickite; halloy. — halloysite; pyroph. — pyrophyllite; tourm. — tourmaline; chl. — chlorite; mont. — montmorillonite; K-spar. — K-feldspar; ab. — albite; epid. — epidote; ank. — ankerite; py. — pyrite; po. — pyrrhotite; mag. — magnetite; hem. — hematite; sid. — siderite; A — Al_2O_3; C — CaO; K — K_2O; F — FeO.

The fact that such assemblages are present in the neoproducts of both phases proves that the evolution of the hydrothermal processes followed a continuous line especially determined by the chemistry of the solutions characterized by : the supply of CO_2, H_2O and H_2S in solutions with a low oxidation-reduction potential under the conditions of a propylitic assemblage; a strong leaching of Na, Fe^{2+}, Mg^{2+} and Ca^{2+} in rocks of solutions with a higher oxidation-reduction potential during the achievement of intermediate and advanced argillic assemblages; the strong enrichment of solution in K displaying a higher oxidation-reduction potential in the course of the formation of the sericitic assemblage as well as an essential enrichment of the solutions in K, Al, H_2 and SO_3^{2-} during the formation of the alunitic assemblage.

Proceeding to the analysis of the structural factor an obvious link between this one and the development of the hydrothermal areas, especially the argillaceous alteration, is revealed. The areas enter into the above mentioned volcano-tectonic alignments, at the periphery of the rooting structures, within the breccias and also around them, including large portions of eruptive, volcano-sedimentary and sedimentary rocks. The circulation of solutions from the main ways to the mentioned rocks was achieved using both the contacts between different types of rocks and the cooling, parting and flow planes, as well as all kind of fractures and pores present in their mass.

The lithology of metamorphosed rocks influenced the hydrometasomatic processes owing to a different degree of permeability as well as by the variations of the chemical and mineralogical composition. These determined the tidy arrangement of the neomineral assemblages, especially as regards their quantitative aspect, and led occasionally to insignificant qualitative differentiations.

Distribution and zonality of neomineral assemblages

The distribution of the hydrothermal alterations suggests the classification of the neomineral assemblages into two distinctive areas : Lazului Valley-Coasta Mare and Afina Hill-Romii Brook. The first series trending N—S has a length of about 3 km and a width of 1—2 km. This area covers the most part of the region, is located within a strong tectonized zone pierced by numerous veins and dykes of andesite rocks, and is encompassed by the necks from Măcriş, Coasta Mare, Geamăna, Paua, Momeasa, Cetraş and Buha Hills. Here is also located the Voia subvolcano. Northwards the outline is broken off by the Buha-Lata structure, while westwards it is limited by the necks from Momeasa, Geamăna and Paua Hills. The southern part of this area continues outside of the study perimeter, while eastwards it is bound—within the southern slope of the Măcriş Hill—with the second area which is trending NW—SE, and is developed especially in the Şesi Valley Basin.

The horizontal zonality of the hydrometasomatic neoproducts within the mentioned area is conspicuous (Fig. 3b); the centre comprises

alunitic and advanced argillic assemblages while at the periphery the intermediate argillic and propylitic assemblages are found again.

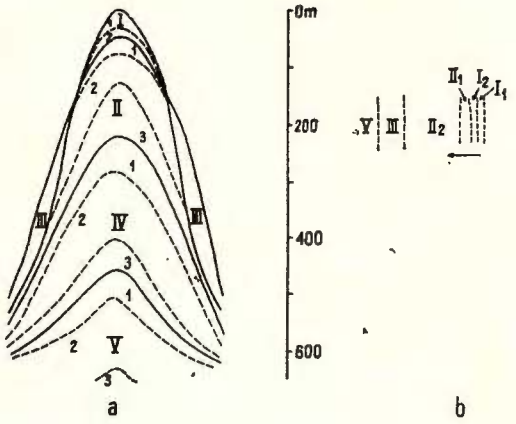

Fig. 3. — Zonality scheme of neomineral assemblages within the Voia region: *a*, vertical; *b*, horizontal.
I. Alunitic assemblage: 1, quartz-alunite; 2, alunite-quartz-argillaceous minerals.
II. Advanced argillic assemblage: 1, argillaceous minerals-quartz-alunite; 2, argillaceous minerals-quartz-carbonates; 3, argillaceous minerals-quartz-carbonates-sericite.
III. Intermediate argillic assemblage: feldspar-argillaceous minerals-quartz-biotite-carbonates-chlorite.
IV. Sericitic assemblage: 1, sericite-argillaceous minerals-gypsum-quartz; 2, sericite-carbonates-quartz-adularia; 3, sericite-carbonates-chlorite-albite-adularia.
V. Propylitic assemblage: 1, chlorite-albite-sericite-carbonates-adularia; 2, chlorite-albite-carbonates-epidote; 3, epidote-chlorite-carbonates-albite.

The sericitic assemblages displaying a slight development at the surface are especially representative with depth where, so as it results from the boring data, the zonality is also noticed (Fig. 3a). According

to this zonality the advanced argillic and intermediate argillaceous assemblages occupy the upper part of the hydrothermalized column, having above them the alunitic assemblage, and below, the sericitic one.

The grading from the advanced argillic assemblage into assemblages from depth towards roof is achieved by the disappearing of the paragenesis II_2 and the appearance of the II_1, I_2, II_3 and IV parageneses. Pyrite and marcasite are ubiquitous and vary between 3—15%. The polymetallic sulphides do not surpass 2%.

The intermediate argillic assemblage has a more limited extension at the surface, as compared to the advanced argillic one. Towards depth, however, it presents a tendency of penetrating into the marginal parts of both the advanced argillic and the sericitic types. The main paragenesis of this type of alteration: plagioclase, feldspar-argillaceous minerals-quartz-carbonates-biotite-chlorite comprises at the boundary with the other assemblages sericite, adularia, albite and hydromica. Pyrite and marcasite sulphides, so as those within the advanced argillic assemblage, are always present (1—3%), while the polymetallic sulphides occur but sporadically.

Mineralogical data

The rocks subjected to alteration characteristic of the argillaceous assemblage present a wide range of colours; they preserve to a great extent the initial structure and texture and comprise essential modifications in their initial mineralogical composition. Their colour is usually light grey, but neither there are missing dark grey, dirty white, yellowish hues.

The texture and structure of rocks is maintained and easy to be recognized excepting in the zone located at the confluence of the Măcriș Valley with the Paua Valley, a small part of the Macriș Hill and in some other points where they are no more preserved.

The mineralogical aspects of the argillic alteration type, as it results from the microscopical and roentgenographical data, are extremely various and are determined by a great diversity of neominerals caused by a different behaviour of primary components and also by the specific characters of hydrometasomatic reactions. Within the intermediate argillaceous stage the reactions have affected to a great extent the fissures and phenocrystals of andesites in comparison with the groundmass which underwent a slight transformation. The situation is radically changed in the case of rocks which have undergone modifications owing to advanced argillaceous alteration, where the strongly corroded primary quartz is almost the single mineral that has not been affected by any transformation; the skeleton relics of feldspars are sporadically occurring, the groundmass is replaced by quartz and argillaceous minerals whereas the fissures comprise almost exclusively argillaceous minerals and quartz.

The mineralogical composition of argillaceous assemblages is schematically given in Table 1, where for the five types of metamorphosed andesite there are also presented neominerals of propylitic, sericitic and alunitic assemblages.

The detailed study of the mineralogical composition of metamorphosed rocks concerning their primary components, groundmass and fissures is informatively presented also for other assemblages, and may be seen in Tables 2, 3 and 4. Besides these data the fact that the argillic and sericitic alterations comprise the greatest number of neominerals may be readily established. This number is gradually reduced both qual-

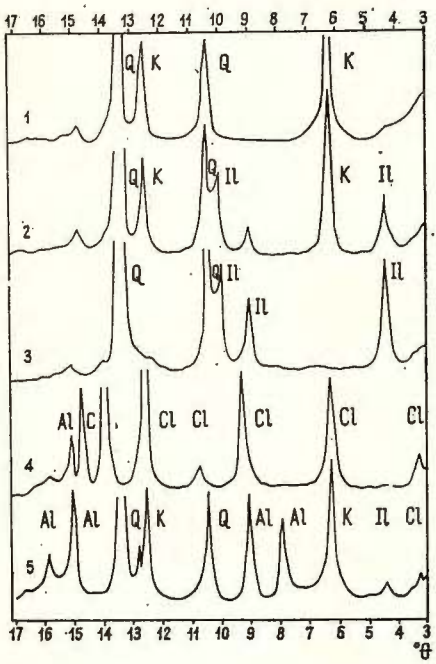

Fig. 4. — X-ray diffraction patterns of some altered rocks (Cu Kα, Ni filter).

itatively and quantitatively while entering the zone including alunitic and propylitic assemblages.

The roentgenographic data resulted from analyzing 43 samples underline the presence within the intermediate ad advanced argillaceous assemblages of kaolinite, illite, dickite and very rare pyrophyllite with which there are frequently associated sericite, quartz, carbonates, alunite, amorphous argillaceous minerals, pyrite, marcasite and more seldom biotite, feldspars and polymetallic sulphides.

Among the above mentioned argillaceous minerals, dickite occurs sporadically while kaolinite and illite often intimately associated under the form of fine and medium crystallized aggregates have a large development, frequently surpassing 50% of the rock mass.

The amorphous argillaceous minerals, as well as a part of kaolinite and alunite located in the upper part of the zone comprising clay mineral assemblages do probably have a supergene origin.

The diffractograms in Figure 4 show simple parageneses for the advanced argillaceous assemblages: quartz and kaolinite within the

TABLE 1

The main assemblages of minerals of the Voia Tertiary volcanites

Rock	Product character	Mineral assemblages						Eruption phase	Hydrothermalization and mineralization phases
		propylitic		Intermediate argillic	Advanced argillic	Alunitic	Sericitic		
		I epidote	II chlorite						
αq h bi±px (Cetraș)	Rooting and lavas	F,H,B,Q, Ep, Cl, Cb, P, Fe.O.	F,B,Q, Cl, Cb, Ar, Q, P.	F,B,Q., Kl, Il, Q, Cb, Sr,Cl,Dx,Ad, P, M.	Q, Il, Kl, Q, Cb, Hm, Sr, Cl, P, M.	Q, Al, Q, Il, Kl, Cl, P, M.	F, Q, Sr, Il, Kl, Q, Cb, Cl, P, M, P.S.	III	III
αq bi h ±px	Rooting and lavas			F,H,B,Q, Cl, Cb, Il, K, Sr, Q, P, M.				II	II
αq bi h	Lavas			F,B,H,Q, Cl, Kl, Il, Q, P.				II	II
αq h bi ±px (Săcărimb)	Rooting, lavas and pyroclastics		F, H, B, Q, Cl, Cb, Ab, M,Il,Ep, P,Fe.O.	F, B, H, Q, Il, Kl, Q,Cb, Sr, Fe.O,P,M, P.S.	Q, Il,Kl,Q,Cb, Hm,Sr,P, M, P.S.		F, Q, Sr, Il, Kl, Q, Ad, Ab, P, M, P.S.	II	II
αq h±bi	Lavas and pyroclastic rocks		F, H, B, Q, Cl, Ab, Cb, Kl, Il, Sr, P, Fe.O.	F, B, H, Q, Il, Kl, Q, Cb, Ab, Sr, Fe.O, P, M, P.S.	Q, Kl, Il, Q, Cb, Sr, Ad, Hm, P, M, P.S.	Q, Al, Kl, Q, Cb, P. M.	F, Q, Bi, Sr, Il, Kl, Hm, Mm, Cb, Gp, Ad, P, M, P. S. Au.	II	II

For symbols see the Table 4.

TABLE 2

Mineralogical composition of neomineral assemblages of the Săcărîmb quartziferous andesite

Primary components	Substitution minerals	Assemblages				
		Propylitic		Intermediate argillic	Advanced argillic	Sericitic
		I epidote	II chlorite			
H	Ep	++	+			
	Cl	+	+++	+		
	Ca	+	++	++	++	++
	Cb	+	++	++	+	++
	Sr		+	+	+	+++
	Mn		+	+	++++	++
	K		+	+++	++++	++
	Q		+	+++	++++	+++
	Gp			++	+++	++
	P		+	++	+++	+
	M			+	++	+
	Fe.O.	+	+	+		
B	G.B.		+	+		
	Cl		+++	+		
	Sr		+	+	++	++++
	Hm		+	+++	++++	++
	Ca		++	++	+++	++
	Q		+	++	++++	+++
	P		+	++	++	++
	M					+
	Fe.O.		+	+		
Px(Hp+A)	Cl		+++	+		
	Sr			+	+	++++
	Ca		++	++	++	++
	Cl		+	++	++	++
	Ar		+	+++	++++	++
	Q		+	+++	++++	+++
	P		+	++	++	+
	M				+	+
	Fe.O.		+		+	+
An	Ep		+			
	Al		+	+		
	Ad		+	+	+	++
	Sr		+	+	+	++++
	Il		+	+++	++++	++
	Kl		+	+++	++++	++
	D		+	+	+	+
	Ca		++	++	+++	++
	Cl		++	++	+++	++
	Q		+	+	+++	+++

Table 2 (continued)

Primary components	Substitution minerals	Assemblages				
		Propylitic		Intermediate argillic	Advanced argillic	Sericitic
		I epidote	II chlorite			
An	Cl		+++			
	Gp			+	++	+
	P		+	++	+++	+++
	M			+	++	++
	P.S.				+	+
Gr	Cl		+++	+		
	Cb		++	++	++	++
	G.B.		+	+	++	++
	Sr		+	+	+	++++
	Kl		+	+++	++++	++
	Il			+++	++++	++
	Q		+	+++	++++	++++
	Gp				++	+
	P		+	+	+++	++
	M				++	+
	Fe.O.		+	+		
F_s	Ep		+			
	Cl		++	+		
	Q		+	+	++++	++++
	Cb		+	++	++	+
	Ca		+	++	++	+
	Sr		+	+	+	++++
	Ad		+	+	+	++
	Al		+	+		
	Kl+Il		+	+++	++++	+++
	Gp				+	+
	Ba				+	+
	P		+	++	+++	+++
	M			+	++	+
	P.S.				+	+
	Fe.O.		+			

For symbols see the Table 4.

Cetraş quartziferous andesites from the Căpitanului Brook (sample 1) and in the Săcărîmb andesite, (here, along the Măcriş Valley, quartz and kaolinite are associated with illite — sample 2); under the form of the same andesite but from the Crîşmarului Brook occur quartz and illite (sample 3). In the same figure, a characteristic paragenesis of the propylitic assemblage is given: chlorite-carbonates-feldspars-alunite found within the Cetraş quartziferous andesite (sample 4) or another, namely

TABLE 3

Mineralogical composition of neomineral assemblages of the Cetraș quartziferous andesite

Primary components	Substitution minerals	Assemblages					
		Propylitic		Intermediate argillic	Advanced argillic	Alunitic	Sericitic
		I epidote	II chlorite				
H	Ep	++	+				
	Cl	++++	+++	+			
	Ca	+++	+++	++	+	+	
	Cb	+++	+++	++	+	+	
	Sr						+++
	Ar	+	+	+++	++++Il,K	++Il, K	++Il, K
	Q			+	++	++++	+++
	Al	++	+	+++	+++	++++	
	P				++++	+++	
	M			+	++	+++	
	Fe.O.	+	+				
B	G.B.	++					
	Cl	+	+++	+			
	Sr		+	+	+		+++
	Hm			++	+++		
	Co	++	++	++	++		
	Al					+++	
	Ca	++	++	++	+		
	Q			+	++	++	++
	Fe.O.	+	+	+			
Px(Hp+A)	Cl	+	+++				
	Sr			+	+		+++
	Ca	+	++	++	++	+	+
	Cb	+	++	++	++	+	+
	Ar		+	+++	++++	+	++
	Q			+	++	+++	+++
	Al					+++	
	P		+	+	++	++	++
Ol-An	Ep	+++	+				
	Ab	+	++	+			
	Ad		+	+			
	Sr			+	++++		
	Il		+	+++	++++	+	
	Kl		+	+++	++++	+	
	D			+	+		
	Ca	++	++	++	++	+	++
	Cb	++	++	++	++	+	++
	Q		+	++	+++	++++	+++
	Cl	+	++	+			
	Al			+	+	++++	
	Gp			+	++	++++	+++
	P	+	+	++	+++	+++	+++

Table 3 (continued)

Primary components	Substitution minerals	Assemblages					
		Propylitic		Intermediate argillic	Advanced argillic	Alunitic	Sericitic
		I epidote	II chlorite				
	M				++	++	+
	P.S.			+	+		+
Gr.	Ep	+++	+				
	Cl	+	+++				
	Cb	++	++	++	+		
	Ca	++	++	++	+	+	
	Sr				+		
	Kl			++	+++		
	Il		+	++	+++	+	
	Al					++++	
	Q		+	++		++++	
	P	++	+	++	+++	+++	
	M	++	+	++	+++	++	
	P.S.				+		
F_s	Ep	+++	+				
	Cl	+	+++				
	Q		+	++	++++	++++	+++
	Cb	++	++	++	+		
	Ca	++	++	+	++		
	Sr				+		++++
	Ad	+	+	+			+
	Ab	+	+				
	K-Il		+	+++	++++		+
	Al					++++	
	Ba				++		
	Gp				+++		
	P	++	++	++		+++	+++
	M			+		++	+
	P.S.+ +C.C.				++		+++

For symbols see the Table 4.

TABLE 4

Mineralogical composition of neomineral assemblages of the Barza quartziferous andesite

Primary components	Substitution minerals	Assemblages				
		II Propylitic epidote	Intermediate argillic	Advanced argillic	Alunitic	Sericitic
H	Cl	+++	+			
	Ca	++	++	++		+
	Cb	++	++	++		+
	Sr	+	+	+		++++
	Mm	+	+	++		+
	Il	+	+++	++++	+	++
	Kl	+	+++	++++	+	++
	Al				++++	+
	Q	+	+++	++	+	+++
	Ab	+	+			
	Ad	+	+	+		+
	Gp		+	+++	+	+
	An			+		+
	P	+	++	+++	++	++
	M		+	++	+++	+
	Fe.O.	+	+			
	P.S.					+
B	G.B.	+				
	Cl	+++	++			
	Sr	+	+	+		+++
	Il-Kl			++	+	+
	Hm	+	++	+++		+
	Ca	++	++	+		+
	Cb	++	++	+		+
	Q	+	++	+	+	+
	Al				++++	
	P	+	+	++	++	++
	M			+	+	+
	Fe.O.	+	++			
F	Cl	+				
	Ca	++	+++			+
	Cb	++	+++			+
	Sr	+	+	+		+++
	Il	+	+++	++++	+	++
	Kl	+	+++	++++	+	++
	D	+	+			
	Q	+	+++	++	+	++
	Ab	+++	++	+		
	Ad	+	+	++		+
	Al			+	+++	+
	Gp		+	++		+
	An		+	+		

Table 4 (continued)

Primary components	Substitution minerals	Assemblages				
		II Propylitic epidote	Intermediate argillic	Advanced argillic	Alunitic	Sericitic
	P	+	++	+++		+++
	M		+	+		+
	P.S.		+	+		++
Gr.	Cl	+				
	Ca	++	++	++		
	Cb	+++	++	++		
	Sr	+	+	+		+++
	Il	+	++	++++	+	+
	Kl	++	+++	++++	+	+
	Q	+	+++	++++	++++	+++
	Al				+	
	Ab	+	+			
	Ad	+	+	+		+
	Gp			+		+
	P	+	++	+++	++	+++
	M		+	++	+	+
	P.S.		+	++		+
F_s	Cl	+				
	Cb	++	++	+++	+	+
	Ca	++	++	+++	+	+
	Sr	+	+	+		++
	Il	+	+++	++++	+	+
	Kl	+	+++	++++	+	+
	Q	+	+	++	+	+++
	Al				++++	+
	Ab	+				
	Ad	+	+	+		
	Gp		+	++++		+
	An		+	+		+
	P	+	++	+++	+++	+++
	M		+	++	++	++
	P.S.		+	+		++
	Fe.O.	++	+			

Symbols of primary components: H — hornblende; B — biotite; Px — pyroxenes; Hp — hypersthene; A — augite; Ol-An — oligoclase-andesine; Gr — groundmass; F_s — fissures and veins; F — feldspars.

Symbols of neominerals: Gr — groundmass; F_s — fissures and veins; Ep — epidote; Ab — albite; Ad — adularia; Ca — calcite; Cb — carbonates; Sr — sericite; Kl — kaolinite; Il — illite; D — dickite; Hm — hydromica; G.B. — green biotite; Ar — argillic minerals; Q — quartz; Gp — gypsum; Al — alunite; Ba — barite; Fe.O. — ferrous ferric oxides; P — pyrite; M — marcasite; P.S. — polymetallic sulphides; C.C. — cupriferous complex.

++++ very frequent
+++ frequent
++ unfrequent
+ rare

the alunitic one, quartz-alunite-kaolinite-illite-chlorite present in the same rock but being located within the Coasta Mare Hill (sample 5).

Conclusions

The assemblages characteristic of the argillaceous alteration are located within the central zone of the two hydrothermally altered areas, and at the upper part of the hydrothermalized and mineralized column. The main parageneses recognized within this alteration are dominated by the presence of illite, kaolinite and quartz. The associated metallic minerals are chiefly represented by pyrite and marcasite, whereas polymetallic sulphides constitute local occurrences with insignificant values. The latter were found in more representative amounts within the sericite assemblage localized in more deep-seated volcanic structures.

References

Berbeleac I. (1970) Aluniţii de la Voia (Munţii Metaliferi), *D.S. Inst. Geol.* LVI, Bucureşti.

— (1975) Studiul petrografic şi metalogenetic al regiunii Vălişoara (Porcurea) (Munţii Metaliferi), *An. Inst. Geol. Geof.*, XLVI, Bucureşti.

Borcoş M., Stanciu Constantina (1963) Altération hydrothermale de l'andesite quartzifère dans le gisement Haneş, *Carp.-Balk. Geol. Assoc., VI Congr.*, Varşovia.

— (1965) Hidrometamorfismul andezitului cuarţifer neogen din sectorul Almaşul Mare (Zlatna, Munţii Metaliferi), *Stud. cerc. geol.*, 10, 2, Bucureşti.

— Bratosin Irina, Colios Elena, Ianc Rossete (1972) Observaţii petrogenetice şi geochimice asupra vulcanitelor din ciclul II de erupţie din Munţii Metaliferi, *D.S. Inst. Geol.*, LVIII, Bucureşti.

Ghiţulescu P. T., Socolescu M. (1941), Étude géologique et minière des Monts Metallifères, *An. Inst. Geol. Rom.* XXI, Bucureşti.

Giuşcă D., Stanciu Constantina, Dimitriu A., Medeşan Alexandra, Udrescu Constanţa (1965) Contributions à la géochimie des processus de séricitisation et adularisation des andésites, *Carp.-Balk. Geol. Assoc., VII Congr., Sofia, Reports, III*, Sofia.

Ianovici V., Giuşcă D., Ghiţulescu P. T., Borcoş M., Lupu M., Bleahu M., Savu H. (1969) Evoluţia geologică a Munţilor Metaliferi. Edit. Acad., Bucureşti.

Meyer Ch., Hemley J. (1967), Wall rock alteration geochemistry of hydrothermal ore deposits, New York.

Rădulescu D. (1953), Contribuţiuni la cunoaşterea fenomenului de propilitizare a rocilor vulcanice. *Rev. Univ. C. I. Parhon, ser. St. Nat.*, Bucureşti.

— Borcoş M., (1968), Spat subsequenter alpiner Magmatism in Rumanien, *Acta Geol.*, XI, 1—3, p. 139—152, Budapesta.

Stanciu Constantina, Dimitriu A., Udrescu Constanţa (1967) Studiul geochimic al procesului de sericitizare a andezitului cuarţifer din Munţii Metaliferi (Zăcământul Bucium şi Concordia), *Stud. cerc. geol.*, 12, Bucureşti.

INFLUENCE OF LITHOLOGICAL INHERITANCE ON DEVELOPMENT OF SOME SOILS IN OLTENIA [1]

BY

ION BURNEA[2], LUCIA BURNEA[2], GHEORGHE GÂȚĂ[3]

Sommaire

Influence de l'héritage lithologique sur la formation de certains sols d'Olténie. Les principaux composants de la fraction argileuse sont l'illite et la vermiculite dioctaédrique pour les profils des sols de Podari et de Simnic (luvisols) et les minéraux intergrades pour le profil des sols de Preajba (acrisols). La composition minéralogique varie faiblement en sens vertical indiquant une nette influence des héritages lithologiques.

A synthesis of clay mineral repartition in the Oltenia soils (Gâță et al., 1975) points out the influence of lithological inheritance on crystallo-chemical composition of clay fractions of these soils.

The paper reported here presents three soil profiles namely the luvisols from Podari (Dolj) and Simnic (Dolj) and the acrisol from Preajba (Gorj) evidencing both the inheritance and the pedological processes.

Materials and methods

Descriptions of the studied soils are summarized in the Table 1.

Particle size distribution analyses were obtained by the pipette method, *pH* electrometric determination by glass electrod, organic matter by Knopp, total nitrogen by Kjeldahl, extractable nutrients (P_2O_5 and K_2O) by lactate-acetate method.

In addition the exchange capacity and exchangeable cations were determined after displacement by ammonium acetate solution (Cer-

[1] Paper presented at the 2nd National Clay Conference, April 11—12, 1975, Bucharest.

[2] Universitatea din Craiova, str. Al. I. Cuza 31, Craiova.

[3] Institutul pentru știința solului, Bd. Mărăști 61, București.

TABLE 1

Some characteristics of studied profiles

Profile	Horizon	Depth cm	Parent material
Podari (luvisol)	A_a	0—20	clay and silty clay deposits of Pleistocene age
	B_{t_1}	25—56	
	B_{t_2}	56—88	
	B_{t_3}	88—170	
Simnic (luvisol)	A_a	0—28	silty clay deposits and aeolian sand of Holocene age
	B_{t_1}	28—45	
	B_{t_2}	45—116	
	B_{t_3}	116—150	
Preajba (acrisol)	A_1	0—15	silty clay and clay deposits of Sarmatian-Meotian age
	A_2/B	31—44	
	B	44—110	

n e s c u, 1939). The mineralogical composition of separated clay fractions was determined for each sample by *X*-ray diffraction techniques, IR absorption curves and thermal analyses (G â ţ ă, 1972)[4].

Results and discussions

The particle size distribution of the samples in the three profiles shows an increasing content of clay fraction (< 1 μ) in *B* horizon as compared with *A* horizon within the Podari-Simnic-Preajba sequence (Tab. 2). The *pH* values increase with depth in each profile from 5.7 7.1 for the Podari profile, 6—6.8 for the Simnic profile and from 4.9 to 5.8 for the Preajba profile. On the contrary the organic matter, total P_2O_5 and extractable nutrients decrease with depth, and for luvisols they have almost the same values (in the Preajba samples smaller amounts are noticed) (Tab. 3).

As regards C.E.C. and V% the Podari and Simnic profiles present almost the same values, namely 27.6—31.3 méq./100 g, 26.4—30.3 méq./ /100 g and 71—80.6%, 71—78.2% respectively. In the Preajba profile these values are lower, i.e. 14.8—28.2 méq./100 g and 50—55% for V (Tab. 4).

The mineralogical composition of clay fractions was determined by means of *X*-ray diffraction patterns. The predominant component is illite approaching the expandable minerals of the luvisols from Podari and Simnic and approaching the intergrade minerals of the acrisol from Preajba soil. As shown in Table 5 the basal spacing position of expandable and intergrade minerals varies only insignificantly with depth.

[4] Thesis of Doctor's Degree, Arch. of the Polytechnical Institute, Bucharest.

This means that the above predominant minerals are inherited from parent material of the profile. The resemblance of the clay fractions in the profile from Podari and Simnic (B u r n e a et al., 1971), might be probably due to the same reddish-brown parent material for the two soils. It is not out of question that the new Holocene deposits from Simnic did arise from the older Pleistocene deposits.

The variation of basal spacings might be due to the genetical processes. For the Podari profile only in *A* horizon the *c*-parameter of expandable minerals is increased for the K-saturated fraction and decreased for the ethylene-glycol-saturated fraction than for the other fractions belonging to *B* horizon. For Ca-saturated fractions the basal spacings have the same values. This change of the interlayer mobility is presumably due to the formation of some intergrade minerals.

For the Simnic profile these chloritization processes are more accentuated. The intergrade components in *A* horizon present 13.8 Å — 13.9 Å for K and Ca-saturated fractions and only 14.9 Å for ethylene-glycol-saturated fractions. Moreover, the other ethylene-glycol-saturated fractions of horizon have their *c*-parameter below 16 Å.

For the clay fractions of the Preajba profile the intergrade minerals are always occurring in all the horizons.There is neither collapse for the K-saturated fractions, nor increase for the ethylene-glycol-saturated fractions in comparison with the Ca-saturated fractions.

The infrared spectra show for each fraction an absorption band at 919—924 cm^{-1} due to Al—O—H bending vibrations (S t u b i c a n, R o y, 1961).

Moreover the OH stretching region always shows an intense absorption band at 3620—3622 cm^{-1}. The assignment of these absorption bands to clay minerals points out the dioctahedral structure of predominant minerals : illite-intergrade minerals and expandable minerals (B u r n e a et al., 1969). The thermal analyses are in agreement with the *X*-ray diffraction and infrared data. Owing to a high illite content and the presence of expandable minerals the peak temperatures of dehydroxylation are over 555°C for the clay fractions of Podari and Simnic profiles (Tab. 6). For the Preajba clay fractions the peak temperatures during the dehydroxylation reaction are lower because of their content in intergrade minerals. In addition the losses of weight of the dehydroxylation are below 45 mg/g for Podari and Simnic clay fractions and over 48.7 mg/g for Preajba clay fractions (in agreement with G â ţ ă, C r ă c i u n, 1975).

Conclusions

The influence of lithological inheritance on the studied profiles is pointed out by the insignificant variation noted in the mineralogical composition of the clay fractions separated from their horizons.

The predominant components in the clay fractions are illite and dioctahedral vermiculite for Podari and Simnic profiles and intergrade minerals for the Preajba profile.

TABLE 2

Grain size composition of soil samples

Profile	Horizon	Depth cm	Grain size fractions (%)					
			>0.2 mm	0.2–0.02 mm	0.02–0.01 mm	0.01–0.002mm	0.002–0.001mm	<0.001 mm
Podari (luvisol)	A_0	0–20	12.09	32.31	11.3	11.2	3.4	29.8
	B_1	25–56	8.43	35.07	8.3	10.0	3.2	35.0
	B_2	56–88	9.21	27.79	8.3	8.2	2.6	43.9
	B_3	88–170	8.64	29.46	8.2	9.0	1.3	43.4
Simnic (luvisol)	A	0–28	16.29	36.21	9.4	8.9	2.2	27.0
	B_1	28–45	12.47	34.53	8.4	8.2	1.2	35.2
	B_2	45–116	13.92	35.88	7.0	8.8	1.7	32.7
	B_3	116–150	14.92	36.58	7.1	9.3	1.7	30.4
Preajba (acrisol)	A_1	0–15	7.09	35.81	14.6	18.2	5.4	18.9
	A_2/B	31–44	5.08	33.62	11.7	14.9	4.4	30.3
	B	44–110	9.91	31.69	11.7	12.6	4.4	29.7

TABLE 3

Some chemical characteristics of soil samples

Profile	Depth cm	*pH*	Organic-water %	N %	P_2O_5 %	Extractable nutrients	
						mg P_2O_5/100 g soil	mg K_2O/100 g soil
Podari (luvisol)	0–20	5.7	1.47	0.100	0.085	10.52	11.6
	26–56	5.8	1.70	0.070	0.063	9.37	11.6
	56–88	5.8	1.38	0.040	0.024	8.58	16.6
	88–170	7.1	1.20	0.020	0.005	6.07	18.8

Table 3 (continued)

Simnic (luvisol)	0—28	6.0	1.38	0.080	0.076	9.72	12.0
	28—45	6.5	1.70	0.065	0.054	7.16	13.4
	45—116	6.7	1.45	0.935	0.021	6.45	13.2
	116—150	6.8	1.60	0.012	0.014	6.23	14.4
Preajba (acrisol)	0—15	4.9	0.60	0.062	0.075	4.08	5.6
	31—44	5·2	0.46	0.041	0.050	3.14	6.2
	44—110	5.8	0.70	0.010	0.016	2.78	7.8

TABLE 4

Exchangeable cations and exchange capacity of soil samples

Profile	Depth cm	Exchangeable cations												
		méq./100 g soil							% from C.E.C.					
		Ca^{2+}	Mg^{2+}	Na^{+}	K^{+}	SB	SH	C.E.C.	Ca^{2+}	Mg^{2+}	Na^{+}	K^{+}	H^{+}	V%
Podari (luvisol)	0—20	16.06	3.10	0.15	0.38	19.69	7.95	27.64	58.10	11.21	0.54	1.37	28.77	71.24
	26—56	17.69	4.43	0.24	0.57	22.93	7.18	30.11	58.75	14.71	0.80	1.89	23.88	76.12
	56—88	18.42	4.98	0.46	0.63	24.69	7.24	31.73	58.05	15.69	1.45	2.02	22.81	77.19
	88—170	19.14	4.48	0.89	0.60	25.11	6.06	31.17	61.40	14.37	2.25	1.92	19.44	80.56
Simnic (luvisol)	0—28	11.92	2.42	0.18	0.47	19.99	8.16	28.15	51.49	10.45	0.77	1.67	28.99	71.01
	28—45	14.78	2.86	0.32	0.61	18.57	7.85	26.42	55.94	18.25	1.21	2.30	29.71	70.29
	45—116	16.51	3.16	0.55	0.96	21.18	7.02	28.20	58.54	11.20	1.95	3.40	28.81	75.19
	116—150	18.23	3.95	0.50	1.21	23.89	6.43	30.32	51.12	13.02	1.64	3.90	21.20	78.20
Preajba (acrisol)	0—15	5.34	0.30	1.24	0.39	7.27	7.48	14.75	35.74	2.03	8.41	2.64	50.70	49.96
	31—44	5.12	0.93	1.43	0.36	7.84	6.94	14.78	34.64	6.29	9.67	2.44	46.96	53.04
	44—110	5.45	0.95	1.79	0.23	8.42	6.88	15.30	35.62	6.21	11.70	1.50	45.00	55.00

TABLE 5

Basal spacings (in Å) of clay fractions of soil samples (expandable and intergrade minerals)

Profile	Horizon	Cation saturated		
		K	Ca	ethylene glycol
Podari (luvisol)	A_a	13.6	14.4	15.4
	B_{t_1}	13.0	14.6	16.3
	B_{t_2}	12.3	14.5	16.4
	B_{t_3}	12.8	14.6	16.4
Simnic (luvisol)	A_a	13.8	13.9	14.9
	B_{t_1}	13.3	14.5	15.3
	B_{t_2}	12.9	14.5	15.9
	B_{t_3}	13.4	14.6	16.0
Preajba (acrisol)	A_1	13.8	14.0	13.9
	A_2/B	13.9	13.9	14.0
	B	13.8	13.9	13.8

TABLE 6

Peak temperatures and losses of weight in the dehydroxylation reactions (clay fractions < 1 μ)

Profile	Horizon	peak temperature °C	loss of weight mg/g
Podari (luvisol)	A_a	565	44.6
	B_{t_1}	560	42.6
	B_{t_2}	560	44.6
	B_{t_3}	565	44.9
Simnic (luvisol)	A_a	565	48.3
	B_{t_1}	565	44.9
	B_{t_2}	565	43.6
	B_{t_3}	565	43.6
Preajba (acrisol)	A_1	550	50.4
	A_2/B	548	48.9
	B	550	48.7

The genetical processes are characterized by a transformation of vermiculite into intergrade minerals more accentuated in the *A* horizons of luvisols.

REFERENCES

Burnea, I., Burnea Lucia, Gâţă G. (1969) Studii spectrale asupra naturii cristalochimice a fracţiunilor argiloase aflate în solul podzolic din zona Subcarpatică a Olteniei. *An. Univ. Craiova*, ser. II, vol. I(XI), *Biologie-St. Agric.*, Edit. Ceres, Bucureşti.

— (1971) Studiu mineralogic comparativ asupra fracţiunilor sub 1 μ existente în solurile din zona centrală a Olteniei. *An. Univ. Craiova*, ser. III, vol. III (XIII), *Biologie-St. Agric.*, Edit. Ceres, Bucureşti.

Cernescu N. (1939) Determinarea capacităţii de schimb şi a cationilor schimbabili la sol. *Inst. Geol., Stud. tehn. econ.*, C, 5, Bucureşti.

Gâţă G., Crăciun, C. (1977) On the dehydroxylation reaction of clay fractions from some Romanian soils. *Proc. of the 2nd National Clay Conference-Bucharest, Inst. Geol., Geof., Stud. tehn. econ.*, I, 14, Bucureşti.

— Burnea I., Maxim I., Sorop G., Crăciun C. (1975). Contribuţii la cunoaşterea compoziţiei mineralogice a fracţiunilor argiloase din solurile Olteniei. Lucrări ştiinţifice — volum omagial, Univ. Craiova.

Stubican V., Roy R. (1961) Isomorphous substitution and infrared spectra of layer-lattice silicates. *Amer. Min.*, 46, p. 32—51, Washington.

THE ABNORMAL MONTMORILLONITE IN BENTONITES FROM THE VICA-GURASADA REGION[1]

BY

CONSTANTIN CRĂCIUN[2]

Sommaire

Montmorillonite anormale des bentonites de Vica-Gurasada. Les analyses thermiques mettent en évidence l'existence de deux variétés de montmorillonite au point de vue du comportement thermique. La variété normale présente un seul effet endothermique qui marque le phénomène de déhydroxilation, alors que celle anormale présente un effet endothermique double. Les analyses chimiques dénotent des teneurs élevées en fer et potassium pour la variété anormale alors que les analyses diffractométriques R.X. dénotent des valeurs proches des réflexions des deux variétés.

The montmorillonite clay minerals are undoubtedly the subject of numerous thermal studies. Different investigators (Grim, Kulbicki, 1961; Mackenzie, 1970; Todor, 1972) showed that under the same experimental conditions the dehydroxylation temperature of montmorillonite minerals varies from one sample to another. Thus the so-called „normal" montmorillonite shows a medium endothermic peak at about 700°C due to the loss of hydroxyl groups, while the so-called „abnormal" montmorillonite displays two dehydroxylation steps (two relatively lower endothermic peaks at about 550°C and 690°C — Mackenzie, 1970).

The presence of abnormal motmorillonite was noted in some localities (Mackenzie, 1970): Almeria (Spain), Dunning (Scotland), Kent (England).

The purpose of this paper is to point out the presence of such a montmorillonite in the bentonites from the Vica-Gurasada region.

[1] Paper presented at the 2nd National Clay Conference, April 11—12, 1975, Bucharest.

[2] Institutul pentru ştiinţa solului, Bd. Mărăşti 61, Bucureşti.

Materials and methods

The colloidal fractions $< 1\,\mu$ separated from bentonites within the Vica-Gurasada region were subjected to *X*-ray diffraction, thermal and chemical analyses. The *X*-ray data were taken on a URS-50 IM diffractometer with a copper target. The thermal analyses were performed with a derivatograph M.O.M. O.D.—103 with ceramic crucibles. The heating rate of 10°/minute has been used.

Results and discussions

The *X*-ray diagrams for bentonites disclose the presence of montmorillonite (dominant mineral), cristobalite, quartz and plagioclase feldspar.

The thermal analysis confirms the presence of montmorillonite as principal constituent of bentonites. The DTA curves show endothermic reactions at about 140°C, 700°C (or 550°C and 690°C) and a low S-shaped endothermic-exothermic peak couple at about 880°C—940°C. The first peak is due to the loss of sorbed moisture, the second to dehydroxylation and the third to structural change.

TABLE 1

Dehydroxylation temperature and weight loss (%) of some bentonites

Sample	Temperature of dehydroxylation	Weight loss %	
Vica bentonite	700°C		3.8
Gruiul Alb bentonite	575°C	1.7	
	690°C	0.6	2.3
Gurasada bentonite 1	708°C		3.1
Gurasada bentonite 2	556°C	1.5	
	674°C	1.4	2.9
Gurasada bentonite 3	704°C		2.5
Gurasada bentonite 4	692°C		4.0
Gurasada bentonite 5	545°C	1.5	
	672°C	1.5	3.0
Gurasada bentonite 6	562°C	1.3	
	697°C	1.7	3.0

Table 1 shows the temperature of endothermic peaks due to the dehydroxylation and weight loss which accompanies this thermal reaction of bentonites. There is a difference among the samples. The Vica and Gurasada 1, 3, 4 bentonites show only a single endothermic peak at about 692—708°C, while the Gruiul Alb and Gurasada 2, 5, 6 show two endothermic peaks at about 545°—575°C and 672°-697°C respectively.

The two peak intensities are lower than those of the samples with a single dehydroxylation peak. The second peak of the abnormal montmorillonite shows a lower temperature than the normal montmorillonite, excepting sample 6.

All the thermogravimetric curves display a gradual, continuous weight loss between the two inflexions which mark the loss of sorbed moisture and OH groups respectively. This weight loss suggests the presence of one exchangeable cation of high hydration energy like Ca which balances the charge defficiency of the lattice. The presence of Ca is proved by a small shoulder at about 200°C (DTA). Also the DTA curves show a distinct weight loss at about 200°C. Usually the weight losses accompanying the release of the OH groups rendered as area peak vary from a simple to a double value, and for this reason it is very difficult to reach now a conclusion.

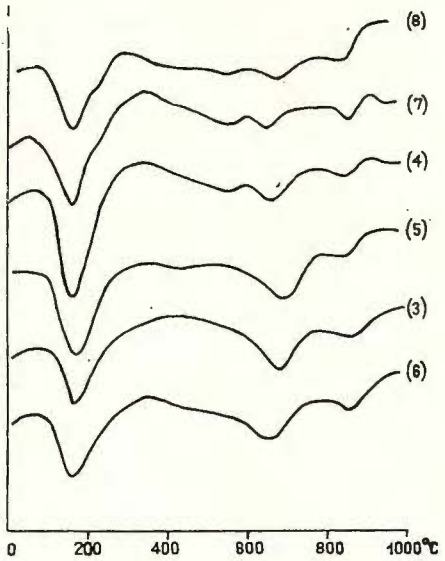

Fig. 1. — DTA curves of the clay fractions from Gurasada bentonites.

In order to obtain new informational data, a clay fraction $< 1\mu$ from these bentonites was separated and analysed.

Figure 1 shows the DTA curves of colloidal fractions separated from bentonites without chemical treatment. On the diagram there may be noticed that the amplitude of the single endothermic peak (normal sample) is higher than that for each of the amplitudes of the two peaks (abnormal sample).

Table 2 shows the dehydroxylation temperatures and the corresponding weight losses of these colloidal fractions. The variation range

TABLE 2

Dehydroxylation temperature and weight loss (mg/g) of clay fractions (< 1μ) of the Gurasada bentonites

Sample	Temperature of dehydroxylation	Weight loss mg/g	
Gurasada bentonite 1	697°C		27.4
Gurasada bentonite 2	578°C 687°C	10.6 11.5	22.1
Gurasada bentonite 3	697°C		19.7
Gurasada bentonite 4	692°C		21.8
Gurasada bentonite 5	586°C 680°C	20.2 11.9	32.1
Gurasada bentonite 6	556°C 695°C	9.7 20.9	30.6

of these values is the same for bentonites and clay fractions both for the normal and abnormal samples. The TG curves indicate weight losses between 19.7 and 32.1 mg/g. The weight losses of montmorillonites with two dehydroxylation peaks have a different distribution for the two effects.

It has been mentioned that some samples show a double endothermic peak. The presence of samples with single and double effects suggests the occurrence in the Gurasada region of two types of montmorillonite: one „normal" which displays only a single dehydroxylation effect, and another „abnormal" with a double dehydroxylation effect. It is noteworthy that the energy required to initiate dehydroxylation (which is reflected in the peak temperature) varies from one type to another.

The differences concerning the bound energy of hydroxyl groups in the lattice of the two types of montmorillonite should be related to the differences in their composition and/or structure. It seems that these differences are too slight to be observed by the *X*-ray diffraction analysis.

The *X*-ray diffraction diagrams in Figure 2 indicate the presence of montmorillonite and cristobalite in both cases. The clay fraction saturated in potassium, calcium and ethylene glycol shows in general the same *c*-axis spacings.

In Table 3 no differences can be observed between „normal" and „abnormal" varieties as to the position of diffraction lines.

The chemical analyses of the two samples: Gurasada 1 (normal) and Gurasada 6 (abnormal) disclose some differences between the two varieties (Tab. 4).

Thus the abnormal montmorillonite shows a higher content of iron and potassium and a higher value of the cation exchange capacity. The low content of sesquioxides in bentonites namely below 0.05% Al_2O_3 and 0.25% Fe_2O_3 shows that most of these cations (iron and aluminium) belong to the montmorillonite lattice.

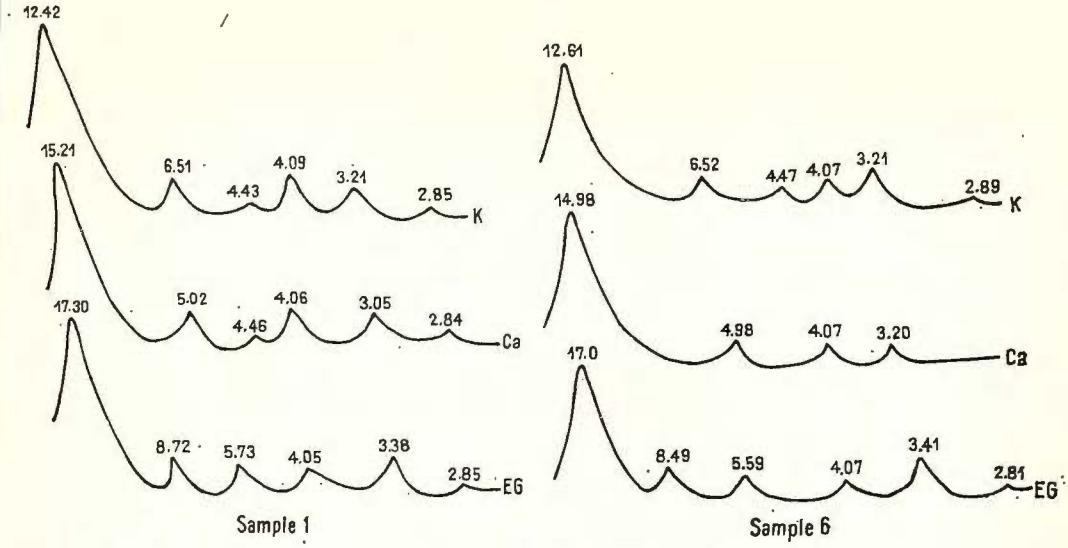

Fig. 2. — *X*-ray diffraction patterns of the two types of the Gurasada montmorillonite (sample 1 — normal montmorillonite; sample 6 — abnormal montmorillonite).

TABLE 3

Basal spacings of the glycolated clay fractions of bentonites

Sample	001	002	003	005
Gurasada bentonite 1	17.3	8.72	5.73	3.38
Gurasada bentonite 2	17.2	8.57	5.61	3.39
Gurasada bentonite 3	17.0	8.45	5.56	3.37
Gurasada bentonite 4	17.0	8.50	5.60	3.36
Gurasada bentonite 5	17.0	8.49	5.59	3.41
Gurasada bentonite 6	17.0	8.48	5.60	3.38

TABLE 4

Chemical analyses of the two varieties of Gurasada bentonite

Oxydes	Gurasada 1 (normal)	Gurasada 6 (abnormal)
SiO_2	72.42	67.26
Al_2O_3	11.97	13.31
TiO_2	0.00	0.18
Fe_2O_3	1.92	5.22
CaO	2.30	3.30
MgO	2.44	2.58
Na_2O	0.08	0.08
K_2O	0.16	0.42
H_2O	8.36	7.63
Total	99.66	99.98

The problem of „normal" and „abnormal" montmorillonites is rather complex, and only few informational data on the true nature of the difference between the two varieties are as yet available. In the case of the Gurasada bentonites this problem remains open until reliable analytical data will be accumulated.

It is not out of question that other analyses like electron microscopy, infra-red spectroscopy and even a *X*-ray detailed study should yield new data which will represent a substantial contribution to the explanation of the different thermal behaviour of both varieties of montmorillonite.

REFERENCES

Grim R. E., Kulbicki G. (1961) Montmorillonite: high temperature and classification. *Amer. Min.*, 46 p. 1329—1369, Washington.

Mackenzie R. C. (1970) Differential Thermal Analysis, vol. I, Academic Press, London.

Todor, D. N. (1972) Analiza termică a mineralelor. Edit. Tehnică, București.

CHARACTERIZATION OF MICA-LIKE MINERALS BY MEANS OF X-RAY DIFFRACTION [1]

BY

GHEORGHE GÂȚĂ [2]

Sommaire

Caractérisation des minéraux de type mica par la diffraction X. Les indices géométriques des diagrammes de rayons *X* mis en corrélation avec quelques propriétés cristallochimiques des minéraux micacés des sols de Roumanie suggèrent l'utilisation de la largeur du pic (001) mesurée à sa mi-hauteur en tant qu'indice de cristallinité (I_L), le rapport des intensités des réflexions (001) et (002) en tant qu'indice de complexité (I_C) et le rapport entre la hauteur du pic (001) et la hauteur obtenue pour la position de la réflection plus 0,5 Å (vers les petits angles) en tant qu'indice de transformation (I_T). Pour la même fraction argileuse ces trois indices varient en fonction du cation adsorbé. Pour leur calcul on recommande les diffractogrammes des échantillons saturés d'éthylène-glycole qui présentent des réflexions nettes et bien dégagées. Ces trois indices et la teneur en potassium de la maille des micas varient plutôt faiblement, aussi le terme d'illite pourrait-il être utilisé plus loin dans le sens proposé par Grim et al. (1937).

The term "illite" was proposed by Grim et al. in 1937 for the mica-like minerals from sediments and soils. They pointed out that "the term is not proposed as a specific mineral name, but as a general term for the clay mineral constituent of argillaceous sediments belonging to the mica group". Later, in 1966, Gaudette et al. showed that this term referred to the nonexpandable 10 Å mica-like minerals with a variable but substantially lower potassium content than the well-crystallized micas and also with a variable tetrahedral and octahedral cation population.

Several of the illites described in some papers are indeed mixed-layer minerals and this type of mica-like minerals are inserted in a continuous

[1] Paper presented at the 2nd National Clay Conference, April 11—12, 1975, Bucharest.

[2] Institutul pentru știința solului, Bd. Mărăști 61, București.

TABLE 1

Diffraction line positions and the geometrical indices for some illites in the Romanian soils (ethylene glycol-saturated clay fractions)

Sample	Horizon	Depth (cm)	Soil	Diffraction line (Å)	I_L	I_T	I_C
Corneşul Mare (Parîng)	*Ee*	6—10	podzol	9.82	11.0	1.24	1.90
Corneşul Mare (Parîng)	*Ee*	10—15	podzol	10.0	17.0	1.22	2.31
Piatra Arsă (Bucegi)	*Ee*	4—10	podzol	9.85	9.7	2.16	1.50
Vîrful cu Dor (Bucegi)	*AE*	0—10	cambisol	10.09	10.7	1.47	2.70
Rînca (Parîng)	*Bv*	120—130	cambisol	10.21	13.5	1.00	1.70
Păltiniş (Sibiu)	*Bv*	40—65	cambisol	10.15	7.6	2.67	3.05
Ardusat (Maramureş)	*Ea*	27—47	acrisol	10.13	12.8	1.72	3.37
Ardusat (Maramureş)	*Bt*	77—100	acrisol	10.03	15.3	1.11	2.27
Rogoz (Maramureş)	Bt_1	77—90	acrisol	10.13	15.8	1.11	2.56
Rogoz (Maramureş)	Bt_2	99—110	acrisol	9.96	13.4	1.65	3.73
Lăpuş (Maramureş)	Bt_1	68—90	acrisol	10.09	18.5	1.28	4.23
Lăpuş (Maramureş)	Bt_2	100—120	acrisol	9.93	11.5	1.64	3.23
Negreşti (Satu Mare)	*Bt*	120—140	acrisol	9.90	11.5	1.86	3.99
Morăreşti (Argeş)	*Bt*	110—120	planosol	10.01	16.8	1.40	2.10
Adîncata (Neamţ)	*Bt*	70—80	luvisol	10.01	9.2	2.87	2.42
Agapia (Neamţ)	*Bt*	120—140	luvisol	9.97	12.0	1.37	2.43
Dămieneşti (Bacău)	*C*	140—160	luvisol	10.02	15.5	1.41	2.09
Lespezi (Iaşi)	*C*	150—165	luvisol	10.17	9.0	1.92	2.30
Baia de Fier (Gorj)	*Bt*	10—20	luvisol	10.11	18.8	1.50	2.73
Bîrseşti (Gorj)	*Bt*	110—120	luvisol	10.13	11.5	1.58	3.43
Buziaş (Timiş)	*Bv*	73—96	luvisol	10.02	11.6	1.95	2.07
Podari (Dolj)	*Ap*	0—18	luvisol	10.11	11.2	1.71	4.63
Banu Mărăcine (Dolj)	*Ap*	10—20	luvisol	9.99	12.0	1.49	4.33
Trifeşti (Iaşi)	*C*	140—150	chernozem	10.17	9.5	1.52	4.49
Mihail Kogălniceanu (Constanţa)	*C*	59—70	chernozem	10.01	7.2	3.12	2.32
Hîrşova (Constanţa)	*D*	115—125	castanozem	9.95	8.0	2.14	2.32
Ostrov (Constanţa)	*D*	470—490	loess	10.07	12.0	1.38	4.33
Rasova (Constanţa)	*D*	320—340	loess	10.01	13.2	1.50	3.12
Baziaş (Caraş Severin)	*D*	330—345	loess	10.02	8.8	1.51	2.12
Feteşti (Ialomiţa)	*D*	400—415	loess	10.02	7.3	2.43	1.96
Sînpetru German (Timiş)	*D*	700—720	loess	10.18	12.0	1.61	3.99
Vinga (Timiş)	*D*	320—340	loess	9·86	9.3	2.11	1.88
Suceava (Suceava)	*Bt*	150—160	phaeozem	9.94	8.0	1.79	1.38
Horezu (Vîlcea)	*Am*	0—14	gleysol	9.94	12.9	1.53	2.56
Bistriţa (Năsăud)	*Bv*	95—105	gleysol	10.04	13.9	2.12	2.34
Gîrcina (Neamţ)	*C*	80—95	rendzina	10.01	10.4	2.92	2.50
Roşiori (Bacău)	*Bv*	59—69	rendzina	9.90	9.5	2.85	1.87
Ilia (Hunedoara)	*Ap*	0—23	fluvisol	9.91	15.8	1.77	3.12

series between mica-like minerals (mica-hydromica-illite) and expandable minerals. A lower potassium content of illite cannot be generally ascribed to mixed-layer minerals because the *X*-ray diffraction patterns of some illites do not show any mixed-layer.

The objective of this paper was to study by means of *X*-ray diffraction the mica-like minerals of colloidal fractions from soils and sediments for a comparison between the geometrical indices of *X*-ray patterns and the structural properties of these minerals (degree of crystallinity, mixed layering intensity, complexity of octahedral and tetrahedral sheets).

Materials and methods

Analysed soil samples consisted of clay fractions $< 1\ \mu$ separated from the horizons of some arable soils and nonarable mountainous soils so that most of the Romanian soil types are represented (Tab. 1). Besides, some micas and illites were selected for this study. Experimental data on illites published by G a u d e t t e et al. (1966) were also used to check the validity of the establised indices.

Micas used were ground in a vibrational mill Siebtechnik for a minute and the $< 2\ \mu$ fractions were separated by means of an Alpine 100 MZ apparatus, operating with a rotating zig-zag classifier and a high efficiency cyclone. The clay fractions from soils and the illites were separated from water suspensions by means of pipette method. For each mineral fraction duplicate oriented aggregates of K-saturated and Ca-saturated samples were preparated on glass slides. The Ca-saturated samples were saturated with ethylene glycol and scanned.

X-ray diffraction patterns were obtained by means of a URS-50 IM *X*-ray diffractometer, using Ni-filtered CuKα radiation. Scans were made at 1°θ per minute and the speed of the recording paper was 10 mm/minute.

The basal spacing position of mica-like minerals and three indices (Fig. 1) were determined on diffractograms : I_L — the width at the half-intensity of (001) line peaks (K u b l e r, 1968), I_C — the (001)/(002) intensity (peak height) ratio (W h i t e, 1962) and I_T — the ratio (001) peak intensity to the intensity at the position of basal spacing plus 0.5Å (sharpness ratio — W e a v e r, 1960).

Another index $I_1 = AH$ (Fig. 1) and the K_2O content of mica-like components by distributing the entire K_2O content of Ca-saturated clay fractions to the mica-like mineral content were also determined.

Results and discussions

The *X*-ray diffraction patterns of muscovites, biotites and illites show basal spacings around 10 Å and a significant variation of the three indices (Tab. 2, 3) although all the experimental conditions were kept constant. These differences are particular either to the effects of preparation method or to the crystallochemic nature of clay fraction minerals.

The preparation technique of oriented samples by evaporation at the room temperature of the clay suspension may present a low reproductibility due to a variable degree of the crystallite orientation and to the segregation during sedimentation (G i b b s, 1965). Due to these

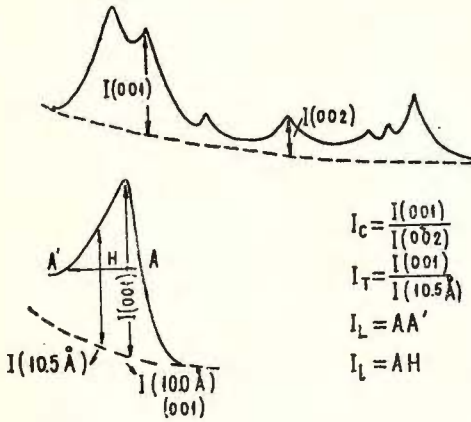

Fig. 1. — Measurements and calculation of geometrical indices of *X*-ray diffraction pattern.

TABLE 2

Variation of geometrical indices of X-ray diffraction patterns and some data on chemical composition of micaceous minerals

Mineral	peak position (Å)	AH	I_L	I_T	I_C	Chemical composition (%)			
						Al_2O_3	Fe_2O_3	MgO	K_2O
Voineasa muscovite	9.93	1.6	3.3	7.40	1.38	36.52	0.97	0.68	10.29
Voineasa muscovite	9.98	1.7	3.6	4.06	1.31	33.71	3.55	1.02	9.46
Buziaș biotite	10.01	1.6	3.2	3.54	2.84	14.63	24.67	8.82	9.11
Cibin biotite	9.98	1.5	3.0	3.62	3.25	12.98	22.86	9.64	8.92
Buresse illite (H a l m a col.)	9·95	2.9	5.6	3.17	2.21	22.33	9.76	3.89	6.12
Fithian illite (M i t c h e l col.)	9.97	3.4	6.8	1.57	2.70	21.38	10.56	1.62	5.98
Illinois illite (M o r t l a n d col.)	9.91	3.6	7.5	1.48	2.37	21.47	10.73	3.62	5.78
Grundite (B o l t col.)	9.99	3.9	10.7	1.22	3.76	26.07	8.87	2.59	6.11

effects, the values of indices may depend on the quantity of material on the slide or on the concentration of the micaceous minerals in the mixtures and the concomitant presence of minerals with the peaks partially superposed on the mica-like lines. For diminishing this kind of errors, determinations of the clay fraction $< 1\ \mu$ were used, in order to avoid

TABLE 3

Variation of geometrical indices of X-ray diffraction patterns of the illites, calculated after Gaudette, Eades and Grim data (1966)

Illite minerals	I_L	I_T	I_C	Chemical composition (%)			
				Al_2O_3	Fe_2O_3	MgO	K_2O
Beavers Bend	2.4	4.8	2.0	23.30	10.94	1.70	6.69
Marblehead	4.8	2.5	2.1	24.90	1.97	3.60	7.98
Rock Island	3.2	2.4	2.4	26.30	2.99	2.00	6.87
Fithian	7.2	1.7	3.1	21.12	11.32	1.50	5.90
,,Grundite"	11.2	1.3	4.0	28.05	8.16	2.33	6.48

TABLE 4

Variation of geometrical indices of Buresse illite with the quantity of sample on the slide

Quantity mg/cm²	I_L	I_T	I_C
0.41	5.0	3.29	2.37
0.60	5.2	3.20	2.39
1.40	5.5	3.17	2.24
1.85	5.7	3.17	2.21
1.85	5.6	3.17	2.22
2.01	5.6	3.14	2.18
3.06	5.8	3.15	2.17
4.52	6.3	3.02	2.03

TABLE 5

Geometrical indices of X-ray diffraction patterns of illite mixed with montmorillonite or kaolinite

Buresse Illite %	Valea Chioarului montmorillonite			Arghires kaolinite		
	I_L	I_T	I_C	I_L	I_T	I_C
100	5.6	3.17	2.21	5.6	3.17	2.21
90	5.7	3.12	2.22	5.7	3.17	2.19
75	5.8	3.19	2.09	5.8	3.14	2.20
50	5.8	3.14	2.14	5.8	3.18	2.06
25	5.6	3.15	2.08	5.8	3.18	2.10
10	5.8	3.19	2.07	5.9	3.15	2.11

as much as possible a variation due to the accentuated differences in the size of crystallites.

The *X*-ray indices of Buresse illite are changing rather sligthtly depending on the quantity of sample on the slide (Tab. 4). Indeed, for quantities between 0.4 and 4.5 mg/cm^2, the mean values were $I_L = 5.6 \pm 0.6$, $I_T = 3.17 \pm 0.14$ and $I_C = 2.21 \pm 0.04$. By using a quantity of sample between 1.5 and 3.0 mg/cm^2, these variations are only of 5.6 ± 0.15, 3.16 ± 0.02 and 2.20 ± 0.02, values which are precise enough for characterizing the mica-like minerals.

The influence of mineral segregation and of dilution effects on the values of the indices, as resulting from Table 5, were tested with two series of mixtures, illite-montmorillonite and illite-kaolinite. The segregation should have been more intense for the illite-montmorillonite mixtures because both the size of montmorillonite particles and their specific gravity are smaller than those of the illite. For illite and kaolinite the size of particles and the specific gravity are almost the same. However, the fluctuations of the I_T values are insignificant with a slight increase for illite-kaolinite mixtures when the illite content decreases. This result is probably due to the change in the degree of particle orientation for the flat crystals with almost the same size (Tab. 5). Moreover, for both series of mixtures the variation of I_T values appears in the limits of reproductibility. On the contrary, the I_C index shows an evident diminishing of the experimental values as a function of the illite content, this effect being more accentuated for the illite-montmorillonite mixtures.

In conclusion the values of the geometrical indices change slightly with the illite content, but still depend on the quality of sample on the slide. Therefore, under our working conditions the only use of the slide with 1.5—3 mg/cm^2 sample was established.

In the Table 2 the experimental data for AH values show a slight variation of the results for dioctahedral micas and illites, which have the means 1.6 ± 0.1 and 3.4 ± 0.5 respectively, pointing out the small asymmetry of the diffraction line of about 10 Å. This asymmetry is as well expressed by the I_T index which varies inverse proportionally with AH and also with the other two indices I_L and I_C when the structural potassium diminishes.

I_L index presents the same variation as the AH, but the values for micas and illites insert in the ranges 3-3.6 and 5.6-7.5 respectively. The comparison of these results (Tab. 2) and those calculated from diagrams (Tab. 3) by Gaudette et al. (1966) confirms our results, namely I_L becomes greater with the release of interlayer potassium, and may probably represent a numerical estimation of the atomic arrangement degree in the lattice i.e. of the crystallinity of illite. For example, in the case of grundite the values 10.7-11.2 show the presence of a relatively accentuated mixed layering which developed the asymmetry of the 10 Å peak. But a better estimation of the asymmetry appears more precisely expressed by the I_T index which is decreasing when the alteration of the micaceous minerals increases, and the degree of transformation

of the mica-like minerals becomes higher. The I_T index, which is decreasing when the slope of the peak in the lower θ angle side decreases, may be considered as a measure of the transformation processes of the micaceous minerals.

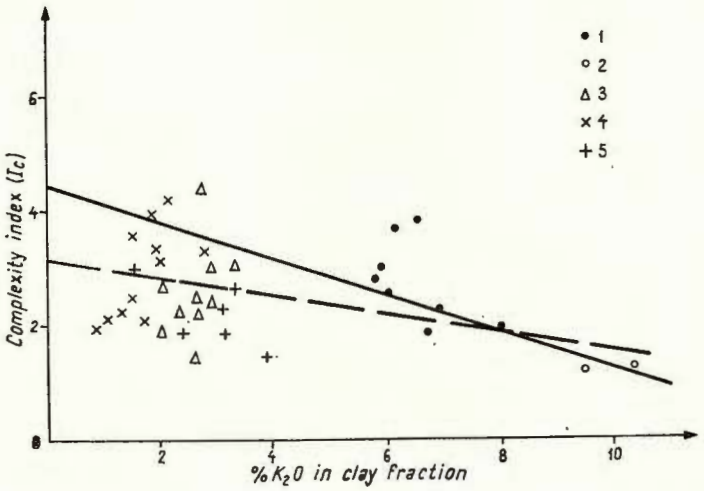

Fig. 2. — Relationship between complexity index I_C and per cent of K_2O in clay fractions from the Romanian soils and some micaceous minerals. 1, illite; 2, muscovite; 3, illite-expandable series; 4, illite-intergrade series; 5, mountainous clay fraction.

As it results from Tables 2 and 3 the I_C index changes its value with the ordering degree and structural complexity of the lattice of the mica-like minerals. For the dioctahedral micaceous minerals the presence of magnesium and iron in the octahedral layer and the release of potassium from the interlayer determine ever higher values for the I_C index. For these dioctahedral minerals, including those calculated after G a u d e t t e et al. (1966) all the points of a function I_C — K_2O content appear along a curve which may be considered, in the first approximation, as a straight line for the range 5.8-10.3% K_2O, except grundite. Below 5% K_2O, in the case of clay fractions from soils only a cloud of points appears which are generally grouped in areas depending on the type of soil (great soil group) or on the lithologic heritage (Fig. 2).

In the graph representing the relationship between I_C index and K_2O content in the lattice of mica-like minerals (Fig. 3) the points are not so scattered as in the diagram of the Figure 2. While for muscovites and illites the regression line is $y = 4.51 - 0.31x$ with $r = -0.84$, where $y = I_C$ and $x = \%\ K_2O$, for all the points from diagrams of the Figures 2 and 3 these mathematical relations are $y = 3.20 - 0.15x$ with $r = -0.39$ and $y = 3.83 - 0.22x$ with $r = -0.57$ respectively. Moreover,

the representative points in the graph 2 are grouped into two areas, namely a group for illites and muscovites and the other for illite-like minerals from clay fractions of soils.

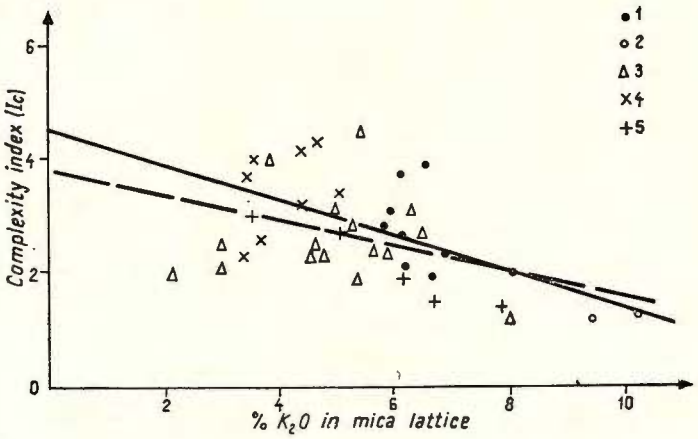

Fig. 3. — Complexity index I_C as a function of K_2O per cent in mica lattice of clay fractions from the Romanian soils and some micaceous minerals. 1, illite; 2, muscovite; 3, illite-expandable series; 4, illite-intergrade series; 5, mountainous clay fraction.

The statistical results point out a closer correlation between I_C and K_2O content in mica-like lattice and thus confirm the occurrence in Romanian soils of mica-like minerals with a relatively wide-ranged variation in the interlayer potassium, which also shifts the height value of (001) and (002) peaks of these micaceous minerals.

The experimental data concerning the geometrical indices of micas and illites suggest the use of I_L as crystallinity index, I_T as a transformation index and I_C as a complexity index. All these three indices change with the type of adsorbed cation in the clay fraction of the same sample. The peak position exceeds the mica and illite range 9.93-10.01 Å (Tab. 2); the experimental data for illites from soils are between 9.82 Å and 10.52 Å for all monoionic samples (Tab. 6), the values getting higher and higher when the content of mixed layer components increases. For instance, within the Cornești Mare soil the peak position is 10.52 Å due to the presence of 15% chlorite-like mineral and 85% of illite in a randomly mixed layer system.

Generally, for the same clay fraction, the I_L indices decrease with the cation succession potassium, calcium and ethylene glycol, and the peak of the ethylene glycol-saturated sample is the sharpest one (Tab. 6). With potassium and calcium-saturated clay fractions there are several cases when this index cannot be precisely determined since the peaks appear only as a shoulder of the chlorite-like, vermiculite or montmoril-

lonite peak. For a small I_L the illite crystallinity is high, and at high I_L values the mixed layer components are present.

The I_T index diminishes when I_L increases and its variations are included between 0.61 for the Corneşu Mare soil with integrade minerals and 3.12 for the Mihail Kogălniceanu soil with an illite and dioctahedral vermiculite as predominant minerals. Frequently there is an increase when the saturation cation changes from potassium to calcium and to ethylene glycol, but these variations are small enough.

TABLE 6

Geometrical indices of illite minerals in some Romanian soils

Soil	Cation	Diffraction line (Å)	Geometrical indices		
			I_L	I_T	I_C
Corneşul Mare	K	10.52	24.0?	0.61	4.79
	Ca	9.95	11.7?	1.34	2.10
	E.G.	9.82	11.0	1.24	1.90
Vîrful cu Dor	K	10.26	12.6?	1.27	2.47
	Ca	10.25	21.0?	1.20	3.04
	E.G.	10.09	10.7	1.47	2.70
Lăpuş	K	10.07	24.0?	1.03	3.67
	Ca	10.14	16.0	1.10	3.30
	E.G.	9.93	11.5	1.64	3.23
Suceava	K	10.02	16.0	1.24	4.56
	Ca	10.08	13.0	1.45	2.22
	E.G.	9.94	12.9	1.53	1.38
Baziaş	K	9.93	14.8	1.41	2.61
	Ca	10.03	12.8	1.81	3.42
	E.G.	10.01	13.2	1.50	3.12
Bistriţa	K	9.91	—	1.12	3.00
	Ca	10.01	24.0	1.16	1.99
	E.G.	10.04	13.9	2.12	2.34
Hîrşova	K	10.03	15.0	2.10	2.44
	Ca	10.08	10.3	1.09	2.31
	E.G.	9.95	8.0	2.14	2.32

I_C index also varies with the adsorbed cation, and usually its lowest value is for the ethylene glycol-saturated clay fractions.

Due to these variations the three indices should be determined only for an established cation. As the ethylene glycol-saturated clay fractions show the sharpest peak this type of samples is used for measuring I_L, I_T and I_C. In the Table 1 the position of the diffraction lines and the geometrical indices for some illites from Romanian soils are presented.

The (001) peak positions cover the interval 9.82-10.21 Å, the high values characterizing the occurrence of the mixed-layer systems.

I_L index varies between 7.2 for a horizon of a Mihail Kogălniceanu calcareous chernozem formed on loess and 18.8 for an horizon *B* of a Baia de Fier brown forest soil formed on the Sarmatian deposit.

The low values of illites with a high crystallinity occur for the soils developed on loess and certain detrital deposits, and the high values for the illites from some acid soils. The I_T indices of the studied clay fractions vary from 1.00 to 3.12 with values which are difficult to be related with the genetic type of soil (great soil group) or lithologic inheritance: 2.27-4.23 for the clay fractions from „lessivé" soils (alfisols) in the north-western part of Romania, around 2.0 for the soils developed on loess, 1.7-2.3 for the illite from the clay fractions in the soils developed on granite in the Parîng Mountains etc. However, its variations do not cover a too large interval; all the indices range between 4.49 for the Trifești chernozem and 1.38 for the Suceava phaeozem (Tab. 1).

Conclusions

Some geometric indices of the *X*-ray diffraction patterns such as: the peak position of (001) line of illite, I_L — the width at the half-intensity of (001) peak, I_T — the (001) peak intensity/intensity at a position of basal spacing plus 0.5 Å ratio, and I_C — the (001)/(002) intensity ratio vary as a function of crystallinity transformation degree, isomorphous substitutions in the illite lattice and the nature of adsorbed cations.

The experimental data of these geometrical indices connected to some crystallochemical properties of mica-like minerals suggest the use of I_L as a crystallinity index, I_T as a transformation index and I_C as a complexity index. As all these three indices change with the adsorbed cation for the same clay fraction, and the peak of etylene glycol-saturated sample is the sharpest one, the ethylene glycol-saturated specimens are recommended for determining the indices. A peak near 10 Å with the small I_L and I_C, and a I_T greater than 2.0 characterizes the illites with ligh crystallinity. On the contrary, an evidence of the occurrence of mixed layer components is a high peak position, a great value for I_L and a small value for I_T. The I_C index correlates with potassium content of illites and appears in connection with the lithologic inheritance.

For the Romanian soils the indices and the potassium content vary in a relatively small range: 7.2-18.8; 0.61-3.12; 1.30-4.49 and 3.40-6.94 for I_L, I_T, I_C and % K_2O content of mica-like minerals, respectively. For this reason, the term illite should be further used in the meaning proposed by Grim et al. (1937).

REFERENCES

Gaudette H. E., Eades J. L., Grim R. E. (1966) The nature of illite. *Clays and clay minerals, 13th Conf.* (1964), p. 33—48, *Pergamon Press*, New York.

Gibbs R. J. (1965) Error due to segregation in quantitative clay mineral *X*-ray diffraction mounting techniques, *Amer. Min.*, 50, p. 741—751, Washington.

Grim R. E., Bray R. H., Bradley W. F. (1937) Mica in argillaceous sediments. *Amer. Min.*, 22, p. 813—829, Washington.

Kubler B. (1968) Evaluation quantitative du métamorphisme par la cristallinité de l'illite. Etat des progrès réalisés ces dernières années. *Bull. Centre Rech. Pau, S.N.P.A.*, 2, p. 385—397, Pau.

Weaver C. E. (1960) Possible uses of clay minerals in search for oil. *Clays and clay minerals, 8th Conf.* (1959), p. 214—227, *Pergamon Press*, New York.

White J. L. (1962) *X*-ray diffraction studies on weathering of muscovite. *Soil Sci.*, 93, p. 16—21, Baltimore.

THERMAL SHIFTS OF BASAL SPACINGS OF SOME CLAY FRACTIONS FROM THE ROMANIAN SOILS[1]

BY

GHEORGHE GÂȚĂ, CONSTANTIN CRĂCIUN[2]

Sommaire

Variation au chauffage des réflexions de certaines fractions argileuses des sols de Roumanie. Le chauffage à 500°C des fractions argileuses saturées de K, séparées de certains sols, modifie la réflexion des minéraux expandables à environ 10 Å et des minéraux intergrades à 11—12 Å. Le traitement thermique à 300°C n'est pas rassurant, fort probablement à cause de l'utilisation d'une période de chauffage trop courte.

The mineralogical composition and the crystal structure of clay fractions in acid soils are related with the aluminium mobility in these soils (Jackson, 1964). Thus the variation of exchangeable cations and the relation to integrade minerals depend on the retention and release of hydroxy-aluminium and iron in the interlayers. Concerning the mobility of the interlayer material, many studies were carried out about both the hydroxy-aluminium-clay fraction equilibria and the changing of these systems during the thermal treatment (Carter et al., 1963; Weismiller et al., 1967; Conyers et al., 1969).

In the last years Martin Vivaldi et al. (1963) and Ho, Handy (1966) pointed out the variation of some properties at different temperatures only for montmorillonite.

The objectives of this paper were to investigate the thermal shifts of the basal spacings of the illite-integrade minerals from the Romanian soils in comparison with some soils of illite-expandable mineral series.

[1] Paper presented at the 2nd National Clay Conference, April 11—12, 1975, Bucharest.

[2] Institutul pentru știința solului, Bd. Mărăști 61, București.

Materials and methods

Several K-saturated fractions ($< 1\ \mu$) separated from bentonites and some Romanian soils have been examined. The soil samples belong both to illite-integrade minerals (Jackson, 1964; Gâță et al., 1968; De Coninck, Herbillon, 1969) and illite expandable minerals (see Table).

The oriented aggregates were prepared by sedimenting and drying on glass slides at room temperature. Each slide was heated for an hour successively at 105-200-300-400-500°C.

The *X*-ray diffraction patterns were obtained with a URS-50 IM equipment using Ni-filtered Cu Kα radiation generated at 35 kV and 6 mA.

Results and discussions

The thermal shifts of basal spacing of the clay fractions separated from the Valea Chioarului bentonite and the Săcălaz soil are presented in the Figure 1. With bentonite the heat treatment changes the diffraction line (001) from 11.8 to 11.3 Å when the temperature varies between 20°C and 300°C. After heating to 400°C and 500°C a greater shift occurs in the basal spacing position, and the *c*-axial dimension becomes 10.3 Å and 9.9 Å respectively.

With Săcălaz soil fractions the K-saturated sample presents three diffraction lines over 10 Å, namely at 13.68, 12.29 and 10.18 Å. By heating to 105°C these lines change their positions to 12.83, 10.99 and 10.22 Å. At 200°C only two lines remain at 12.43 and 10.05 Å, the first ascribed to expandable minerals and the second to illite. With increased treatment temperature the line of expandable minerals varies to 12.04 and 11.55 Å and the illite line to 10.11 Å and finally to 9.92 Å when the temperature reaches 300°C and 500°C respectively. The Ca-saturated and ethylene glycol-saturated samples show a doublet 14.42—11.50 Å and 17.08—12.62 Å (beside the 10 Å line), the predominant minerals being also expandable. In this clay fraction do also occur some mixed layer minerals which collapse at 500°C only to 11.55 Å.

From the illite-intergrade mineral series (Fig. 2) the Jepii Mari *D* horizon (41-50 cm) and the Rogoz *Ee* horizon (30—57 cm) were studied. The two clay fractions display small differences between calcium-saturated and ethylene glycol-saturated samples because the (001) lines remain at about 14 Å and 9.8—10 Å for intergrade and illite components.

During the heat treatment the Jepii Mari K-saturated fraction preserves unchanged its about 10 Å peak, but shifts its intergrade peak from 13.5 Å at room temperature to 13.8—13.1—13.3—12.6 and 12.06 Å at 100-200-300-400 and 500°C respectively.

For the Rogoz K-saturated fraction the content of intergrade minerals is greater as its 13.8 Å line has a higher intensity than the illite line, but its mixed layers have a smaller content of chlorite-like components because the 12.3 Å peak intensity at 500°C is small enough. Moreover

the change of peak positions at 100°C from 13.8 Å to 12.66 Å and the shift of intergrade peak intensity during the heat to 500°C should be pointed out.

The values for the basal spacing for the different samples are summarized in the Table. An indication for the distinction of the expandable minerals is also given by the *c*-axis values of the ethylene glycol-saturated

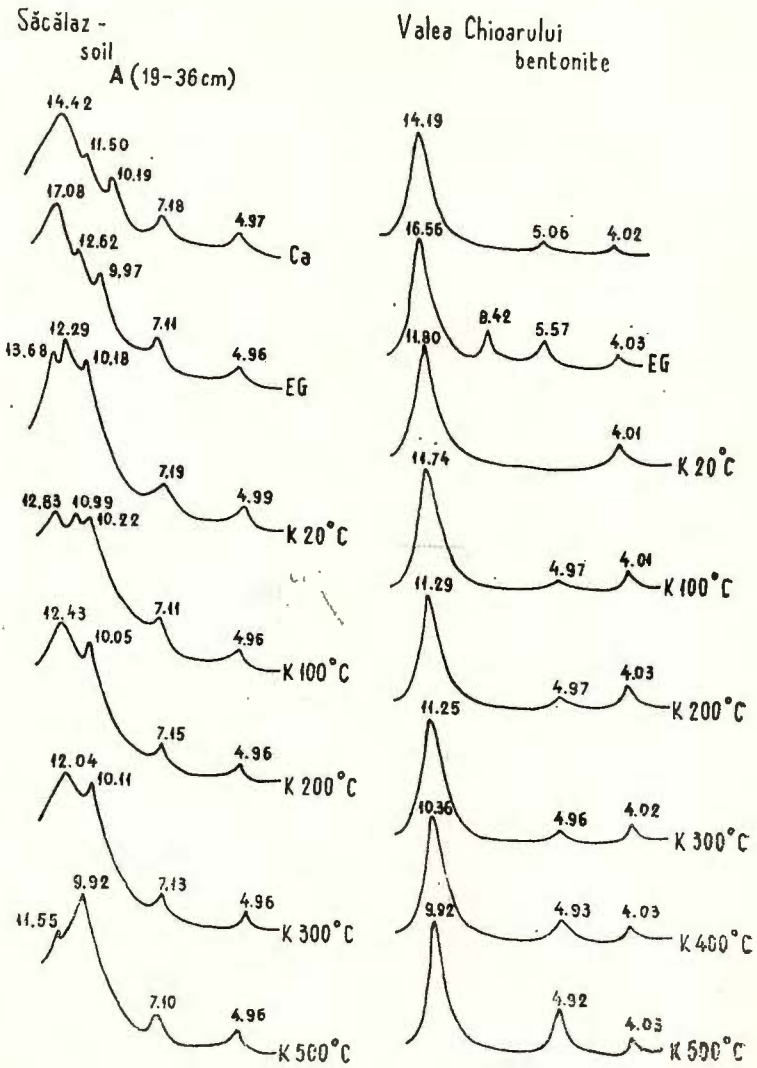

Fig. 1. — Thermal shifts of basal spacing of the K-saturated clay fractions separated from the Valea Chioarului bentonite and the *A* horizon of the Săcălaz chernozem.

samples. The bentonites with about 17 Å basal spacings for ethylene glycol-saturated samples collapse from 11-12 Å at room temperature to 10.3—11.3 Å at 300°C and 9.8—9.9 Å at 500°C respectively. Therefore the collapse gives a mica-like parameter at 300°C for the Gurasada bentonite and at 500°C for the Valea Chioarului bentonite.

All illite-expandable minerals from soils present a 10 Å peak at 500°C but at 300°C only the Călmăţui fraction shows this *c*-axis, while

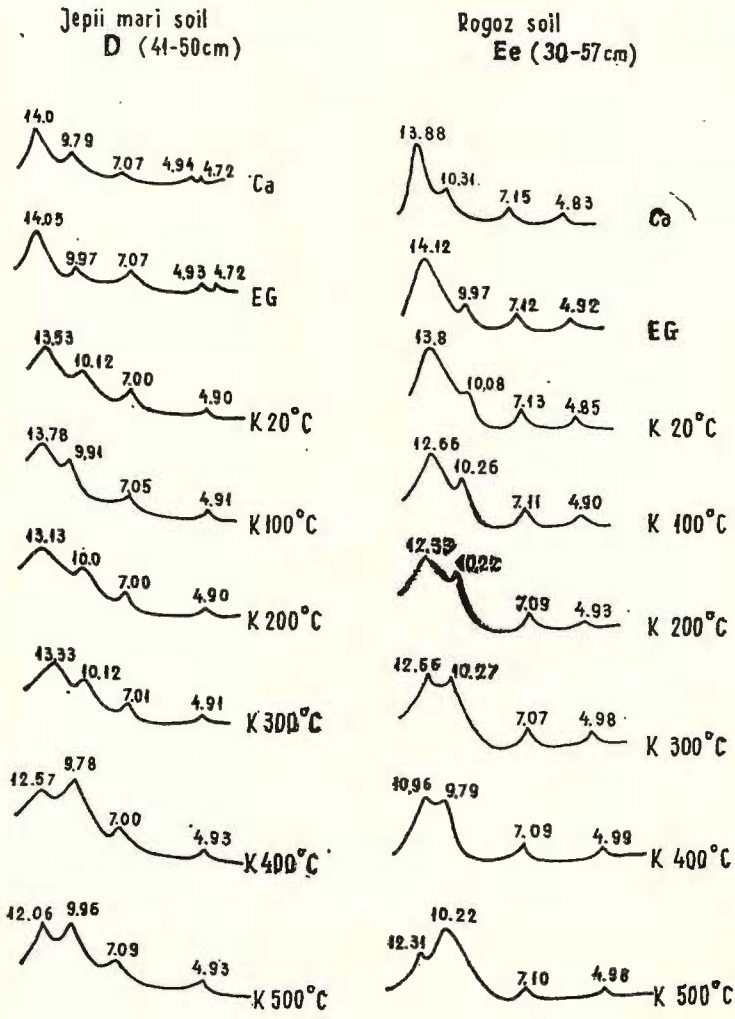

Fig. 2. — Variation of the *X*-ray diffraction patterns of the K-saturated clay fractions separated from the *D* horizon of the Jepii Mari podzol (41—50 cm) and the *Ee* horizon of the Rogoz acrisol (30—57 cm).

TABLE

Thermal shifts of basal spacings of some K-saturated clay fractions from Romanian soils

Sample	Soil	Horizon	Depth cm	Basal spacings (Å)			
				E.G.	20°C	300°C	500°C
BENTONITES							
Gurasada (Hunedoara)				17.0	11.1	10.3	9.8
Valea Chioarului (Baia Mare)				16.6	11.8	11.3	9.9
ILLITE-EXPANDABLE MINERALS							
Pielești (Dolj)	vertisol	*Bt*	50—60	17.8	14.4	13.1	10.9
Cornești (Timiș)	chernozem	*Bt*	77—115	17.3	12.7	12.2	10.1
Călmățui (Brăila)	halosol	*As*	0—2	15.7	12.8	9.9	9.8
ILLITE-INTERGRADE MINERALS							
Lăpuș (Maramureș)	acrisol	*A*	0—10	14.7	14.6	13.8	13.5
Păucinești (Hunedoara)	acrisol	*BD*	200—240	13.7	12.9	12.9	12.4
Agapia (Neamț)	luvisol	*Ap*	0—18	13.7	13.5	12.5	11.9
Adîncata (Neamț)	luvisol	*Ap*	0—20	13.9	13.8	13.9	11.1
Ostrov (Hunedoara)	luvisol	*D*	49—60	14.0	13.9	14.0	13.2
Preajba (Gorj)	acrisol	*Bt*	55—75	15.2	13.4	13.4	12.1
Sîncraiul Almașului (Alba)	acrisol	*Ee*	35—55	15.5	13.2	13.1	11.0
Ardusat (Maramureș)	acrisol	*Ee*	7—27	15.0	14.1	12.9	11.3

the Pielești and the Cornești fractions collapse to 13.1 Å and 12.2 Å respectively. As regards the 10.9 Å shoulder of the Pielești fraction at 500°C this should be given by some intergrade components which collapse to only about 11 Å.

The K-saturated fractions of the illite-intergrade series show their peaks in the range 13.7—15.0 Å. The Lăpuș clay fraction presents predominant chlorite components which have slight shifts during heat treatment; at the same time the Păucinești fraction collapses slightly with an increasing temperature (300°C to 500°C) from 12.9 to only 12.4 Å.

The other illite-intergrade minerals occur as subordinate components in the clay fractions of the heated samples and appear on the *X*-ray diffraction patterns over 300°C only as secondary peaks besides the 10 Å basal lines. Thus the Ostrov fraction contains chlorite components with no collapse during the heat treatments. The Agapia and Preajba fractions have their collapse at 500°C about 12 Å whereas the Adîncata, Sîncraiul Almașului and Ardusat fractions about 11 Å. In our working conditions, the heating test at 300°C appears to be unconvincing because many clay fractions with intergrade or expandable minerals present such a basal spacing about at 13 Å.

Conclusions

The illite-expandable minerals from some Romanian soils show only a basal spacing at about 10 Å after the heat treatment to 500°C.

After a heating to 500°C, the illite-intergrade minerals from some Romanian soils collapse to 11-12.4 Å or might display no collapse as a function of the nature of their intergrade components.

As regards the thermal treatment at 300°C it proved to be unsuitable, probably because of the short period of heating.

REFERENCES

Carter D. L., Harvard M. E., Young Y. L. (1963) Variation in exchangeable K and relation to intergrade layer silicate minerals. *Soil Sci. Soc. Amer. Proc.*, 27, p. 283—287, Madison-Wisconsin, U.S.A.

Conyers E. S., Wilding L. P., Mc. Lean E. O. (1969) Influence of chemical weathering on basal spacing of clay minerals. *Soil Sci. Soc. Amer. Proc.*, 33, p. 518—523, Madison-Wisconsin, U.S.A.

De Coninck F., Herbillon A. (1969) Evolution minéralogique et chimique des fractions argileuses dans des alfisols et des spodosols de la Campine (Belgique). *Pédologie* 19, p. 159—272, Paris.

Gâţă G., Gâţă Elena, Dincu I., Schramek C., Constantinescu C. (1968) Contribuţii la cercetarea unei serii de minerale argiloase din substratul mineralogic al unor soluri din sudul României. *An. I.C.I.F.P. — Pedol.* 35, p. 139—151, Bucureşti.

Ho Clara, Handy R. L. (1966) Modification of Ca-montmorillonite by low temperature heat treatment. *Proc. 13th Nat. Conf. Clays and Clay Minerals*, p. 353—365, *Pergamon Press*, Oxford.

Jackson M. L. (1964) Chemical composition of soils. Chemistry of the soil. Ed. Bear Reinold Publ., p. 71—141, New-York.

Martin-Vivaldi J. L., Mac Ewan D. M. C., Gallego M. R. (1963) Effects of thermal treatment on the c-axial dimension of montmorillonite as a function of the exchange cation. *Proc. Internat. Clay Conf. Stockholm, Pergamon Press*, p. 45—51, London.

Weismiller R. A., Ahlrichs J. L., White J. L. (1967) Infrared studies of hydroxy-aluminium interlayer material. *Soil Sci. Soc. Amer. Proc.* 31, p. 459—463, Madison-Wisconsin, U.S.A.

ON THE DEHYDROXYLATION REACTION OF CLAY FRACTIONS FROM SOME ROMANIAN SOILS [1]

BY
GHEORGHE GÂȚĂ, CONSTANTIN CRĂCIUN[2]

Sommaire

Sur la réaction de dehydroxylation des fractions argileuses de quelques sols de Roumanie. Le comportement thermique le long des processus de dehydroxylation est déterminé par la structure cristalline et la composition minéralogique des fractions argileuses. Généralement les minéraux de la série illite-intergrade présentent l'effet endothermique à des températures moins élevées, une chaleur de réaction plus élevée et une perte en poids plus grande par rapport à la série illite-minéraux expandables. La teneur en potassium n'influence que faiblement ces propriétés thermiques.

A great number of thermogravimetrical and differential thermal curves of clay fractions from the Romanian soils are almost identical although their mineralogical composition displays a wide-ranged variation. Thus the shape and the intensity of the endothermic peak at high temperature of both illite-intergrade mineral and illite-expandable mineral series vary to a small extent (Gâță, Gâță Elena, 1962; Todor, 1972). Generally the thermal reaction shows a dehydroxylation heat which fluctuates relatively little around a mean apparently the same for a large number of samples. This uniformity suggests the necessity to determine the dehydroxylation heat of the clay fraction from the Romanian soils and to study the relationship between these reaction heats, the temperature peaks and the crystallochemical structure of these fractions.

Materials and methods

The clay fractions ($< 1\ \mu$) were isolated from the majority of Romanian soils: podzols, cambisols, acrisols, luvisols, planosol, chernozems, castanozem, phaeozems, gleysols and vertisols. The mineralogical composition of these fractions were estimated by means of *X*-ray diffraction

[1] Paper presented at the 2nd National Clay Conference, April 11—12, 1975, Bucharest.

[2] Institutul pentru știința solului, Bd. Mărăști 61, București.

patterns (G â ţ ă, 1973) [3]. As shown in the Fig. 3, the analysed samples belong to the two alteration series, illite-intergrade and illite-expandable minerals (J a c k s o n, 1964).

TABLE

Brief description of the analysed samples

Sample	Horizon	Depth cm	Soil
Dengher (Parîng Mountains)	*CD*	50—60	podzol
Cornesul Mare (Parîng Mountains)	A_2	6—10	podzol
Piatra Arsă (Bucegi)	A_2	4—10	podzol
Bolboci (Bucegi)	D_s	60—80	podzol
Rînca (Parîng Mountains)		120—130	cambisol
Păltiniş (Sibiu)	*BD*	88—104	cambisol
Păltiniş (Sibiu)	B_1	40—65	cambisol
Lăpuş (Maramureş)	B_1	68—101	acrisol
Lăpuş (Maramureş)	B_2	101—121	acrisol
Rogoz (Maramureş)	B_2	77—91	acrisol
Rogoz (Maramureş)	B_2	91—111	acrisol
Ardusat (Maramureş)	A_2g	27—47	acrisol
Ardusat (Maramureş)	*Bg*	77—100	acrisol
Negreşti (Satu Mare)	*Bg*	120—140	acrisol
Adîncata (Neamţ)	B_2	70—90	luvisol
Agapia (Neamţ)	B_2	120—150	luvisol
Dămieneşti (Bacău)	*C*	140—160	luvisol
Călugăreni (Bacău)	*B*	47—57	luvisol
Suceava	B_2	150—160	phaeozem
Lespezi (Iaşi)	C_1	153—163	luvisol
Trifeşti (Iaşi)	C_2	140—160	chernozem
Gîrcina (Neamţ)	C_1	80—95	gleysol
Morărăşti (Argeş)	*Bg*	108—120	planosol
Filfani (Argeş)	C_2	175—185	vertisol
Melineşti (Dolj)	*AB*	30—40	vertisol
Baia de Fier (Dolj)	B_4g	110—120	luvisol
Horezu (Gorj)	*AC*	48—58	gleysol
Bistriţa Năsăud	*An*	35—45	gleysol
Buziaş (Timiş)	B_1	51—71	luvisol
Valcani (Timiş)	*G*	140—170	vertisol
Vinga (Timiş)	N_2		loess
Sînpetru German (Timiş)	*D*	700	loess
Baziaş (Timiş)	*D*	300	loess
Feteşti (Ialomiţa)	*D*	400	loess
Hîrşova (Constanţa)	*D*	115—125	castanozem
M. Kogălniceanu (Constanţa)	*C*	59—70	chernozem
Ostrov (Constanţa)	*D*	470—490	loess

[3] Thesis of Doctor's Degree, Arch. of the Polytechnical Institute, Bucharest.

The thermal analyses were recorded with a derivatograph M.O.M. (Hungary) using as sensibility scales 1/10, 1/10 and 500 for differential thermal analysis, differential thermogravimetry and thermogravimetry respectively. For all analyses the heating rate of 10° per minute was used. Ceramic crucibles and the same volumetric quantities of samples have been always used for analyses. Thus the variations of the sample

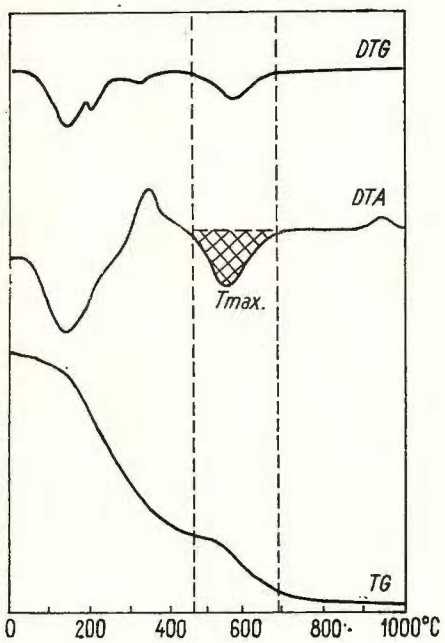

Fig. 1 — The derivatogram for a clay fraction from a soil sample and the measurement of dehydroxylation heat on DTA. curve.

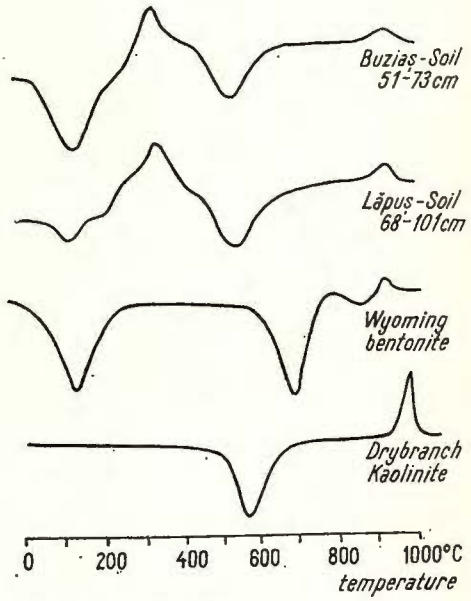

Fig. 2. — DTA. curves for two standard clay minerals and the clay fractions from some Romanian soils.

weight were inserted into the range 0.94-1.29 g; the weight of reference samples, Al_2O_3 calcined, was the same for all analyses, namely 1.04 g.

The heat of reaction of each sample was estimated from the peak area on the DTA curve (Fig. 1) by means of a calibration diagram plotted with $CaCO_3$-Al_2O_3 mixtures (Bruijn, van der Marel, 1954; Gâţă, 1964; Mackenzie, 1970). Moreover, some thermal analyses for clay fractions and two for standard clays, Wyoming bentonite and Drybranch kaolinite are presented in the Figure 2.

Results and discussions

Brindley (1963), Brindley et al. (1967 a, 1967 b), Rouxhet et al. (1969) and Rouxhet (1970) studied the kinetics and mechanism of dehydroxylation processes of some micas and clay minerals as a function of temperature and vapour pressure.

In the paper presented here the dehydroxylation reaction of the clay fractions from soils is recorded on the DTA curve as an endothermic peak ranging from 535°C to 590°C. This peak is sharp enough excepting the one from some clay fractions of the podzols formed on granite-gneiss rocks (Corneşul Mare, Dengherul). It is very difficult to establish the base line for these analyses due either to the organic material content still present in samples or to the relatively high content of free sesquioxydes, especially aluminium hydroxides.

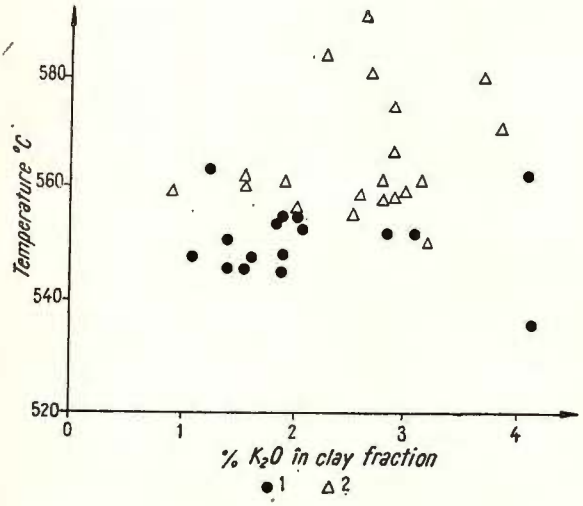

Fig. 3. — Peak temperature of the dehydroxylation reaction as a function of potassium content. 1, illite-intergrade minerals; 2, illite-expandable mineral series.

The dependence of peak temperature on the potassium content in the clay fractions of the Romanian soils (Fig. 3) does generally show two groups of points: an area over 554°C for illite-expandable mineral series, and the other one under this temperature for the illite-intergrade minerals. There are some points which have not their suitable places, namely Suceava (554°C) and Baziaş (550°C) with expandable clay fractions in the low range temperature (535—554°C) and Ardusat (563°C) and Gîrcina (562°C) with intergrade mineral fraction at the high range temperature (554 — 590C°). These exceptions may be justified by the mineralogical composition of the fractions; the Baziaş fraction contains besides expandable minerals a relatively small quantity of chlorite-like components, the intergrade minerals of the Ardusat fraction have their interlayer spacing to 15.59 Å, and the Gîrcina fraction has a high content of illite (64.2%) which increases the dehydroxylation temperature since under our working conditions the Buresse and Fithian illite show their temperature peaks at 580°C, respectively 560°C. Then the high dispersion of the points shows a slight correlation between the peak temperature and the potassium content of the clay fractions, the former being affected by the kaolinite content, size and crystallinity of the particles as well as other factors.

The dehydroxylation temperature and also the heat of reaction of the studied clay fractions appear to be different in the two series. The illite-intergrade minerals with peak temperature below 554°C generally have a heat reaction higher than the illite-expandable minerals, excepting the clay fractions from some mountain soils with an illite-chlorite interstratification, which occasionally has only a single large diffraction basal spacing to 11.2—12.4 Å for ethylene glycol-saturated fractions.

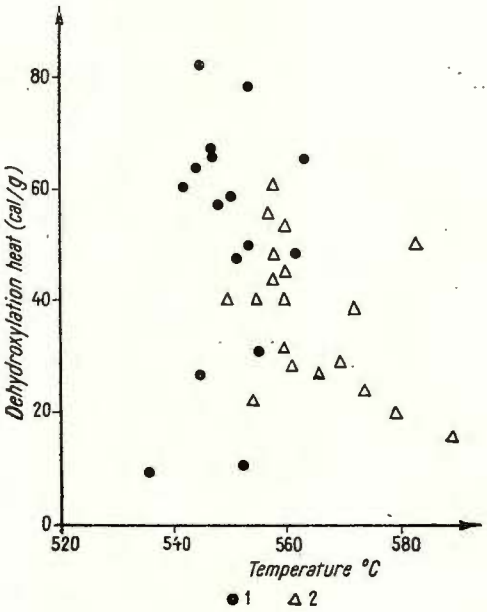

Fig. 4. — The variation of reaction heat with peak temperature for the dehydroxylation processes of clay fractions from some Romanian soils.
1, illite-intergrade minerals; 2, illite-expandable mineral series.

The heat of reaction as a function of peak temperature (Fig. 4) shows the same large dispersion of the points with the same exceptions as in the Figure 3. In the diagram there may be distinguished three areas: the first for illite-expandable minerals over 554°C with reaction heats between 16 and 56 cal/g, the second for illite-intergrade minerals below 554°C with the reaction heat in the range of 48—82.5 cal/g, and the third also below 554°C for some mountain mixed layer minerals with reaction heats between 9 and 31 cal/g.

The variation of loss of weight with peak temperature (Fig. 5) shows a rather close correlation with two groups of points: one for illite-expandable minerals and the other one for illite-intergrade minerals. The same exceptions are noticed for Baziaș, Gîrcina and Ardusat fractions, and in addition two isolated localities for the mountain mixed-layer fractions namely Dengherul and Cornești Mare soils. The representative points are included between two straight lines with the equations: $p_1 = 1.32t_1 - 760$ and $p_2 = 1.55\,t_2 - 900$ where p_1 and t_1 are the loss of weight in mg/g, and the reaction temperature in °C, respectively.

When the reaction heat is expressed in terms of its loss of weight there occurs again a large dispersion of points distributed in two regions, namely one for illite-expandable minerals with lower dehydroxylation

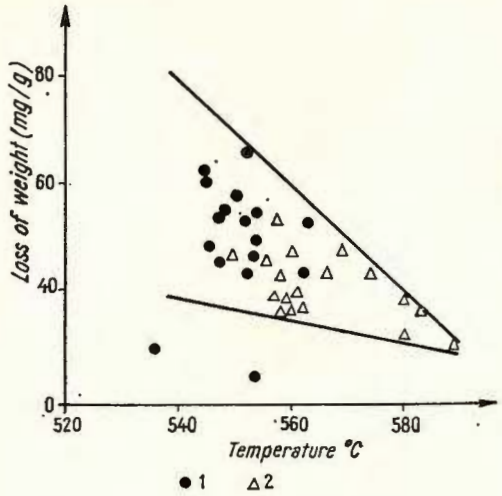

Fig. 5. — The relationship between the loss of weight and peak temperature of clay fractions from some Romanian soils.
1, illite-intergrade minerals; 2, illite-expandable mineral series.

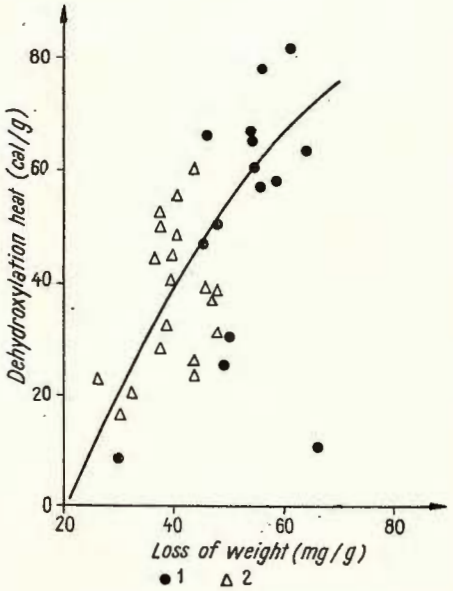

Fig. 6. — Reaction heat vs. loss of weight curve for clay fractions from some Romanian soils.
1, illite-intergrade minerals; 2, illite-expandable mineral series.

heats (< 60 cal/g) and loss of weight (< 47 mg/g), and the other one for illite-intergrade minerals with higher heats and losses in the dehydroxylation reactions (Fig. 6).

There are some points which are plotted in the limit region between the two clouds of points as the Păltiniş, Sînpetru German, Lăpuş, Ardusat fractions in the intergrade area and the Vinga, Baziaş, Baia de Fier, Filfani clay fractions in the illite-expandable mineral area. Moreover, there are points with a changed place as Dengherul and Gîrcina fractions in the illite-expandable mineral area, and on the contrary, the Buziaş

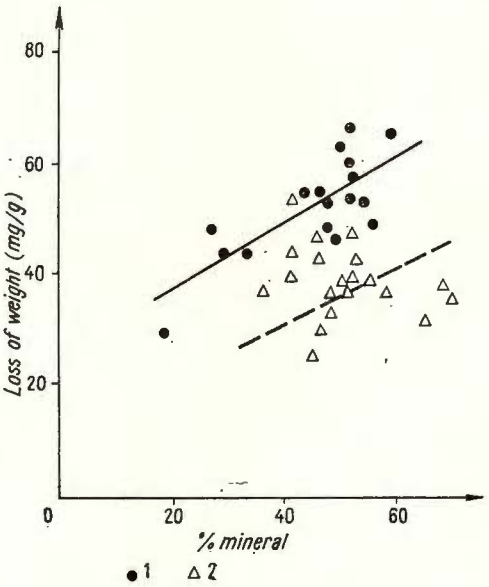

Fig. 7. — The relationships between the loss of weight and expandable mineral or chlorite-like component for clay fractions from some Romanian soils.
1, illite-intergrade minerals: 2, illite-expandable mineral series.

fraction in the illite-intergrade mineral area. The relationship between the heat of reaction and the loss of weight may be given by the statistical curve of the conics type (parabola or hyperbola), and approximately by a straight line.

The relatively slight correlation of the reaction heat or loss of weight versus the structural potassium suggests a relationship between these values and the content of expandable or chlorite-like components. Such a diagram also shows two groups of points (Fig. 7). For example, the dependence of the loss of weight on the expandable mineral or chlorite-like components is presented in two fields of representative points which may be statistically grouped between two straight lines. Indeed the intergrade minerals generally have a loss of weight higher than the illite-expandable minerals with a few exceptions when the points are in the same intermediate region such as for instance the Baziaş, Lăpuş and Păltiniş fractions.

Conclusions

The crystal structure and the mineralogical composition determine the thermal behaviour of clay fractions separated from Romanian soils. Thus the dehydroxylation temperature, the reaction heat and the loss of weight vary within the intervals of 535—590°C, 9—82.5 cal/g and 30—66 mg/g respectively.

Generally with a few exceptions due to the high illite content, the illite intergrade minerals show a lower peak temperature (544—554°C), a higher reaction heat (48—82.5 cal/g) and a greater loss of weight (47—66 mg/g). On the contrary the illite-expandable mineral series presents a higher peak temperature (554—590°C), a lower reaction heat (16—56 cal/g) and a lower loss of weight (26—48 mg/g). Frequently some intermediate values appear in the case of the chlorite-illite mixed layer minerals characterized by a single large diffusion line of ethylene glycol saturation (Dengherul, Corneşul Mare, Păltiniş).

The potassium content determines rather slightly these thermal properties.

REFERENCES

Brindley G. W. (1963) Role of crystal structure in solid state reactions of clays and related minerals. *Proc. Internat. Clay Conf., Stockholm*, p. 37—44, *Pergamon Press*, London.

— Achar B. N. N., Sharp J. H. (1967 a) Kinetics ans mechanism of dehydroxylation processes: II Temperature and vapor pressure dependence of dehydroxylation of serpentine. *Amer. Min.*, 52, p. 1697—1705, Washington.

— Sharp J. H., Patterson J. H., Achar B. N. N. (1967 b) Kinetics and mechanism of dehydroxylation processes: I Temperature and vapor pressure dependence of Kaolinite. *Amer. Min.*, 52, p. 201—211, Washington.

Bruijn C. M. A., van der Marel W. H. (1954) Mineralogical analyses of soil clays. *Geol. en Mijnbouw*, 16, p. 69—83, 's-Gravenhage.

Gâță G. (1964) Factorii care condiționează rezultatele cantitative în analiza termică diferențială. *Știința Solului*, 2, p. 58—66, București.

— Gâță Elena (1962) Studiul argilei din unele soluri formate pe loess. *An. I.C.C.A. — Pedologie*, 30, București.

Jackson M. L. (1964) Chemical composition of soils. Chemistry of the soil. Ed. Bear. Reinold Publ., New York.

Mackenzie R. C. (1970) Differential thermal analysis. Academic Press, London.

Rouxhet P. G. (1907) Kinetics of dehydroxylation and OH—OD exchange in macrocrystalline micas. *Amer. Min.*, 55, p. 841—853, Washington.

— Touillaux R., Mestdagh M., Fripiat J. J. (1969) New consideration about the dehydroxylation processes of minerals. *Proc. Internat. Clay Conf. Tokio — Japan*, 1, p. 109—119, *Israel Univ. Press.*, Jerusalim.

Todor D. N. (1972) Analiza termică a mineralelor. Edit. Tehnică, București.

QUANTITATIVE DETERMINATION OF KAOLINITE IN ILLITE-BEARING CLAYS BY DIFFERENTIAL THERMAL ANALYSIS [1]

BY

RADU LĂCĂTUȘU[2]

Sommaire

Détermination quantitative de la kaolinite des argiles à illite à l'aide de l'analyse thermodifférentielle. L'étude présente une méthode pour déterminer la quantité de kaolinite à partir du mesurage des surfaces des effets endothermiques des courbes thermodifférentielles. Les résultats sont comparables aux données obtenues par diffraction *X*, les erreurs relatives étant comprises entre 8 et 12%

The quantitative determination of clay minerals does still present essential difficulties related to many factors due to experimental conditions and the crystallochemical structure of these minerals. In addition these minerals are most frequently occurring as a mixture of minerals, and in these cases appear analytical interferences.

The differential thermal analyses permit to achieve readily the quantitative determinations of the clay minerals when their thermal peaks are not superposed. Thus by measurement of one parameter of a thermal characteristic effect (intensity, area or cosec. of angle determined by the sides of the thermal peak) and comparison with the calibration curve, satisfactory results may be obtained. (Mackenzie, 1957; Barshad, 1965; Gâță, 1964, 1972 [3]).

When mixed minerals occur, the thermal effects are superposed, and their quantitative determination and particularly an accurate qualitative determination are difficult to be carried out. In this case even a quantitative determination is possible only if a mineral shows a certain characteristic effect. This paper presents such a case referring to the kaolinite determination.

[1] Paper presented at the 2nd National Clay Conference, April 11—12, 1975, Bucharest.

[2] Institutul pentru știința solului, Bd. Mărăști 61, București.

[3] Thesis of Doctor's Degree, Arch. of the Polytechnical Institute, Bucharest.

Material and methods

As material for study there have been used the fraction $< 1\ \mu$ of Aptian clay from South Dobrogea, Aghireș kaolinite (fraction $< 1\ \mu$) like standard material and the $< 1\ \mu$ clay fraction separated from the *D* horizon of the Turda soil (leached chernozem) as dilution material for testing the recovery degree of kaolinite.

The thermal analyses were performed with a "Linseis" apparatus with Pt—Pt Rh thermocouples. The heating rate of 20°C/minute has been used.

The *X*-ray data were obtained by means of the URS-50 IM diffractometer. The sample for *X*-ray study was saturated in potassium, calcium and etylene glycol.

Results

Under our working conditions the differential thermal curve of kaolinite shows an endothermic effect at about 580°C due to the release of OH-groups from the lattice, and an exothermic effect at about 950°C due to the structural change (formation of $\gamma\ Al_2O_3$ or even of mullite). The differential thermal curve of illite presents an endothermic peak at about 130°C owing to the loss of sorbed moisture, an endothermic peak at about 560°C owing to the dehydroxylation effect, and an endothermic-exothermic S-shaped system due to the structural change (destruction of the lattice of illite and the formation of spinel — Mackenzie, 1957; Grim, 1953; Todor, 1972).

A differential thermal curve for a mixture of these two minerals (kaolinite and illite) shows an endothermic effect at about 140°C due to the loss of sorbed moisture, characteristic of 2 : 1 minerals, a second endothermic effect at about 570°C due to the loss of OH groups both from the kaolinite and illite lattice and a third exothermic effect at about 950°C characteristic only of kaolinite.

Intensity and area of the exothermic effect are proportional to the quantity of kaolinite. When the quantities of kaolinite are small this effect is not distinct.

The experimental data on thermal differential analysis prove that when the heating rate is faster, the thermal effect becomes much more obvious (Grim, 1953; Mackenzie, 1967; Gâță, 1964; Todor, 1972). By using a heating rate of 20°C/minute we have obtained — when dealing with clay samples whose mineralogical composition is chiefly formed of kaolinite and illite — more distinct exothermic effects which permitted to achieve more precise measurements, especially when the kaolinite contents amount to at least 10%.

In order to obtain the standard curve, the fraction $< 1\ \mu$ of Aghireș kaolinite was used in dilution with calcinated Al_2O_3 as inert material. The same heating rate (20°C/minute) has been used for standard sample.

G â ţ ă pointed out (1964) that the area of the exothermal peak is the most suitable parameter for quantitative determinations. Hence the same parameter was also used by us.

Table 1 shows data of the standard kaolinite curve as a function of the area of exothermic effect at about 950°C. The measured value

TABLE 1

Standard curve of kaolinite as a function of exothermic peak area at 950°C

Kaolinite %	The area of exothermic peak at 950°C mm²	
	measured	calculated
10	0.0	−6.47
20	6.7±3.01	2.63
30	11.0±2.80	11.76
40	18.3±2.19	20.98
50	27.3±2.00	30.00
60	38.0±1.80	39.13
70	50.2±1.61	48.25
80	58.4±1.14	58.38
90	65.0±1.41	66.50
100	77.3±1.34	77.53
S = − 15.6167 + 0.9125 % kaolinite r = 0.9958		

represents the average of three repetitions. The mean square error of measurement is greater in the case of higher concentrations of kaolinite.

The graphic relation between measured and calculated data of the areas of thermal effects in the kaolinite interval ranging from 30 to 100% is a straight line with an equation of the $a + bx$ type (Tab. 1).

The correlation coefficient obtained from calculation of this straight line is very high (0.9958). Practically in the kaolinite concentration interval varying between 20—100% this straight line may be used for the quantitative determination.

By application of this method for the quantitative determination of kaolinite from Aptian clays in South Dobrogea, satisfactory results were obtained. Some of these results are presented in Table 2. They may be compared with the ones yielded by the *X*-ray diffraction according to the method described by G â ţ ă (1972) [4]. Generally the values obtained by the *X*-ray diffraction are lower. However, the two series of values

[4] Op. cit. pt. 3.

TABLE 2

Comparative results concerning kaolinite determination by DTA and X-ray diffraction (%)

No.	Samples	kaolinite DTA	kaolinite *X*-ray
15	Speranța quarry — white clay	68.8	62.1
20	Speranța quarry — pink clay	47.0	40.8
27	Țugui quarry — white clay	49.0	40.3
36	Țugui quarry — yellow clay	38.3	31.4
39	Jugănaru quarry — pink clay	43.2	45.0
68	Haralambie Valley — white clay	36.7	32.5
69	Haralambie Valley — white clay	63.5	55.0
102	Gherghina quarry — yellow clay	54.4	47.3
104	Gherghina quarry — yellow clay	48.2	45.2
108	Gherghina quarry — black clay	28.1	25.0
121	Mircea Vodă—Satu Nou zone — white clay	30.0	31.9
123	Mircea Vodă—Satu Nou zone — yellow clay	42.2	39.9

kaolinite (DTA) = 0.6654 + 1.1224 % kaolinite (*X*-ray)
r = 0.9613

TABLE 3

Recovery of added kaolinite

added kaolinite %	recovered kaolinite %	differences
90	88.3	−1.7
80	79.2	−0.8
75	73.6	−1.4
60	63.6	+3.6
50	54.3	+4.3
40	45.7	+5.7
25	31.0	+6.0
20	29.9	+.99

are graphically located along a straight line with a high correlation coefficient, namely r = 0.9613 (Tab. 2).

The recovery degree of kaolinite added in a clay fraction ($< 1\ \mu$) separated from the *D* horizon of the Turda leached chernozem comprising illite and dioctehedral vermiculite as predominant minerals is rendered

in the Table 3. One may observe that as the quantity of added kaolinite increases its recovery degree marks an increase.

The relative error of this method is included between 8 and 12%.

REFERENCES

Barshad I. (1965) Thermal Analysis Techniques for Mineral Identification and Mineralogical Composition. In Methods of Soil Analysis, Part. 1, Madison, U.S.A.

Gâţă G. (1964) Factorii care condiţionează rezultatele cantitative în analiza termică diferenţială. *Ştiinţa solului*, 2, p. 58—66, Bucureşti.

Grim R. E. (1953) Clay Mineralogy. Mc. Graw Hill, New York.

Mackenzie R. C. (1957) The differential Thermal Investigation of Clays. Mineralog. Soc. (Clay Minerals Group), London.

Todor D. (1972) Analiza termică a mineralelor. Edit. Tehnică, Bucureşti.

ESSAIS MÉTHODIQUES DES MINÉRAUX ARGILEUX ÉTALON DE ROUMANIE [1]

PAR

LUCIAN MATEI, ADELA POJAR[2]

Abstract

Methodical Tests Relating to Standard Clay Minerals of Romania. The Aghireş kaolinite and the Valea Chioarului montmorillonite have been selected as standard clay minerals of Romania. In this respect it is necessary to characterize the composition and the physical-mechanical properties of both minerals as it represents the first purpose of the paper. The second one consists in tracing the dependence relationships between the physical-mechanical parameters of clay minerals and their lattice structure.

En choisissant la kaolinite d'Aghireş et la montmorillonite de Valea Chioarului comme minéraux argileux étalon pour la Roumanie, leur caractérisation est indispensable. Aussi nous proposons-nous dans cette étude de déterminer quelques caractères des minéraux argileux étalons stricto sensu et de préciser le comportement physico-mécanique des étalons et de quelques mélanges dosés, afin de mettre en évidence le degré de dépendance des propriétés physico-mécaniques de la structure réticulaire des minéraux argileux.

Tous les essais, y compris ceux physico-mécaniques, ont été effectués sur des échantillons dont le minéral argileux analysé a été enrichi par la méthode de la séparation de la fraction $< 2\ \mu$ aux cylindres de sédimentation.

L'utilisation des minéraux argileux purs a éliminé les erreurs introduites dans les analyses physico-mécaniques par la présence des liants (oxydes et hydroxydes de fer, matières organiques et carbonates) autant que par la dilution par des minéraux clastiques.

[1] Communiqué à la deuxième Conférence Nationale des Argiles, 11—12 Avril, 1975, Bucarest.

[2] Institutul de cercetări şi proiectări pentru economia apelor, Splaiul Independenţei 294, Bucureşti.

L'interprétation générale des résultats doit tenir compte du fait que le degré de cristallinité des minéraux, leur surface spécifique, les déformations du réseau, la nature des cations échangeables et les teneurs en minéraux argileux influencent sensiblement les propriétés physico-mécaniques.

Les résultats des analyses chimiques globales des fractions $< 2\ \mu$ sont consignés dans le tableau 1.

TABLEAU 1

Analyses chimiques pondérales des minéraux étalons (fraction $< 2\ \mu$)

Oxydes	Kaolinite d'Aghireș	Montmorillonite de Valea Chioarului
SiO_2	51,81	69.97
Al_2O_3	32,94	19,17
Fe_2O_3	0,82	1,27
CaO	1,21	0,90
MgO	—	2,41
Na_2O	0,13	1,31
K_2O	0,87	0,18
P.C.	11,68	5,00
Total	99,46	100,01

La capacité d'échange totale des cations est de 20 milliéquivalents/100 g pour la kaolinite et de 88 milliéquivalents/100 g pour la montmorillonite. Les analyses des bases échangeables montrent la prédominance des cations de Na^+ pour la montmorillonite et de ceux de Ca^{2+} et Na^+ pour la kaolinite. Le tableau 2 révèle les caractères des bases échangeables.

TABLEAU 2

Cations échangeables des minéraux argileux étalons

Cations / Minéraux	Ca^{2+} (méq./100 g)	Mg^{2+} (méq./100 g)	Na^+ (méq./100 g)	K^+ (méq./100 g)
Montmorillonite de la vallée du Chioaru	15,40	3,62	67,36	2,07
Kaolinite d'Aghireș	10,37	1,81	7,91	0,37

Grim (1953) considère que la capacité d'échange cationique varie de 3 à 15 milliéquivalents/100 g de kaolinite et de 70 à 100 milliéquivalents/100 g de smectites, exception faite pour la stévensite ; toutes les déterminations ont été effectuées à une valeur du $pH = 7$.

La grande valeur de la capacité d'échange cationique de la kaolinite d'Aghireş peut s'expliquer par l'insatisfaction des valences de la bordure des unités structurales, fait qui conduit au déséquilibre électronique du réseau, qui possède toutefois un degré de cristallisation avancé.

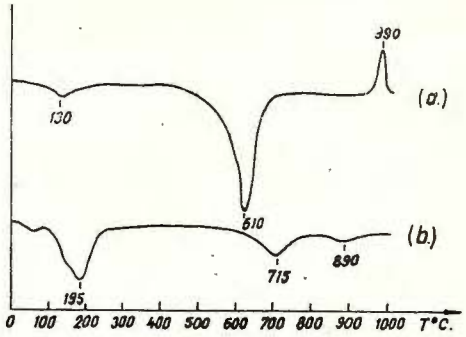

Fig. 1. — Courbes des analyses thermiques différentielles : a, kaolinite d'Aghireş ; b, montmorillonite de Valea Chioarului.

Ce phénomène a été évidencié par les analyses thermo-différentielles (fig. 1) qui montrent un faible phénomène endothermique entre 125 — 130°C, imputable à la perte en eau hygroscopique, un phénomène endothermique à 610°C, dû à la perte en hydroxyle et un effet exothermique représenté par un pic à 990°C dû à la décomposition totale du réseau accompagnée de l'apparition des phases stables à de hautes températures. Les deux derniers effets sont situés à des températures assez élevées pour la kaolinite.

La courbe thermo-différentielle de la montmorillonite de la vallée du Chioaru marque la perte de l'eau d'hydratation des cations à 195°C et l'effet endothermique correspondant présente un aspect caractéristique dû à la présence des cations de Na^+ (B a r s h a d, 1950). Le grand intervalle des températures (175°C) situé entre les deux effets endothermiques de températures élevées autant que l'absence d'un effet exothermique final attestent d'importantes substitutions des cations de Al^{3+} à Mg^{2+} dans les couches octaédriques, avec une structure similaire à celle indiquée par L u c a s , T r a u t h (1965) pour la montmorillonite de type Cheto.

L'aspect des cristallites des minéraux argileux examinés au microscope électronique est présenté dans les figures 2 et 3. Les micrographies électroniques de la kaolinite d'Aghireş révèle des particules bien cristallisées, avec les bords nets, en forme de plaquettes hexagonales allongées parallèlement aux faces (010) ou (110). Les dimensions des cristaux varient de 0,3 à 1,5 μ. Les formes de la Na-montmorillonite sont nébuleuses avec les bords irréguliers et sinueux, les cristaux étant généralement moins gros que ceux de Ca-montmorillonite. La présence des cations de Ca^{2+} entre les couches tétraédriques conduit à la formation d'agrégats de grandes dimensions, dont la forme irrégulière se maintient. Les différences structurales déterminées par la variation de la force d'attraction

entre les particules (M a t h i e u-S i c a u d et al., 1951) dépendent de la quantité de cations échangeables, dans le sens que l'intensité des forces d'attraction augmente, à mesure que le nombre des cations de Ca^{2+} augmente. Lorsqu'il y a saturation ou un léger excès en cations de Ca^{2+} les particules s'ordonnent face à face et bord à bord.

Fig. 2. — Image de la kaolinite d'Aghireș enregistrée avec le microscope électronique.

Fig. 3. — Image de la montmorillonite de Valea Chioarului enregistrée avec le microscope électronique.

Tous les aspects de la structure des minéraux argileux étalon ont été vérifiés par des analyses diffractométriques aux rayons X et par des analyses des spectres d'absorption en infrarouge. Ces investigations attestent que les échantillons de kaolinite et de montmorillonite, outre le minéral argileux principal comportent aussi d'autres minéraux tels : quartz, micas et feldspaths qui étant en quantités très réduites on peut considérer qu'ils n'influencent pas les déterminations physico-mécaniques.

Afin de caractériser au point de vue physico-mécanique les minéraux argileux étalon on a utilisé des échantillons de montmorillonite naturelle autant que saturée de cations de K^+, Ca^{2+} et Mg^{2+}. Les échantillons ne contenant pas de carbonates ont été saturés directement par immersion et agitation dans des solutions 1 N, de KCl, $CaCl_2$ et $MgCl_2$. L'excès de réactif a été écarté par centrifugations répétées avec de l'eau distillée jusqu'à libre de chlore.

Étant donné que nos recherches concernent un matériel sans structure, afin de caractériser le comportement physico-mécanique des minéraux étalons nous avons choisi les paramètres dont la détermination n'exige pas que le matériel soit à l'état naturel.

La séparation de la fraction $< 2\ \mu$, imposée par le but de cet ouvrage, notamment de poursuivre exclusivement l'influence de la structure réticulaire des minéraux argileux sur les paramètres physico-mécaniques, n'exige point des analyses granulométriques.

Initialement on a pris de tous les échantillons une quantité égale de poudre, séchée à la température conventionnelle de 105°C, qui correspond à une évaporation totale de l'eau hygroscopique et à une perte partielle de l'eau d'hydratation des cations. La poudre a été pressée avec des forces égales dans des espaces égaux des anneaux inoxydables de l'appareil Vasiliev (fig. 4).

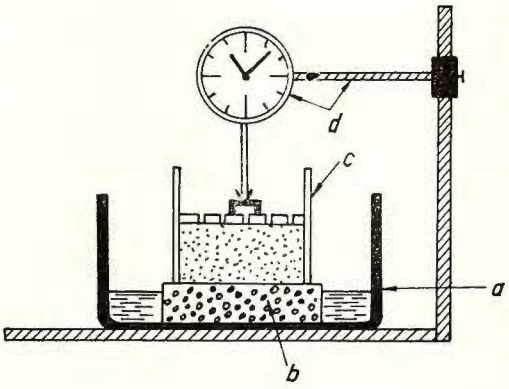

Fig. 4. — Appareil Vasiliev: a, vase d'immersion; b, pierre poreuse; c, anneau inoxydable; d, instrument de mesure.

Soumise au gonflement libre dans un intervalle de temps d'environ 150 minutes la kaolinite d'Arghireş montre un faible gonflement par adsorption d'eau pendant les deux premières minutes, dû à quelques désordres du réseau (fig. 5), suivi d'une ligne droite jusqu'à la fin du processus.

Par contre, la pente des courbes de gonflement de la montmorillonite saturée de cations mono- et bivalents indique un développement différent le long du processus. On constate qu'au moment où le phénomène de gonflement doit, déclancher, la montmorillonite sodique présente une inertie initiale par rapport à la montmorillonite saturée de Ca^{2+}, Mg^{2+} ou de K^+.

Selon toute vraisemblance l'hydratation de la Na-montmorillonite a lieu progressivement et de manière continue en présence d'un excès en eau ; après 300 minutes le gonflement continue avec la même intensité qu'après 60 minutes. Les pentes des courbes de la montmorillonite saturée de Ca^{2+}, Mg^{2+} et K^{+} indiquent l'arrêt des gonflements libres après environ 500 minutes. La K-montmorillonite qui montre une haute adsorbabilité par rapport aux Ca- et Mg-montmorillonites, dans l'intervalle de temps de 150 à 300 minutes, indique toutefois un arrêt plus rapide du phénomène.

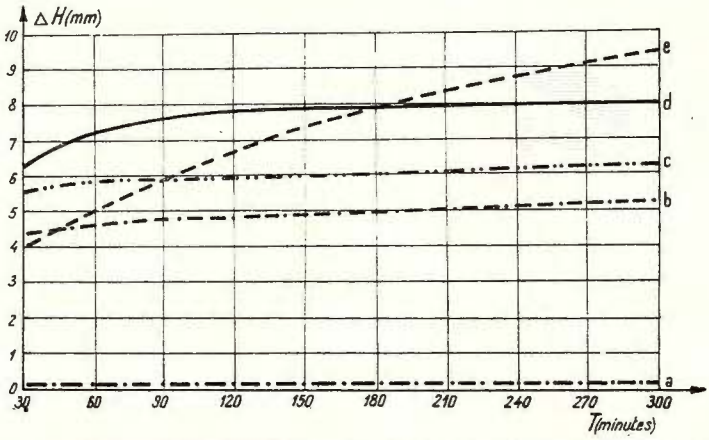

Fig. 5. — Courbes des gonflements libres de la kaolinite d'Aghireș (a) et de la montmorillonite de Valea Chioarului saturée de Ca^{2+} (b), Mg^{2+} (c), K^{+}(d) et Na^{+}(e).

L'explication du comportement particulier de la montmorillonite de Valea Chioarului saturée de différents cations doit être cherchée dans la manière dont a lieu l'hydratation des cations échangeables.

Il est bien connu que dans les conditions d'une faible humidité la Na-montmorillonite n'adsorbe qu'une seule couche monomoléculaire d'eau disposée entre les couches tétraédriques ; il y a des cas où en conditions similaires la Ca-montmorillonite adsorbe deux couches d'eau bien liées et disposées dans le même espace. S'il y a excès d'humidité la Na-montmorillonite peut retenir une multitude variée de couches monomoléculaires d'eau, légèrement orientées, fait qui conduit à la dispersion des particules par l'affaiblissement des forces de liaison entre les feuillets et en conséquence à l'accroissement de la surface d'adsorption. Par contre s'il y a excès d'humidité la Ca-montmorillonite retient le même petit nombre de couches monomoléculaires d'eau.

Les résultats obtenus par l'analyse du gonflement libre révèlent que l'ordre dont les cations échangeables conduisent à l'adsorption des plus grandes quantités d'eau est l'ordre qui correspond à la série générale d'absorbabilité (série H o f m e i s t e r). La capacité de substitution des

cations échangeables de cette série a été minutieusement examinée par H a n s e r (1941) et reprise par R o s s (1943) qui pour la montmorillonite a précisé la série de substitution suivante :

$$Li^+ < Na^+ < H^+ < K^+ < Mg^{2+} < Ca^{2+}$$

Il y a lieu de mentionner la concordance entre la série de H o f m e i s t e r et les résultats de nos déterminations E n s l i n effectuées sur la montmorillinite de Valea Chioarului saturée de cations de Na^+, K^+ et Mg^{2+} (tab. 3).

TABLEAU 3

Quelques propriétés physiques des minéraux étalons liés par l'adsorbtion d'eau et perméabilité

Minéraux	Adsorption E n s l i n (ml)	W_p (%)	W_L (%)	I_p (%)	A_c	K (cm. 10^{-1})
kaolinite	—	28,1	70,5	42,4	0,42	$6{,}5.10^{-6}$
Na-montmorillonite	4,82	37,0	775,0	738,0	7,38	$<5.10^{-8}$
K-montmorillonite	3,08	55,0	360,0	305,0	3,05	$<5.10^{-8}$
Ca-montmorillonite	—	27,0	193,0	116,0	1,66	$6{,}77.10^{-6}$
Mg-montmorillonite	2,50	32,1	263,5	231,4	2,31	$4{,}9.10^{-7}$

L'ordre des cations de la série générale de substitution est vérifié aussi dans le cas de l'influence des cations échangeables du réseau de la montmorillonite sur les valeurs des limites A t t e b e r g et tout spécialement sur celle de la limite supérieure. Bien que ces limites, représentant la teneur en eau qui détermine la modification de l'état de cohésion de l'argile, constituassent une caractérisation empirique, elles sont des critères de classification et d'identification très pratiques au service des ingénieurs.

Etant donné que la quantité d'eau que l'argile adsorbe dépend de la participation de la fraction fine, nous accordons un intérêt tout particulier à comparer sa plasticité avec sa teneur en fractions $< 2\ \mu$. Il en résulte le coefficient d'activité établi par S k e m p t o n (1953) dénommé „activité colloïdale de l'argile" :

$$Ac = \frac{I_p}{\%\ \text{fraction} < 2\ \mu} \qquad \text{(tab. 3)}$$

En ce qui concerne la limite inférieure de plasticité, où l'effet de dispersion n'est pas trop accusé, vu l'humidité faible, la nature des cations échangeables n'entraîne pas des variations spectaculaires des valeurs.

Certes, en ce qui concerne l'adsorption de l'eau du réseau des minéraux argileux, et tout spécialement de ceux à structure réticulaire de type 2 : 1 elle présente une valeur maximum-limite, au delà de cette valeur intervenant la perméabilité du matériau.

On peut également affirmer que le type de réseau réticulaire et la nature des cations échangeables ont une influence décisive. Le tableau 3 révèle que la montmorillonite saturée de Ca^{2+} et Mg^{2+} est relativement susceptible à la circulation de l'eau. Les valeurs de perméabilité ($K = 6,77 \cdot 10^{-6}$ et respectivement $K = 4,9 \cdot 10^{-7}$) sont comparables à celle de la kaolinite ($K = 6,5 \cdot 10^{-6}$) qui est la plus accusée de tous les échantillons. La présence des cations de Na^{+}, très hydrophiles, conduit à de très faibles perméabilités, de l'ordre de $K > 5 \cdot 10^{-8}$.

Les déterminations concernant le comportement physico-mécanique de quelques mélanges à teneurs variées en kaolinite d'Aghireş et en montmorillonite de Valea Chioarului ont été effectuées, elles-aussi, sur des échantillons enrichis en fractions $< 2\ \mu$ par la sédimentation des composants grossiers. L'étude des argiles monominérales telles la kaolinite d'Aghireş et la montmorillonite de Valea Chioarului saturées de cations mono- et bivalents, simplifie, sans doute, le problème à étudier, nous donnant la possibilité d'observer les différences de comportement qui existent entre les minéraux argileux qui dépendent de la structure réticulaire, lors des essais physico-mécaniques. Mais ces argiles sont peu fréquentes, voire très rares, par rapport à celles qui comportent des mélanges de minéraux dont dispose l'ingénieur.

TABLEAU 4

Perméabilité et propriétés physiques des mélanges de minéraux argileux étalons liés par l'adsorbtion d'eau

Mélange		W_p (%)	W_L (%)	I_p (%)	A_c	K ($cm \cdot 10^{-1}$)
Montmorillonite %	Kaolinite %					
0	100	28,1	70,5	42,4	0,42	$6,5 \cdot 10^{-6}$
2,5	97,5	27,6	60,5	32,9	0,33	$6,5 \cdot 10^{-6}$
5,0	95	26,5	58,8	32,3	0,32	$6,5 \cdot 10^{-6}$
7,5	92,5	27,0	69,5	41,5	0,41	$6,5 \cdot 10^{-6}$
10,0	90	26,6	90,9	64,3	0,64	$1,37 \cdot 10^{-7}$
15	85	24,9	101,9	77,0	0,77	$4,62 \cdot 10^{-7}$
20	80	25,1	122,5	97,4	0,97	$4,62 \cdot 10^{-7}$
25	75	26,8	149,0	122,2	1,22	$< 5 \cdot 10^{-8}$
30	70	23,4	156,0	132,6	1,33	$< 5 \cdot 10^{-8}$
40	60	24,7	216,5	191,8	1,92	$< 5 \cdot 10^{-8}$
50	50	24,7	266,0	241,3	2,41	$< 5 \cdot 10^{-8}$
75	25	31,1	502,0	470,9	4,71	$< 5 \cdot 10^{-8}$
100	0	37,0	775,0	738,0	7,38	$< 5 \cdot 10^{-8}$

Le tableau 4 montre la variation des valeurs limites d'A t t e b e r g en fonction du rapport entre le taux en kaolinite et le taux en montmorillonite naturelles.

Etant donné que les roches qui comportent une faible quantité de montmorillonite et un autre minéral argileux comme composant dominant (tout spécialement l'illite) sont les cas les plus fréquents, nous avons examiné minutieusement l'intervalle de concentration en montmorillonite compris entre 0 et 15%.

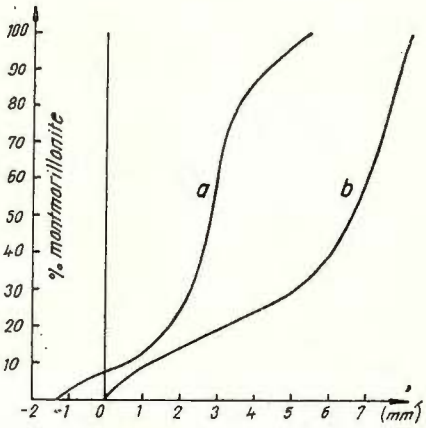

Fig. 6. — Variations des gonflements libres en fonction de la composition du mélange : a, humectation par l'extrémité inférieure, durée = 210 minutes ; b, humectation bilatérale, durée = 210 minutes.

Le mélange de deux composants en proportion connue n'implique pas une moyenne pondérale de l'indice de plasticité (ni des limites de plasticité — Caquot, Kerisel, 1967).

Les déterminations de gonflement libre (fig. 6) où l'humectation de la poudre dosée installée sur la pierre poreuse, comme nous l'avons mentionné précédemment, ont été effectuées par l'imerssion de la pierre dans de l'eau distillée (courbe *a*) autant que par égouttement sur un piston poreux (courbe *b*). Elles ont mis en évidence l'évolution des gonflements en temps et la valeur des gonflements libres finalement de chaque participant.

On remarque que la manière dont a lieu l'adsorbtion de l'eau dépend du type du réseau des deux minéraux participants. Il en est de même de l'aspect approximativement linéaire de la courbe de pression du gonflement — participation proportionnelle des deux composants (fig. 7).

La pression de gonflement, la résistance, au cisaillement (fig. 8), la résistance à la pénétration (fig. 9) et les déterminations de la compression œdométrique (les dernières effectuées jusqu'à une composition de 10% montmorillonite) ont été exécutées sur des échantillons dosés mécaniquement par le mélange de poudres avec une humidité presque nulle ; pour une bonne homogénéisation nous avons utilisé la méthode des quarts.

À des quantités égales de poudres on a ajouté des quantités égales d'eau, jusqu'à l'humidité de 35% qui représente l'humidité moyenne d'une argile normale. Après l'homogénéisation mécanique par pétrissage, des quantités égales de la pâte obtenue ont été introduites dans des volumes égaux connus (matrices œdométriques).

Cependant les poids volumétriques initiaux ne sont pas égaux, car à mesure que la teneur en montmorillonite augmente les goflements instantanés déterminent un hérissement du matériau et alors la participation du „matériau sèche" aux volumes donnés est différente.

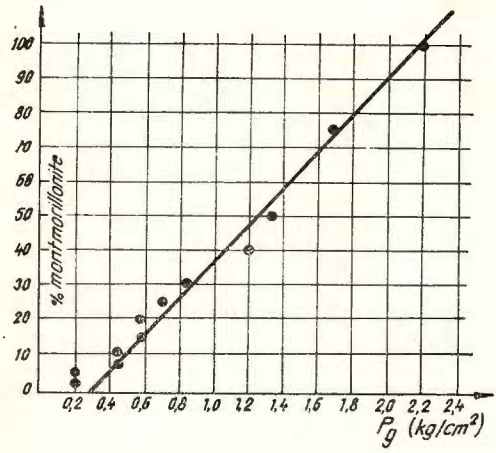

Fig. 7. — Variation de la pression de gonflement en fonction de la composition minéralogique du mélange.

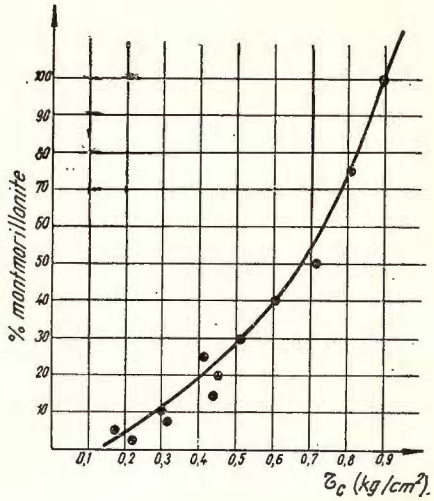

Fig. 8. — Résistance au cisaillement en fonction de la composition minéralogique du mélange.

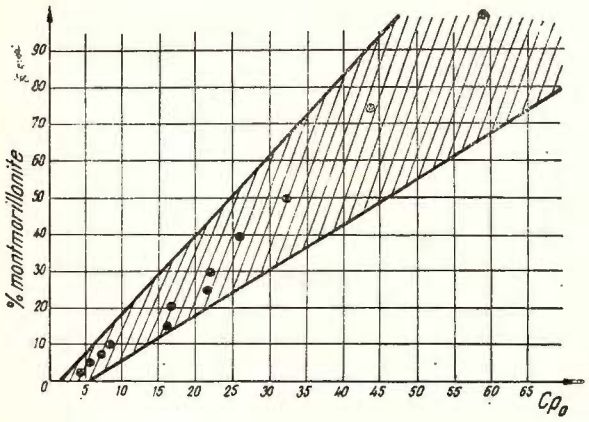

Fig. 9. — Domaine de la variation du coefficient de pénétration en fonction de la composition du mélange (valeurs moyennes pour 120 essais).

Les figures 8 et 9 rélèvent également des résistances au cisaillement et à la pénétration apparemment plus élevées à mesure que la montmorillonite gagne en teneur, fait qui ne correspond pas au comportement mécanique réel de la montmorillonite.

L'explication de ce phénomène nous vient des propriétés plastiques des minéraux argileux, notamment les échantillons avec une teneur élevée en kaolinite, à une humidité de 35% se trouvent dans le voisinage de la limite de plasticité (tab. 4), alors que les échantillons avec une teneur élevée en montmorillonite, toujours à l'humidité de 35%, présentent un déficit en eau adsorbée, manifestant des propriétés de résistance apparemment élevées, fait dû à un état de tension de type „attractif" entre les particules contenant une faible quantité d'eau d'adsorption et les innombrables molécules d'eau polarisées adsorbées par d'autres particules qui sont les premières à prendre contact avec l'eau. Ces forces d'attraction exerçant une action indirecte entre les particules argileuses proprement dites conduisent à l'augmentation apparante (et exigée par l'état d'humidité) de la cohésion des échantillons.

Les déterminations complètes sur la kaolinite d'Aghireş et sur la montmorillonite de Valea Chioarului ont mis en évidence que leurs propriétés physico-mécaniques dépendent de leur composition et de leur structure réticulaire.

On a tout spécialement examiné les relations qui sont utiles pour l'emploi pratique de ces minéraux étalons.

L'examen des résultats obtenus porte à conclure que l'ensemble de la structure réticulaire des minéraux argileux, comportant de nombreuses déformations et substitutions cationiques, détermine d'importantes variations de la manière dont ces minéraux se comportent au contact avec l'eau.

Les principales causes structurales sont :

— le type de réseau réticulaire ; étant donné que les réseaux de type 1 : 1 sont peu sensibles ou insensibles à l'adsorption de l'eau, alors que ceux de type 2 : 1 par leur constitution même sont susceptibles d'adsorber les couches monomoléculaires d'eau ;

— les réseaux réticulaires de type 2 : 1, tout spécialement ceux smectitiques qui attestent une mobilité spéciale en ce qui concerne la distance d'entre les couches au contact avec l'eau, notamment dans le cas du mélange des deux minéraux étalons, à de faibles variations de la montmorillonite on obtient des changements importants des valeurs des paramètres physico-mécaniques ;

— la nature des cations échangeables, tout spécialement en ce qui concerne la charge électrique et le rayon ionique. Les cations monovalents adsorbent la plus grande quantité d'eau ; ils influencent les propriétés physiques rattachées à l'absorption de l'eau suivant un ordre qui correspond à la série d'adsorbabilité générale établie par E. A. Hanser et ensuite par C. S. Ross pour la montmorillonite.

Tenant compte des caractéristiques de la composition chimique, de la structure réticulaire et des résultats obtenus par les analyses physico-mécaniques effectuées sur la kaolinite d'Aghireş et sur la montmoril-

lonite de Valea Chioarului (obtenues en écartant les autres composants minéraux) on recommande celles-ci comme minéraux argileux étalons pour la Roumanie, du reste recommandation déjà faite par le Groupe Roumain pour l'Etude des Argiles.

BIBLIOGRAPHIE

Barshad J. (1950) The Effect of Interlayer Cations on the Expansion of the Mica Type of Crystal Lattice. *Amer. Min.*, 35, p. 225—238, Washington.

Caquot A., Kerisel J. (1972) Tratat de mecanica solurilor. Edit. tehnică, București.

Grim R. E. (1953) Clay Mineralogy. Mc. Graw-Hill Book Comp., New York.

Hanser E. A. (1941) Colloid Chemistry in Ceramics. *Amer. Ceramic Society Journal*, vol. 24, p. 179—187.

Lucas J., Trauth N. (1965) Etude du comportement des montmorillonite à haute temperature. *Bull. Serv. Carte géol. Als. Lorr.*, 18, 4, p. 217—242, Strasbourg.

Mathieu-Sicaud A., Mering J., Perrin-Bonnet J. (1951) Etude sur microscope électronique de la montmorillonite et de l'hectorite saturées par différents cations. *Bull. Soc. Franc. Minéral.-Crist.*, 74, Paris.

Ross C. S. (1943) Clays and soils in relation to geologic processes. *Washington Acad. Sci. Jour.*, 33, Washington.

Skempton A. W. (1953) Soil mechanics in relation to geology. *Proc. of the Yorkshire Geological Society*, 29, Part 1, 3, Leeds.

CLAY MINERALS IN THE PRAID SALT DEPOSITS[1]

BY

GHEORGHE NEACȘU, TIBERIU URCAN[2]

Sommaire

Minéraux argileux du massif de sel gemme de Praid. La composition minéralogique de la fraction argileuse disséminée dans les dépôts de sel gemme de Praid est dominée par l'illite, la kaolinite participe en moindre mesure et la chlorite est en quantités tout à fait subordonnées. Tous ces minéraux présentent un faible degré de cristallinité et proviennent d'une écorce d'altération (allogène). L'étude minéralogique révèle des processus diagénétiques peu intenses et nous renseigne sur les conditions paléoclimatiques qui ont gouverné la précipitation du sel dans les bassins de sédimentation.

The clay minerals occur in the salt deposits either like clayey interbeds or like fine clay material disseminated in the salt mass. The alternation of clay and salt bands is suggesting a climatic control. The presence of the finely disseminated clayey material in the evaporite mass shows that the supply of the weathering crust material from the continent in the sedimentary basin did not disturb the precipitation of salts.

In this paper we studied the mineralogical composition of the finely disseminated clay material in the Praid salt deposits in order to elucidate its genesis and to reconstitute the paleoclimate conditions.

The halite is the main mineralogical component in the analysed samples associated with small amounts of anhydrite, gypsum, calcite and clay minerals determined by the *X*-ray diffractometry study.

After the removal of soluble salts and calcite by repeated hot washings with distillated water and HCl 4%, the $< 1\ \mu$ argillaceous fraction was examined by the *X*-ray diffractometry method.

[1] Paper presented at the 2nd National Clay Conference, April 11—12, 1975, Bucharest.

[2] Întreprinderea geologică de prospecțiuni pentru substanțe minerale solide, str. Caransebeș 1, București.

The Figure presents the basal reflections of the clay minerals obtained on oriented samples by *X*-ray diffraction techniques. The diffractograms revealed the presence of illite, kaolinite and chlorite.

The d (001) basal reflection of chlorite (14.2 Å) noticed on all diffractograms becomes stronger on the heated preparation diffractogram proving the presence of a Fe-rich chlorite.

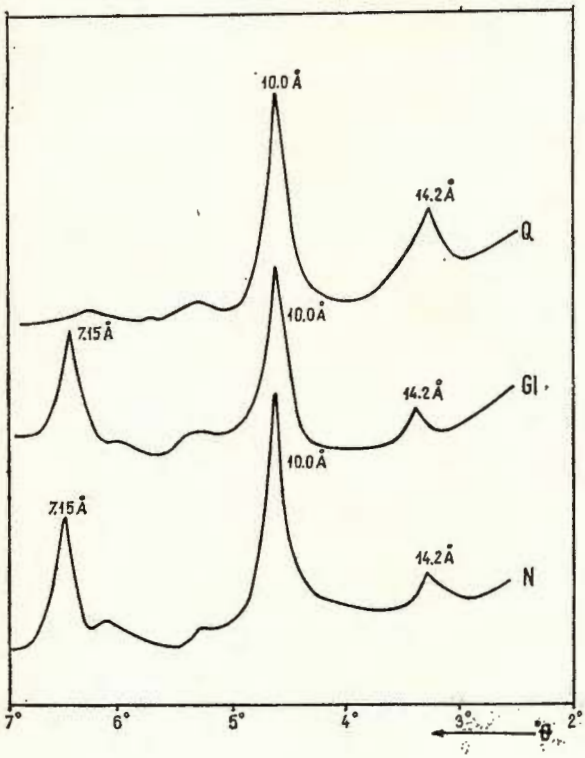

Fig. — *X*-ray diffraction patterns of the $< 1\,\mu$ clay fraction (finely disseminated) in common salt deposits of Praid. (2—7°θ, Cu Kα radiation, Ni filter, 30 kV, 25 mA; symbols: N = natural sample; Gl = glycolated sample; Q = heated for two hours at 600°C sample).

As we can see in the Figure, all the clay minerals show a low degree of crystallinity.

The *X*-ray diffraction study of the argillaceous fractions, contained in the common salt from Praid, points out the following mineralogical composition:

illite	65—75%
kaolinite	20—30%
chlorite	5—10%

The polymorphous 1 Md illite is the main component of the clay fraction. The pM kaolinite occurs in a rather high amount, and the chlorite is subordonate.

The low crystallinity degree of illite, kaolinite and chlorite indicates their allogenic character, their source being the weathering crust of the continent. Both in the sedimentary basin and during diagenesis there may be noticed an abundance of Mg^{2+} and K^{+} cations, favourable to the chlorite and illite forming. Under these conditions it is possible that a small amount of montmorillonite might have turned into chlorite and/or illite.

The low crystallinity degree of illite, kaolinite and chlorite indicates a low intensity of the diagenetical processes too.

As it is well known the kaolinite represents mainly a weathering product, and the saline environments are not favourable to its formation and preservation.

The presence of kaolinite in a rather high amount in the clay fraction of the Praid salt deposits raises another important problem relating to the climate conditions of the salt precipitation. The kaolinite forming in the weathering crust is possible only in a climate rather abundant in precipitations.

The presence both of kaolinite and some plants (nuts, hazel nuts) in the common salt deposits (P a p i u, 1960) is indicative of a hot and occasionally wet climate allowing the development of a varied vegetation.

REFERENCES

P a p i u C. V. (1960) Petrografia rocilor sedimentare. Edit. St., București.

10.50 Å HYDROMICA, A PRINCIPAL COMPONENT OF "KAOLIN" FROM THE HARGHITA AREA [1]

BY

GHEORGHE NEACȘU, TIBERIU URCAN[2]

Sommaire

Hydromica à 10,50 Å, principal composant du kaolin de Harghita. L'étude des argilisations hydrothermales dans les Monts Harghita dénote que si le processus d'argilisation est dans un stade initial les produits sujets à des transformations sont déterminés par la nature des roches et si celui-ci est dans un stade avancé c'est la nature des solutions qui contrôle les produits. L'hydromica 10,50 Å est le principal composant des zones argilisées des Monts Harghita. Le soit-disant „kaolin" de Harghita est constitué d'hydromica 10,50 Å en proportions supérieures à 90%. L'étude du comportement de l'hydromica à 10,50 Å au traitement thermique ou à l'éthylène-glycole porte à conclure que la position anormale de la réflexion (001) vient de la distribution chaotique du K^+ et du stade d'hydratation du matériel. La présence de quelques faibles quantités de couches de type vermiculite irrégulièrement interstratifiées parmi les couches à 10 Å de l'hydromica n'est pas exclue. L'hydromica ayant fait l'objet de cette étude présente un degré avancé de cristallinité, un état de dispersion avancé et une très bonne orientation ; la variété polymorphe 2 M et les caractéristiques roengénographiques de l'hydromica mettent en évidence qu'elle est de beaucoup plus proche des micas bien cristallisées que de l'illite.

Introduction

In a preceding paper (Neacșu, Urcan, 1975), the authors studied the process of the hydrothermal argillization showing the mineralogical transformation which took place in the volcanic rocks, especially in the initial stages of alteration, in the southern part of the Harghita Mountains.

In the first alteration stage when the initial structure of the rock was kept, and the hydrothermal solutions had not an important circulation, there could be observed a close relationship between the mineralogical

[1] Paper presented at the 2nd National Clay Conference, April 11—12, 1975, Bucharest.

[2] Întreprinderea geologică de prospecțiuni pentru substanțe minerale solide, str. Caransebeș 1, București.

composition of the initial rock and the results of the transformation phenomena.

In the beginning stage of argillization the hydrothermal solutions displayed a reduced activity, and independently of their nature, the kind of the transformation products was determined by the mineralogical and chemical composition of the initial rock.

The study of the beginning stage of hydrothermal argillization leads us to the conclusion that the initial transformation took place in these directions :

feldspar	→	kaolinite
hornblende	→	montmorillonite
biotite	→	hydrobiotite

Thus several minerals differing as a function of *pH* conditions, were concomitantly formed due to a local change of the chemical composition of solutions ; this change was controlled by the chemistry of primary minerals which underwent an alteration.

In the present paper we shall study the intensive hydrothermal argillization stages spread in the whole Harghita Mountains area.

The first stage of intensive argillization
Kaolinite forming

When the hydrothermal activity marks an increase, the transformation products are determined by the chemistry of the hydrothermal solutions. The argillization becomes intensive, the main mineralogical compounds of the rocks including the volcanic glass, are argillized. The chemistry of solutions, especially the acid character of *pH*, determines the transformation of all the mineralogical components into kaolinite.

In relation to the intensity of the hydrothermal acid solutions circulation, we could observe some different stages of kaolinization between the fresh rock and the completely kaolinized rock.

The acid *pH* solutions are leaching the alkalies and the earth-alkalies from rock allowing the kaolinite forming.

The characteristic paragenesis for the first stage of argillization is : kaolinite + secondary quartz. Sometimes the amount in secondary quartz increases so that in this case the silicification is frequent.

When the intensity of hydrothermal alterations is less strong, the rock keeps different quantities of feldspar and volcanic glass, while the femic minerals are completely transformed.

In all the hydrothermal argillization processes the kaolinization occurs in a reduced proportion.

The second stage of intensive argillization
Hydromica forming

The hydrothermal solutions rich in K^+ and with a neutral or a weak alkaline *pH*, determine the transformation of all preceding minerals into hydromica. The main amount of silica is partially dissolved so that

in this stage no important silifications are found. Now there are forming almost monomineral rocks constituted by more than 90% hydromica.

When the intensity of alteration is less important one can observe various quantities of preceding minerals, like kaolinite (up to 50%) and secondary quartz (up to 10%).

The hydromicaceous hydrothermal argillization phenomena are characteristic of the hydrothermal argillization in the Harghita Mountains.

The third stage of intensive argillization Montmorillonite and mixed layer forming

Concomitantly with the change of the nature of hydrothermal solutions, which become rich in earth-alkalies (Ca, Mg) and with a more alkaline *pH*, the intensity of the argillization process is less important. This decrease of the intensity of alteration process is deduced from the fact that the new-forming minerals, especially montmorillonite, rarely chlorite and vermiculite, occur in small amounts as independent minerals; they occur especially as mixed layer minerals 10 — (10—14 M); 10 — (10—14 V) and 10 — (10—14 C).

In more than 90% of cases, the reflection of random mixed layers (10.1—10.9 Å) is about 10.50 Å.

The reduced intensity of the alteration process is inferred from the fact that the appearance of new phases stops at an incipient stage of the swelling layer forming (maximum 15%), when we have a random mixed structure with dominant hydromica layers. The total quantity of swelling minerals and chlorite, like independent minerals, is rarely totalizing 3% of the whole rock. Only in the most recent veins montmorillonite as an independent mineral increases up to 25%, and in random mixed layers up to 40%. Nowhere this argillization process leads to the forming of a montmorillonitic, vermiculitic or chloritic argillized rock.

Characteristic of the third stage of intensive argillization is the appearance of small quantities of calcite, while in recent veins calcite is more abundant.

The diffractograms of the natural, glycolated and heated sample in a vein (Fig. 1, sample 731) show the predominant presence of random mixed layers 60% hydromica, 40% montmorillonite (10.9; 12..2; 9.8 Å) and random mixed layers 55% hydromica, 45 chlorite (12.4; 12.2; 11.3 Å) together with montmorillonite (12.4; 17.8; 9.8 Å), hydromica (9.8 Å) and kaolinite (7.1 Å).

About 10% from the analyzed 10.50 Å hydromicas behaved like random mixed layers at glycoling and heating at 600°C.

Figure 1 shows two specimens with random mixed layers 85% hydromica, 15% montmorillonite (sample 726) and 80% hydromica, 20% montmorillonite (sample 727) identified by 10.5; 11.3—11.9; 9.8 Å peaks. In the same specimens were identified by 12.2 and 10.7 Å peaks random mixed layers: 45% hydromica, 55% chlorite (sample 726) and 80%

hydromica, 20% chlorite (sample 727). Together with these appear hydromica (9.8 Å), chlorite (13.4—14.6 Å) and kaolinite (7.1 Å).

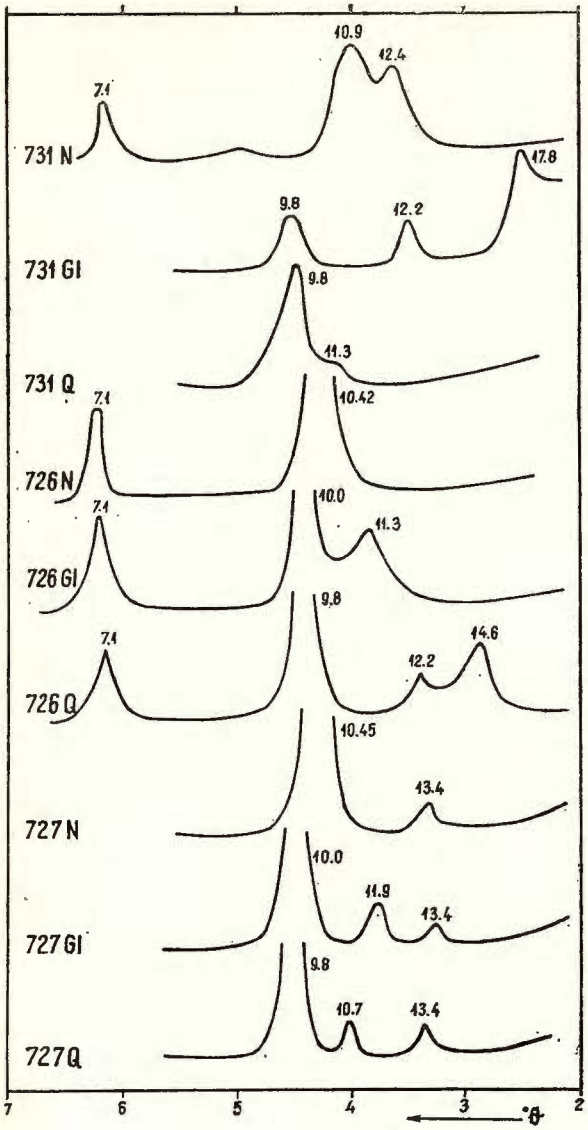

Fig. 1. — The diffractograms of 10.50 Å hydromica containing swelling mixed layers. (Oriented samples : N = untreated ; Gl = = glycolated ; Q = heated for 2 hours at 600°C).

10.50 Å Hydromica

The numerous diffractograms run on samples from the argillization zones in the Harghita Mountains lead to the conclusion that almost 80% of cases are represented by a hydromica with a 10.50 Å basal reflection.

The commercial product called "colloidal kaolin" of Harghita presents the following mineralogical composition :

10.50 Å hydromica	over 90%
kaolinite	about 7%
swelling minerals + quartz	under 3%

More than 90% of 10.50 Å hydromica samples do not swell by glycoling but they successively modify their positions, by heating at 600°C, to 10.0 Å.

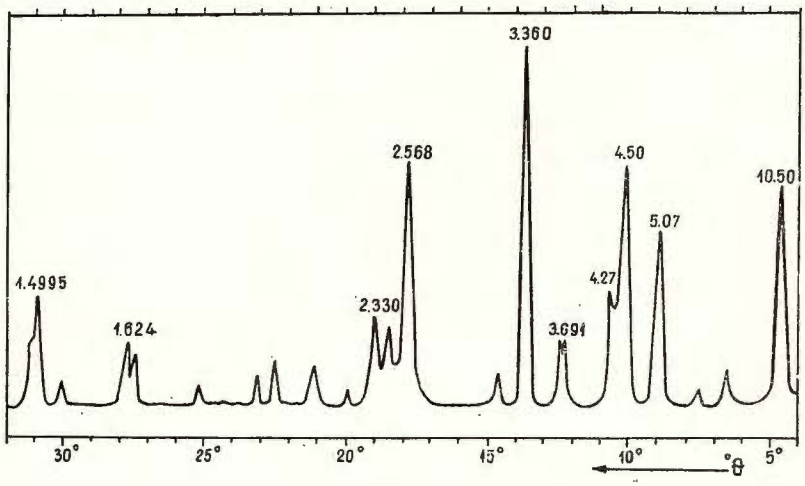

Fig. 2. — The diffractogram of 10.50 Å hydromica. (Unoriented sample).

According to B r i n d l e y (1951) when it is dealing with random mixed layers of swelling type with 10 Å layers, the last one showing a clear-cut predominance, they do not present swelling. He also noted mixed layers 10—14 V of hydrobiotite type which do not present swelling.

In order to explain the abnormal position of 10.50 Å hydromica a detailed roentgenographical study with thermal and chemical treatments has been undertaken.

The roentgenographical characteristics of the 10.50 Å hydromica obtained by *X*-ray diffractometry on unoriented slides, untreated samples, are presented in Table 1 and Figure 2. As we can observe almost all the reflections belong to hydromica. The weak reflection d = 7.18 Å belongs to kaolinite, while the reflection d = 1.818 Å and d = 1.536 Å indicate the presence of a small amount of quartz.

The intensities of the first five basal reflections are high, with exception of the fifth basal order d (005) = 2.028 Å.

The decreasing of the basal reflection intensity, which takes place as follows : d (003); d (004); d (001); d (002); d (005), and especially

the high intensity of the reflection d (002) = 5.07 Å, reveal that this hydromica pertains to the dioctahedral series being an aluminous one.

The same thing results from the d (060) = 1.4995 Å position too, this being characteristic of the aluminous micas (B r i n d l e y, 1951). The reflections of the 10.50 Å hydromica indicate a high degree of crystallinity approaching that of hydromuscovite and micas and not the one of illites.

TABLE 1

10.50 Å hydromica. Unoriented slide, untreated sample *

No	d/n	I_0	No	d/n	I_0	No	d/n	I_0
1	10.50	60	10	3.643	18	19	2.139	15
2	7.18	5	11	3.360	100	20	2.028	20
3	6.05	5	12	3.126	18	21	1.971	12
4	5.07	45	13	3.091	21	22	1.912	9
5	4.50	80	14	2.932	6	23	1.818	10
6	4.27	24	15	2.568	70	24	1.684	20
7	3.951	3	16	2.461	27	25	1.660	20
8	3.829	5	17	2.389	28	26	1.536	9
9	3.695	18	18	2.239	10	27	1.4995	36

* Scanned from 4° to 32°θ, at the rate of 1°/minute; Cu K α radiation, Ni filter, 30 kV, 25 mA; the lattice spacings (d/n) are measured in Å and relative intensities (I_0) on a scale 1-100. The same conditions for Tables 2, 3, 4 and 5.

The reflections (02 l) and (11 l) between 4,4—2,6 Å are indicative of a 2M polymorphy.

The diffractogram of the oriented series shows the intensive series of the first five basal reflections (Tab. 2; Fig. 3). This denotes a high degree of crystallinity, a strong dispersion and a good orientation. The high degree of orientation, the intensification of more than 10 times of the (001) reflection can be explained only by the strong development of the particles in the directions "a" and "b", like a sheet of paper.

The d = 13.70 Å reflection belongs to a swelling mineral, while the d = 7.16 Å and d = 3.571 Å reflections, belong to kaolinite. The d = 13.70 Å reflection disappears by heating at 600°C, like the d = 7.16 Å and d = 3.571 Å reflections, and modifies its position to 17.80 Å by glycoling.

The 1st, 2nd and 3rd order reflections of the hydromica are intensive, whereas the 5th and especially the 4th order reflections display a lower intensity in comparison with the well-crystallized micas. The high intensity of the basal reflections indicates a well-crystallized hydromica, rather Similar to hydromuscovite, not like illite.

The succession of the intensity of the first five basal reflections of the oriented sample is different of the unoriented one, the ratio between them being: d (001) = 100/60; d (002) = 46/45; d (003) = 55/100; d (004) = 4/70; d (005) = 12/20.

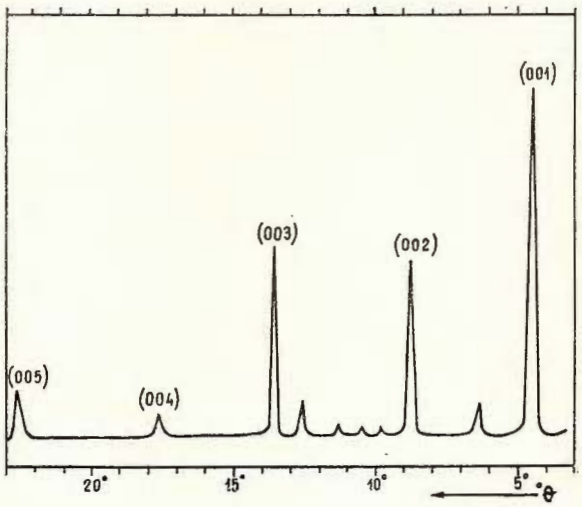

Fig. 3. — The diffractogram of 10.50 Å hydromica. (Oriented slide untreated sample).

TABLE 2

10.50 Å hydromica. Oriented slide, untreated sample

No	d/n	I_0	face	No	d/n	I_0	face
1	13.70	1—2		7	3.935	2	
2	10.47	100	(001)	8	3.571	9	
3	7.16	10		9	3.360	55	(003)
4	5.06	46	(002)	10	2.545	4	(004)
5	4.42	2		11	2.022	12	(005)
6	4.26	3					

d (001) becomes the most intensive on the oriented sample diffractogram (about 10 times higher), and d (004) becomes hardly visible.

The decreasing order of the basal reflection intensity on the oriented sample diffractogram is as follows: d (001); d (003); d (002); d (005); d (004).

Calculating the reflection position based on the 2nd-5th order basal reflections we obtained a value between 10.1—10.2 Å (in average 10.14 Å), higher than the common hydromica. This fact, in connection with the

measured position of the d (001) 10.47—10.50 Å, is indicative of a larger "c_0", probably caused by the number and the exchangeable K^+ position, by the ordering degree of the K^+ positions, by the successive disposal of layers and by the hydration state of the interlayer spacings. The $< 0.1\ \mu$ fraction contains almost only 10.50 Å hydromica that reveals a high degree of dispersion.

TABLE 3

The change of the lattice spacing and intensities of d(001) basal reflection by heating at different temperatures

Temperature	20°C	110°C	325°C	490°C	600°C	700°C	800°C	900°C	950°C	1000°C
d(001)	10.47	10.40	10.36	10.23	10.03	9.98	9.98	9.98	9.98	—
I_0	90	95	100	80	60	45	35	15	5	—

We studied too the behaviour of 10.50 Å hydromica by successive heating up to 1000°C (for 2 hours) of the oriented sample (Tab. 3).

Table 3 shows that the main decrease of the d (001) basal reflection appears by heating for 2 hours at 490°C and 600°C. After 600°C d (001) does not change its position. The change of the d (001) reflection position at 325°C is quite insignificant, and indicates the absence of montmorillonitic layers within the random mixed layers. The more important change of the d (001) reflection position at 490°C and 600°C is indicating either the presence of some vermiculitic layers within the random mixed layers, or a kind of more closed inter-layer water, or a structural reorganization of K^+ inter-layer.

We noticed the presence of the d (001) basal reflection up to 950°C that shows that unhydric metaphasis formed after 600°C is stable up to higher temperatures, like hydromuscovite and muscovite, being different from illites whose structure is completely destroyed at 800—850°C.

The destruction of the unhydric metaphasis, that begins after 900°C at 10.50 Å hydromica, is complete only at 1000°C when the 3 Al_2O_3. . 2 Si O_2 mullite (reflections 5.5; 3.39; 2.59 Å) and quartz (reflections 4.2; 3.34 Å) are forming.

While in the case of illites by heating at 550°—600°C, the d (001) basal reflection becomes stronger and sharper, at 10.50 Å hydromica we observed a slight increase of d (001) basal reflection by heating at 325°C followed by an important reduction of intensity at 490°C, and especially at 600°C the corresponding peak becoming wider. This fact could be interpreted like an effect of diminution of the crystallinity degree of the whole crystalline edifice (contrary to illites).

The change of the (001) basal reflection and its intensities by heating at different temperatures shows that 10.50 Å hydromica has a high degree

of crystallinity like hydromuscovite, and not like illite. The abnormal position d (001) = 10.50 Å is possibly caused by the disordered interlayer K^+ distribution, by the hydration state of layers of by the presence of small amounts of vermiculitic type layers randomly interstratified within 10.0 Å hydromica layers.

TABLE 4

The change of the position and the intensity of the d(001) basal reflection for the 10.50 Å hydromica, saturated with different cations, heated for 2 hours at various temperatures and glycolated

Cations	20°C	110°C	325°C	490°C	600°C	glycolated
K^+	10.40 95	10.37 95	10.34 100	10.20 85	9.98 65	10.35 80
Ca^{2+}	10.52 85	10.44 85	10.38 100	10.25 80	10.04 55	10.35 80
Mg^{2+}	10.41 70	10.38 70	10.34 100	10.25 75	10.03 55	10.30 55
Na^+	10.50 90	10.44 90	10.36 100	10.19 70	9.99 40	10.30 60
NH_4^+	10.48 95	10.44 95	10.37 100	10.26 70	10.04 45	10.30 50

More than 90%of 10.50 hydromica layers do not swell, and by glycoling the basal reflection position becomes 10.30 Å. The diminuation of the basal reflection position of the first order with 0.20 Å seems to indicate a more advanced hydration state. Simultaneously with the diminution of the d (001) basal reflection values takes place a decrease of 10—40% of their intensity by glycoling (Tab. 4).

With a view to proceed to a more detailed study we saturated with different cations (K^+, Ca^{2+}, Mg^{2+}, Na^+ and NH_4^+) by using 1N or 2N chloride solutions shaked for 14 hours.

As we can observe in Table 4, the saturation with cations does not make a sensible change in the d (001) reflection position. The saturation with K^+ and Mg^{2+} seems to cause a small diminution of the d (001) value from 10.50 to 10.40 Å, while the saturation with Ca^{2+}, Na^+ and NH_4^+ does not change the position of the d (001) reflection. The saturation with Ca^{2+} or NH_4^+, followed by glycoling does not produce an increase of d (001) reflection as it is mentioned for some disordered clay micas.

We can also see that the 10.50 Å hydromica saturated with different cations, like the untreated sample (Tab. 3), shows a small change of the d (001) reflection position, and at the same time a small increasing of the intensity by heating at 110°C and 325°C; by heating at 490°C and especially at 600°C, the intensity becomes sensibly lower and the position d (001) reaches about 10.0 Å.

By glycoling the d(001) = 10.5 Å becomes about 10.30 Å, and the intensity marks a decrease due to dehydration.

Taking into account the stability of the micaceous minerals during the treatment with acids in order to eliminate the impurities (especially the swelling layers in randomly mixed structures), we attacked hydromica with boiling 1N HCl, shaking it for 10 hours. The obtained results are given in the Table 5.

TABLE 5

10.50 Å hydromica attacked with boiling 1N HCl for 10 hours after heating for 2 hours at different temperatures or glycoling

Temperature	20°C	110°C	325°C	490°C	600°C	glycoling
d(001)	10.45	10.45	10.37	10.24	10.00	10.30
I_0	80	90	100	65	40	45

As we can notice from Table 5, the attack with 1N HCl does not make a sensible change in the position and the intensity of d (001) basal reflection, and also in the behaviour at different temperatures or by glycoling in comparison with the same untreated samples. The single important change is the change of the colour of the solution which becomes yellow-greenish.

The lack of changes in the 10.50 Å hydromica behaviour by attack with 1N HCl is caused either by the absence of the impurities (especially swelling layers within random mixed layers) or by an attack with an insufficiently strong acid (1N HCl).

Conclusions

The study of the hydrothermal argillization in the Harghita Mountains area shows that in the incipient phase of alteration the nature of the rock determines the nature of the transformation products, while in the intensive argillization (with the stages of kaolinite, hydromica, montmorillonite and mixed layers forming), the nature of the transformation products is due to the nature of the solutions.

10.50 Å hydromica is the main compound of the argillization areas in the Harghita Mountains. The so called "colloidal kaolin" of Harghita is composed of more than 90% 10.50 Å hydromica.

In about 10% of the studied samples 10.50 Å swells being a random mixed layer mineral.

In more than 90% of the studied samples 10.50 Å hydromica does not swell, but on the contrary, reduces d(001) to 10.40 Å indicating an advanced hydration state

A detailed study traced the behaviour by heating at different temperatures of 10.50 Å hydromica untreated, saturated in different cations and attacked with boiling 1N HCl for 2 hours.

From Tables 3, 4 and 5 one can draw the same conclusions considering the disorder as being the cause of the abnormal 10.50 Å position, the probable explanation being the disordered disposal of K^+ and the hydration state of interlayer spacings and/or the presence of the impurities, like swelling layers of vermiculitic type, randomly interestratified with 10 Å hydromica.

10.50 Å hydromica has a high degree of crystallinity, an advanced dispersion and a quite suitable degree of orientation; the 2M polymorphy and *X*-ray patterns show that it is more approached to well-crystallized micas (of hydromuscovite type) than illites, and belong to dioctahedral mica group.

REFERENCES

Brindley G. W. (1951) *X*-ray identification and crystal structures of clay minerals. London.

Neacșu G., Urcan T. (1975) Hydrothermal transformation phenomena in the andesite of Pilișca (Harghita Mountains). *Proc. of the first National Clay Conference — 1973, Bucharest, Inst. Geol. Geof., Stud. tehn. econ.*, I, 13, București.

Mg — HYDROTHERMAL ARGILLIZATION IN THE SASCA MONTANĂ AREA [1]

BY

GHEORGHE NEACȘU, TIBERIU URCAN, RODICA SERGHIE[2]

Sommaire

Argilisation hydrothermale magnésienne de Sasca Montană. Outre les phénomènes de contact thermique et métasomatique, dans la région de Sasca Montană on a identifié nombre de processus hydrothermaux d'altération : argilique, carbonatée, siliceuse, zéolitique etc. Le phénomène le plus répandu est celui d'argilisation. La corrélation des données diffractométriques *R.X.* avec celles microscopiques ont conduit les auteurs à mettre en évidence, pour la première fois, la présence de la saponite, en liaison étroite avec le phénomène de serpentinisation. Ce phénomène a été décrit comme un processus d'altération hydrothermale magnésienne. La seconde génération de saponite, qui apparaît sous forme de filons, est représentée par les macrocristaux résultés d'un enchevêtrement épitaxique de fines paillettes de saponite en milieu hydrothermal.

Within the Sasca Montană area located in the western part of the Reşiţa — Moldova Nouă zone (Banat) there occur several banatitic igneous bodies trending N—S, which determine at the contact with Mesozoic sedimentary rocks, mainly limestones, various types of contact and metasomatic phenomena. The contact rocks, which include the most important copper ore deposits, are represented by garnet skarns and recrystallized limestones.

All these rocks were submitted to the action of the chemically differing hydrothermal solutions, which operated at a wide-ranging temperature. Sericitization, albitization, saponitization (argillization), serpentinization, silicification carbonation, chloritization and zeolitic alteration are to be recognized among the hydrothermal phenomena.

[1] Paper presented at the 2nd National Clay Conference, April 11—12, 1975, Bucharest.

[2] Întreprinderea geologică de prospecţiuni pentru substanţe minerale solide, str. Caransebeş 1, Bucureşti.

Argillization is one of the widely spread processes affecting both the banatitic igneous rocks and the contact rocks.

In this paper we shall study only the Mg-argillization of skarns, the so-called saponitization phenomena.

Mg-montmorillonite (saponite) is occurring in a close connection with the serpentinization processes of skarns and belongs to two generations :

— first generation : fine lamellar spherulite aggregates of saponite spread in the serpentinized and low talcized mass of diopsidic and garnet skarns ;

— second generation : thin oriented flakes of saponite, forming macro-crystals, whose optical features could be determined, developed as veins in the same rocks. It is possible that these saponite macrocrystals, which exceed 0.7/0.4 mm in size, would represent twins and pseudotwins resulting from epitaxial growth of saponite sheets (L o d d i n g, 1972).

Mg-silicates of skarns are either completely or partially substituted for thin sheets of serpentinic minerals like deweyllite, talc and saponite of the first generation.

A mixture of deweyllite, talc and saponite may be observed under microscope in the brown mass of the hydrothermalized skarns which replaces the phenocrystals of Mg-silicates in skarns.

TABLE 1

The lattice spacings (d/n) and relative intensities (I_0) of serpentinized and saponitized skarn *

No	d/n	I_0	No	d/n	I_0
1	14.40	35	10	2.565	58
2	9.40	20	11	2.497	100
3	7.30	27	12	2.148	25
4	4.55	81	13	1.720	16
5	4.20	30	14	1.680	8
6	3.640	36	15	1.529	30
7	3.340	20	16	1.519	68
8	3.180	26	17	1.507	20
9	3.015	13			

* Semioriented slide, scanned from 2° to 31°θ, at the rate of 1°/minute by TUR-M 61 *X*-ray diffractometer. Cu Kα radiation, Ni filter; 30 kV, 25 mA; d/n are measured in Å and I_0 on a scale 1-100. The same conditions for Table 2.

The *X*-ray diffraction study of serpentinized and argillized skarns has also revealed the presence of deweyllite, talc and saponite (Tab. 1; Fig. 1).

As shown in Table 1 and Figure 1 the main reflections of the diffractogram belong to deweyllite with a slight influence of the reflections

of the common serpentine (chrysotyle-antigorite). The saponite was identified by means of the 14.40, 4.55 and 1.519 Å reflections. Subordinately there occurs talc (9.4 Å).

By heating at 600°C for 2 hours the (001) reflection of saponite changes its position from 14.40 Å to 9.40 Å, superposing itself on the (001) reflection of talc (Fig. 1).

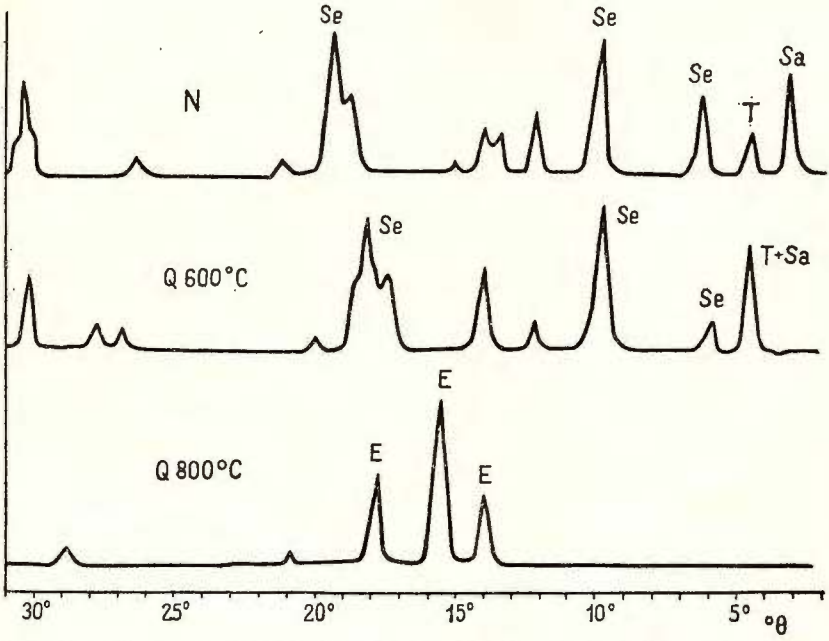

Fig. 1. — Diffractogram of semioriented sample of the Sasca Montană serpentinized and saponitized skarn (Scanned between 2—31°θ, Cu Kα radiation, Ni filter, 30 kV, 25 mA. Symbols: N = untreated sample; Q 600°C = heated sample at 600°C for 2 hours; Q 800°C = heated sample at 800°C for 2 hours; Sa = saponite; T = talc; Se = deweyllite; E = enstatite).

By heating at 800°C for 2 hours both the deweyllite and saponite turn into enstatite (Fig. 1).

When examining with the optical microscope the second generation saponite appears like oriented sheets forming macrocrystals, coloured green-brown pale with a very weak pleochroism having a strong birefringence (second order). Extinction angle is 0°. Elongation positive. The refraction indices of saponite macrocrystals of the second generation are: Ng = 1.555; Nm = 1.525; Np = 1.490.

The saponite macrocrystals are reaching 0.70/0.40 mm in size.

The results of the *X*-ray study of the second generation of saponite are shown in Table 2 and Figure 2.

As we can observe in Table 2 and Figure 2 the main reflections of saponite are : 14.40, 4.57, 2.503 and 1.520 Å. The reflection d = 3.034 Å does also indicate the presence of calcite.

By heating at 600°C for 2 hours, saponite changes the positions of its (001) reflection from 14.40 Å to 9.40 Å, superposing itself on the (001) reflection of talc. By glycoling the d(001) basal reflection of

TABLE 2

The lattice spacings (d/n) and the relative intensities (I_0) of saponite macrocrystals

No	d/n	I_0	No	d/n	I_0
1	14.40	100	7	3.034	40
2	7.30	20	8	2.576	30
3	4.96	10	9	2.503	60
4	4.57	55	10	1.734	20
5	3.820	10	11	1.690	10
6	3.340	20	12	1.520	70

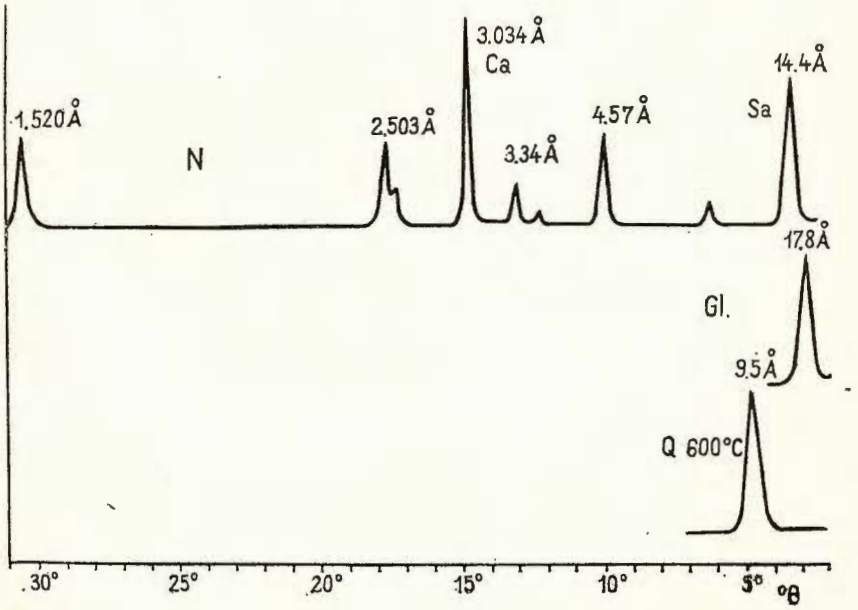

Fig. 2. — Diffractogram of semioriented sample of saponite macrocrystals in the veins (Scanned between 2—31°θ, Cu Kα radiation, Ni filter, 30 kV, 25 mA. Symbols : N = untreated sample ; Gl = glycolated sample ; Q 600°C = heated sample at 600°C for 2 hours ; Sa = saponite ; Ca = calcite).

saponite increases from 14.40 Å to 17.80 Å by absorbtion of two molecular layers of glycerol.

In conclusion within the Sasca Montană area the Mg-hydrothermal argillization-saponitization process has been described for the first time. The first generation of saponite occurs in close connection with the serpentinization phenomena, and the second generation of saponite forming large macrocrystals is found in the veins which penetrated the serpentinized skarns.

REFERENCES

Lodding W. (1972) Diagenesis of macrokaolinites. *Proc. of the Internat. Clay Conf. Kaolin Symposium*, Madrid.

MACROCRYSTALS OF A WELL-ORDERED TRICLINIC KAOLINITE FROM MOLDOVA NOUĂ (BANAT)[1]

BY

VASILICA PIEPTEA, GHEORGHE NEACŞU[2]

Sommaire

Macrocristaux de kaolinite triclinique largement cristallisée de Moldova Nouă (Banat). Dans les cornéennes quartzitiques de Moldova Nouă on a identifié à l'oeil nu des macrocristaux de kaolinite triclinique largement cristallisée, mis en évidence aussi par les analyses de diffraction *X*. Les analyses microscopiques ont établi que les dimensions des macrocristaux de kaolinite examinés sont supérieures à 0,10 mm. Les cornéennes quartzitiques à kaolinite apparaissent au contact d'un corp subvolcanique banatitique avec des calcaires mésozoïques ; en ces conditions la formation de la kaolinite semble avoir eu lieu à la suite des processus endogènes.

Introduction

In this paper the authors are discussing about the occurrence of kaolinite macrocrystals in the banatitic contact zone. The last investigations on the ore deposits have already pointed out the presence of kaolinite owing to the action of hydrothermal acid solutions (Tröger, 1969). Large kaolinite crystals have been quoted in sedimentary rocks : in kaolins from Georgia, USA (Hinckley, 1961 ; Conley, 1966), in Tonstein, Germany (Moore, 1964), in Lower Lias claystone layers, France (Auger, 1972). The large development of kaolinite crystals has also been mentioned in Romania (Papiu et al., 1968 ; Papiu et al., 1971). Mansfield and Bayley (in Lodding, 1972) studied over 50 kaolinite flakes of sand and silt grain-size using the single crystal *X*-ray method, and found that all are twins and pseudotwins intergrowths ;

[1] Paper presented at the 2nd National Clay Conference, April 11—12, 1975, Bucharest.

[2] Întreprinderea geologică de prospecţiuni pentru substanţe minerale solide, str. Caransebeş 1, Bucureşti.

the twin crystals are rotated about 120° to the normal (001). Auger (1972) studied the kaolinite macrocrystals with a scanning electron microscope and stated that they may reach the size of 0.5 mm. Lodding (1972) found by textural analyses kaolinite macrocrystals ranging from 0.07 to 0.20 mm in size.

Occurrences

The kaolinite sample was collected in the Moldova Nouă area from the 5 c gallery, opened on the north-eastern range of the Suvorov subvolcanic body. This gallery crossed the following petrographical complexes :

1. The banatitic body, which consists of porphyritic quartz-diorite with a disseminated copper mineralization (porphyry copper ore deposit).

2. Mesozoic limestones, which are surrounding the plutonic contact and have undergone a thermal and low-grade metasomatic metamorphism. It resulted in recrystallized calcitic limestones (with a small proportion of iron, manganese and magnesia) as well as contact rocks with actinolite. In crystalline limestones the copper mineralization is much more developed than in banatitic rocks, and consists of the same minerals (pyrite, chalcopyrite, seldom digenite and chalcocite).

3. The quartzitic hornfels complex, which also displays a thermic and metasomatic metamorphism. The parent rocks are no more to be seen. As a result of the rise of the temperature and the introduction of Si and K, the primary formations turned into quartzitic hornfelses with micaceous minerals (Pl. I; Pl. II, Fig. 1—2) and further on into micaceous quartzites. The quartzitic hornfelses with micaceous minerals contain idiomorphic pyrite crystals as accessory mineral. In these rocks we have to mention as another characteristic accessory mineral the zircon idiomorphic crystals (Pl. I, Fig. 1—4), which we consider of endogenous nature owing to the pneumatolysis generated by the igneous body (Rittman, 1967). From metre 0 to metre 60 the gallery passed through the complex of quartzitic micaceous hornfelses in which kaolinite forms rare aggregates of microscopic size. At metre 25 we met with a concentration of kaolinite, so that the rock may be considered as kaolinite hornfelses. At the metre 60th the gallery entered the recrystallized limestones.

Petrographical and mineralogical data

Macroscopically the kaolinite hornfels is differing from the micaceous one. While the latter is intensively hard owing to the high content of recrystallized quartz, the former is aphanitic and crumbling ; it is pink coloured due to the presence of scattered hematites. On fine fissures (1 mm in cross-section), there are deposits of pure, white coloured kaolinite as well as deposits of quartz.

The microscopical analysis of the rock proved that it is composed of quartz and kaolinite in almost equal quantities. The grains of quartz

present a detrital-like aspect, being only non-uniformly recrystallized. They generally vary in size (from 0.05 mm to 0.20 mm), and are irregularly shaped. The kaolinite cements the grains of quartz. The two minerals are intimately associated as a result of recrystallization during the metamorphism process. The texture of the rock shows deformations. On fine fissures there are deposits of quartz with low degrees of crystallization (Pl. IV, Fig. 3). Generally isotropic [3] under the crossed nicols, the kaolinite appears also crystallized. Owing to their birefringence kaolinite macrocrystals, frequently ranging from 0.05 to 0.10 mm in size, some of them exceeding 0.10 mm, could be measured. Nm = 1.565. Kaolinite macrocrystals arranged almost perfectly parallel form either slightly bent aggregates or radiating aggregates. These roll-shaped kaolinite aggregates are concentrated in nests and veins (Pl. II, Fig. 4; Pl. III, IV).

Paragenesis

The rock composed of kaolinite and partially recrystallized quartz as principal minerals, contains also accessory minerals. We have to mention the presence of minute idiomorphic rutile crystals, which vary between 0.01—0.05 mm, and generally have an oriented pattern (Pl. II, Fig. 3). In the kaolinite-quartzitic hornfels there have been estimated by chemical analysis 0.159% Fe and 0.7% Ti[4].

The quartzitic hornfelses with micaceous minerals contain as accessory minerals idiomorphic pyrite crystals, larger rutile crystals (up to 0.14 mm) and constantly zircon crystals (up to 0.15/0.05 mm), generally idiomorphic, the latter frequently presenting a zonary structure (Pl. I, Fig. 3).

X-ray diffraction analyses

The *X*-ray diffraction patterns of samples were taken by the TUR-M 61 *X*-ray diffractometer, Cu Kα radiation with a Ni-filter. The samples were scanned from 6° to 32° θ at the rate of 0.5°/minute (shift of arm), 30 kV, 25 mA (Tab.; Fig).

The $< 10\ \mu$ fraction was separated by the sedimentation method in distilled water.

As shown in Table all the lines of perfectly crystallized T kaolinite are to be noticed (B r i n d l e y, 1951); the interplane spacings have the same position as the triclinic kaolinite but their relative intensities are variable. Some reflections are more intensive (4.45; 4.35; 4.16; 4.11;

[3] On the whole thin section kaolinite was set off by using 0.5% methylblue solution (M i e l e n z, 1950 in T r ö g e r, 1969).

[4] The analyses were made in the I.G.P.S.M.S. laboratories by the chemist A n a R ă d u c a n u.

2.24 Å), some are less intensive (particularly 2.37; 1.98; 1.93; 1.84; 1.78; 1.58; 1.54 Å).

The Hinckley crystallinity index of kaolinite macrocrystals is 1.50 higher than Zettlitz and Cornwall kaolinite, indicating a very well-ordered triclinic kaolinite (Hinckley, 1963).

The ratio of the intensities of (001) and (002) reflections increases from 0.97 for unoriented sample to 1.05 for semi-oriented sample and 1.33 for oriented sample.

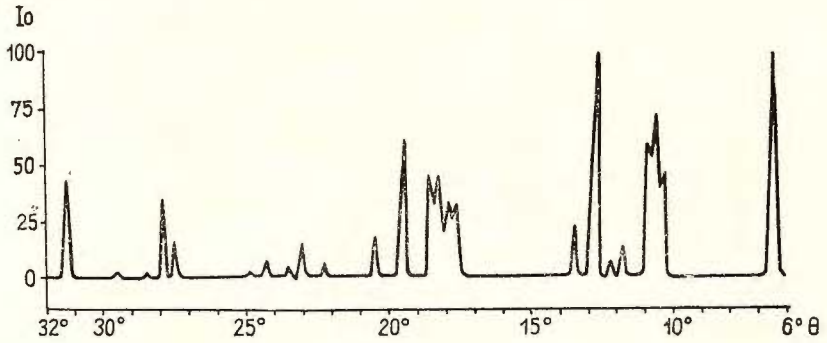

The diffractogram of kaolinite macrocrystals from Moldova Nouă.

TABLE

Lattice spacings (d/n) and relative intensities (I_0) of well-crystallized kaolinite from Moldova Nouă (macrocrystals)

N_0	d/n	I_0	N_0	d/n	I_0	N_0	d/n	I_0
1	7.15	97	12	2.742	4	23	1.978	22
2	4.44	52	13	2.551	50	24	1.933	8
3	4.35	74	14	2.516	38	25	1.890	12
4	4.16	70	15	2.485	61	26	1.840	5
5	4.11	42	16	2.372	20	27	1.780	5
6	3.834	32	17	2.333	78	28	1.678	22
7	3.730	17	18	2.278	67	29	1.657	48
8	3.565	100	19	2.236	24	30	1.614	18
9	3.350	35	20	2.174	8	31	1.575	5
10	3.135	8	21	2.126	15	32	1.537	10
11	3.090	5	22	2.057	7	33	1.485	50

After heating for two hours at 600°C the basal reflection series disappear.

On the bulk sample diffractogram do appear all the quartz reflections.

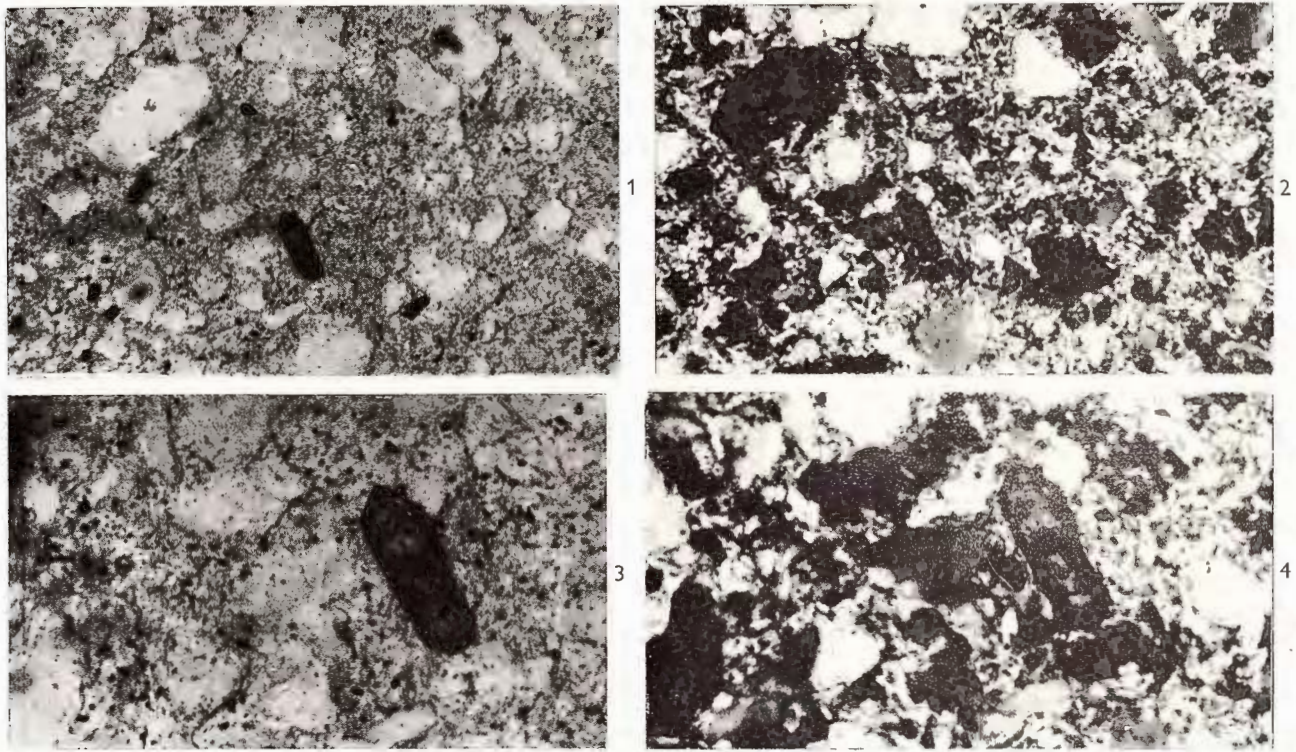

Fig. 1. — Quartzitic hornfels with micaceous minerals. An idiomorphic crystal of zircon is to be seen ; N|| (×65).
Fig. 2. — Idem, N +.
Fig. 3. — The same image enlarged. The idiomorphic zircon crystal presents a zonary structure ; N|| (×160).
Fig. 4. — Idem, N +.

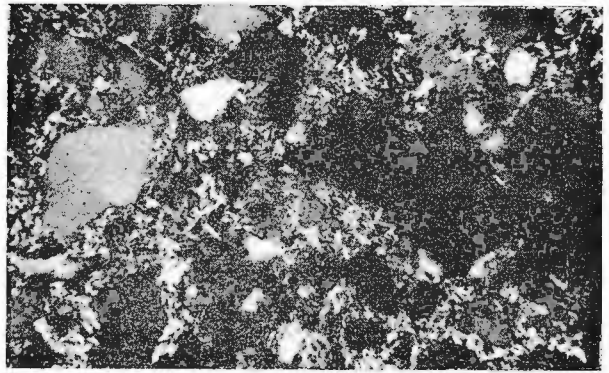

1

2

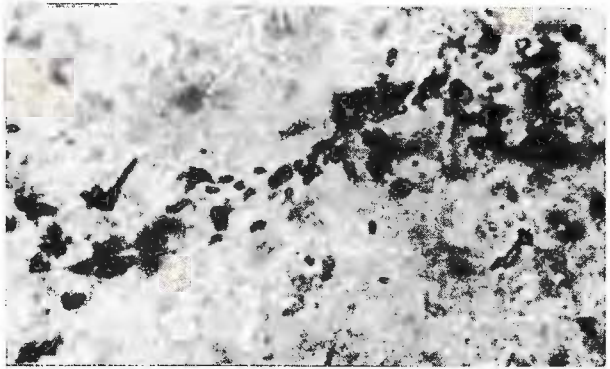

3

4

Fig. 1. — Quartzitic hornfels with micaceous minerals ; N + (× 160).
Fig. 2. — A fissured quartz crystal with a partially euhedral contour is to be seen in a quartzitic hornfels ; N + (× 65).
Fig. 3. — Rutile with parallel orientation in kaolinite hornfels ; N|| (× 320).
Fig. 4. — Kaolinite crystals with parallel orientation form roll-like aggregates which are set off owing to birefringence.

VASILICA PIEPTEA, G. NEACȘU. Well-Ordered Triclinic Kaolinite Macrocrystals from Banat. Pl. III.

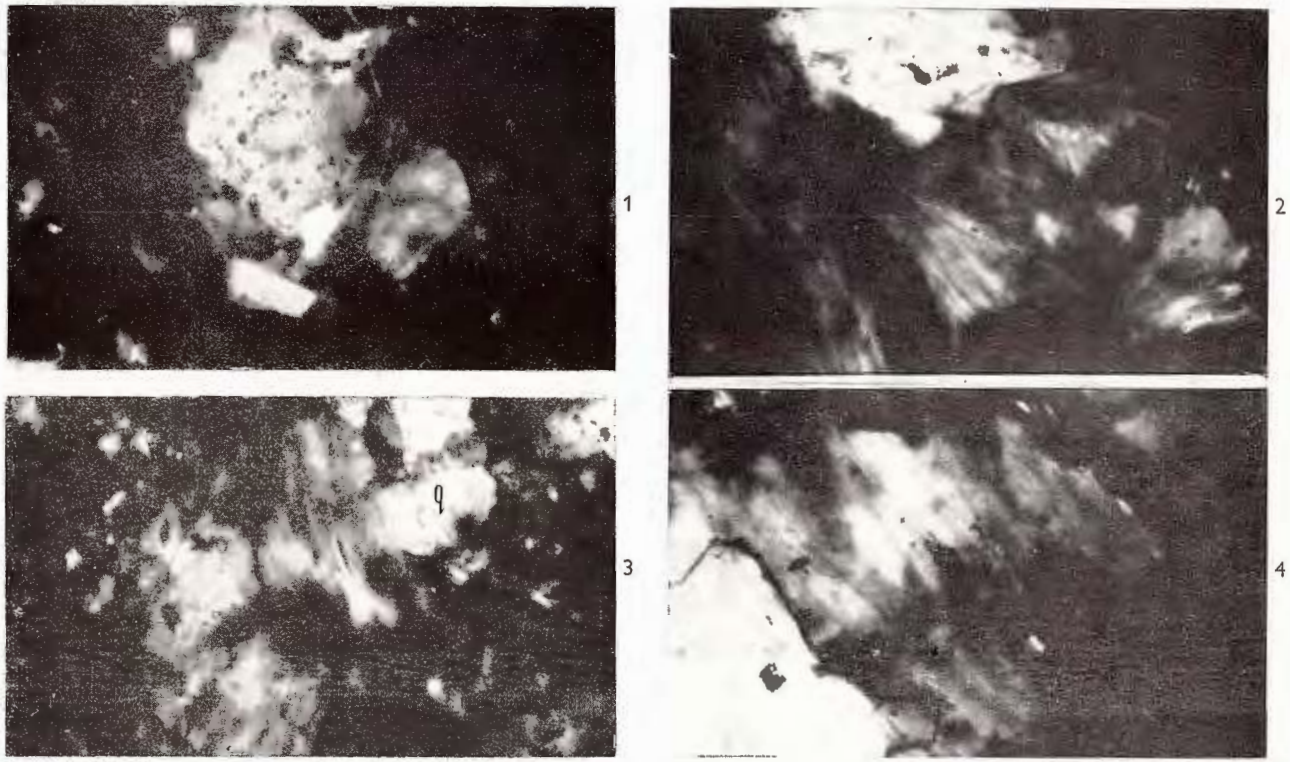

Fig. 1. — In an isotropic mass parallel disposed kaolinite crystals are forming a bent aggregate (at right). At left a quartz crystal with fluid inclusions is noticed ; N + (×320).

Fig. 2. — Kaolinite radiating aggregates. In the upper part of the photo a quartz crystal with fluid inclusions may be observed. N + (×320).

Fig. 3. — Parallel disposed kaolinite crystals forming bent aggregates. The kaolinite is associated with quartz (q) ; N + (× 320).

Fig. 4. — Kaolinite aggregates. At the left side downwards a quartz crystal is noted ; N + (× 320).

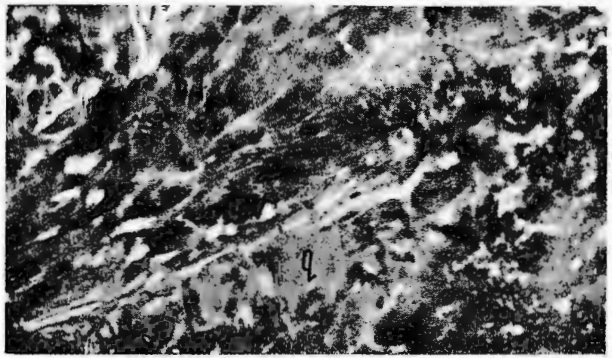

1

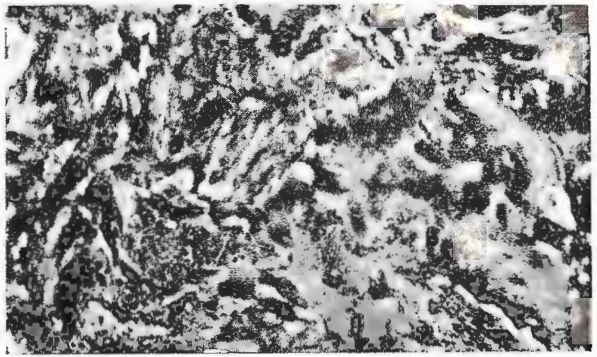

2

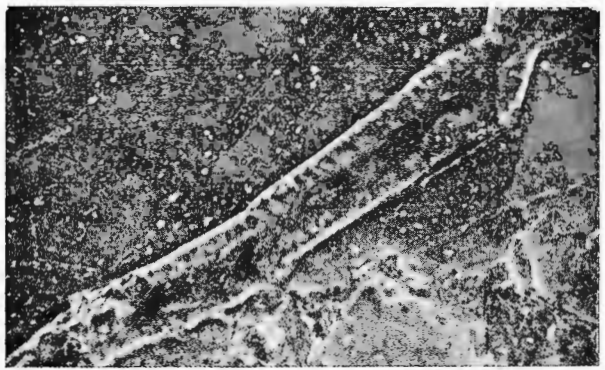

3

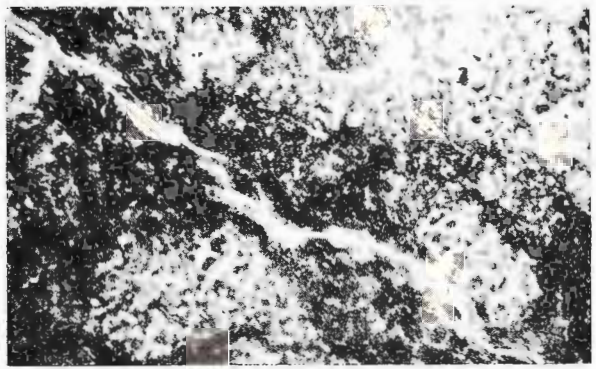

4

Fig. 1. — Paragenesis of quartz-kaolinite. Kaolinite forms radiating aggregates; phase-contrast, (× 200).

Fig. 2. — Between the quartz granoblasts (q) lamellar kaolinite crystals forming bent aggregates ; phase-contrast, (× 200).

Fig. 3. — In kaolinite quartzitic hornfels occur also quartz veinlets; phase-contrast, (× 100).

Fig. 4. — Kaolinite hornfels containing hydrous iron oxydes. Along a fissure a deposition of pure white kaolinite; phase-contrast, (× 100).

Genesis

The oriented disposition of the rutile in the rock indicates the introduction of volatile constituents. This observation is in agreement with the opinion of other researchers. Bonorino, 1959 (in Deer et al., 1967) discussing the hydrothermal alteration of an ore deposit from Colorado (Front Range mineral belt), explains the origin of alteration zones by chemical fronts, developed as a result of gaseous fluid migration. The critical changes of the composition of fluids would have been determined by the modification of the Si : Al ratio, variation of K concentration and of *pH*. In our case some of these conditions would have varied locally. In response to some composition gradients (decrease of K concentration and of *pH*) and also to a lowering of temperature, kaolinite has formed instead of micaceous minerals. It is noteworthy that the kaolinite hornfels presents a lower grade of recrystallization of quartz in comparison with the micaceous one due to the lower temperature of the metamorphism process.

Hence we conclude that the occurrence of kaolinite macrocrystals in the Moldova Nouă area is of an endogenous nature at the contact of the banatitic body with the recrystallized limestones. The relatively high temperature at which the kaolinite had formed is attested by the derived rock, a quartzitic hornfels with kaolinite respectively. The kaolinite macrocrystals have resulted from a pneumatolytic-hydrothermal metamorphic process. The participation of the pneumatolytic metamorphic process is confirmed by the presence of rutile, and so as in the micaceous hornfels, we notice an addition of zircon. In the micaceous hornfels complex there have locally formed kaolinite hornfelses owing to some local changes of the composition and temperature gradients.

We appreciate that the hydrothermal solutions in the Moldova Nouă area could have allowed an enlargement of kaolinite crystals by epitaxial growth.

Acknowledgements. The authors are indebted to the Geological Survey of IPEG Moldova Nouă for assistance in their collecting of samples.

REFERENCES

Auger F. (1972) Cristallisation exceptionelle de kaolinite dans le Lias inférieur de Vendée (France). *Proc. of the Intern. Clay Conference, Kaolin Symposium*, Madrid.

Brindley G. W. (1951) *X*-ray identification and crystal structures of clay minerals. Mineral Soc., London.

Conley R. F. (1966) Statistical distribution patterns of particle size and shape in Georgia Kaolins. *Clays and clay minerals*, 14, p. 257—264, *Pergamon Press*, Oxford.

Deer W. A., Howie, R. A., Zussman J. (1967) Rock-forming minerals. vol. 2, Longmans, London.

Hinckley D. N. (1961) Mineralogical and chemical variations in the kaolin deposits of the Coastal Plain of Georgia and South Carolina. The Pennsylvania State Univ., Ph.D. Thesis.

— (1963) Variability in crystallinity values among the kaolin deposits of the Coastal Plain of Georgia and South Carolina. *Clays and Clay Min., 11th Nat. Conf.*, p. 229—235, *Pergamon Press*, Oxford.

Lodding W. (1972) Diagenesis of macro-kaolinite. *Proc. of the Intern. Clay Conference, Kaolin Symposium*, Madrid.

Moore L. R. (1964) The in situ formation of some kaolinite macrocrystals. *Clay Minerals Bull.*, 5, 31, p. 338—357, England.

Papiu C. V., Minzatu Silvia, Iosof V., Giușcă R., Jacotă G. (1968) Contribuții la cunoașterea alcătuirii mineralogice și genezei lehmului bauxitelor din masivul Pădurea Craiului (Munții Apuseni). *D.S. Inst. Geol.* LIV/1 (1966—1967), București.

— Minzatu Silvia, Iosof V., Udrescu Constanța, Giușcă R. (1971) Alcătuirea chimică mineralogică a formațiunii bauxitifere din bazinul Hațegului. *D.S. Inst. Geol.*, LVII (1969—1970), București.

Pieptea Vasilica, Ciornei A., Weingartner R. (1973) Mineralizația cupriferă de tip diseminat din corpul subvulcanic Suvorov, regiunea Moldova Nouă, *D.S. Inst. Geol.*, LIX/2, 65—67, București.

Rittman A. (1967) Vulcanii și activitatea lor. Edit. tehnică, București.

Tröger W. E. (1969) Optische Bestimmung der gesteinsbildenden Minerale. Teil 2. Schweizerbartische Verlagsbuchhandlung, Stuttgart.

LA CLINOPTILOLITE DANS LES TUFS DE TRANSYLVANIE[1]

PAR

FLORICA POPESCU[2], H. ASVADUROV[3]

Abstract

Clinoptilolite in the Tuffs of Transylvania. The clinoptilolite was identified in some tuffs from Transylvania. The mineralogical and chemical features are similar to the ones described in the relevant literature. The potassium-clinoptilolite was confirmed by its thermic behaviour. The semi-quantitative determination of clinoptilolite from investigated tuffs was achieved using two samples of almost pure clinoptilolite (95% and 96%) found in the Mirşid-47 and Perşani tuffs. Clinoptilolite is potentially valuable for many industrial and agricultural processes.

La clinoptilolite décrite en 1890 par Pirson (en Mumpton, 1960) a été dénommée ainsi par Schaller en 1932. À présent elle est considérée comme une zéolite appartenant au groupe de l'heulandite, mais plus riche en silice (supérieur à 60% SiO_2 d'après Hey, Banister, 1934 et Mumpton, 1960) et dans le contenu de laquelle prédominent les cations Na^+ et K^+ par rapport au Ca^{2+} (Mason, Sand, 1960).

Les applications et l'utilisation industrielle de la clinoptilolite ont eu ces dernières années une large extension (Shepard, 1971). La clinoptilolite est utilisée notamment dans : la purification des eaux polluées ou résiduelles (par l'adsorbtion de l'ion NH_4^+) ; le traitement des déchets radioactifs (par l'adsorbtion des isotops radioactifs de Cs et Sr) ; la séparation industrielle de l'oxygène et de l'azote atmosphérique ; la deshumidification des gas ; l'amélioration et la fertilisation des sols, etc.

[1] Communiqué à la deuxième Conférence Nationale des Argiles, 11—12 Avril, 1975, Bucarest.

[2] Institutul de geologie şi geofizică, str. Caransebeş 1, Bucureşti.

[3] Institutul de cercetări pedologice şi agrochimice, Bd. Ion Ionescu de la Brad 4, Bucureşti.

Comme suite à l'identification de ce minéral dans quelques dépôts tuffacés de la plate-forme de Someş (A s v a d u r o v et al., 1974; P o p e s c u et al., 1975) et tenant compte de son importance scientifique et pratique nous avons considéré nécessaire de faire une étude plus poussée du point de vue minéralogique et chimique.

Le but de ce travail a été de dépister la présence de la clinoptilolite dans les roches tuffacées d'autres régions de la Transylvanie, de préciser la teneur en ce minéral dans ces roches et de mettre en évidence ses caractéristiques minéralogiques et chimiques.

Méthodes de recherche

Nous avons exécuté des analyses sur des échantillons prélevés sur des dépôts tuffacés et sur des tufs d'âge badénien des environs des localités : Mirşid (district de Sălaj), Jichiş, Tărpia, Viile Dej, Bădeşti, Codor (district de Cluj), Şinca Veche, Perşani (district de Braşov), Slătioara, Cuştiui et Bîrsana (district de Maramureş).

Les 30 échantillons étudiés ont été récoltés soit des affleurements, soit à différents niveaux de profondeur (entre 5 et 8 m) des carrières existantes à Şinca Veche, Perşani, Cuştiui et Bîrsana.

Pour tous les échantillons nous avons exécuté les analyses roentgénographiques des fractions < 2 et < 10 μ sur lames orientées autant que des échantillons bruts (en poudre).

L'analyse thermique différentielle et les analyses chimiques ont été exécutées seulement dans le cas des roches qui ont présenté un intérêt spécial. Pour tous les échantillons nous avons déterminé la teneur en K_2O accessible (mg. a 100 g roche) et pour la majorité de ces échantillons nous avons également déterminé les cations échangeables.

Résultats analytiques

En étudiant les échantillons par diffraction des rayons X (tab. 1; fig. 1—4) nous avons constaté dans tous les échantillons collectés et analysés la présence de la clinoptilolite. L'identification d'une clinoptilolite presque pure (96%) dans l'échantillon de Perşani (100—120cm) nous a permis :

a) son étude minéralogique et chimique;

b) son utilisation comme standard dans l'appréciation sémi-quantitative de la teneur des autres roches tuffacées.

La clinoptilolite a été déterminée d'après les équidistances d caractéristiques données par la diffraction des rayons X : 9,00; 7,94; 3,97 et 2,96 Å. La vérification faite par le traitement thermique suivi d'irradiation (tab. 1; fig. 1) a permis l'identification de :

a) la clinoptilolite potassique résistante jusqu'à 750°C pour la majorité des échantillons;

b) la clinoptilolite calcique résistante jusqu'à 550°C (seulement pour les échantillons de Viile Dej et de Bîrsana).

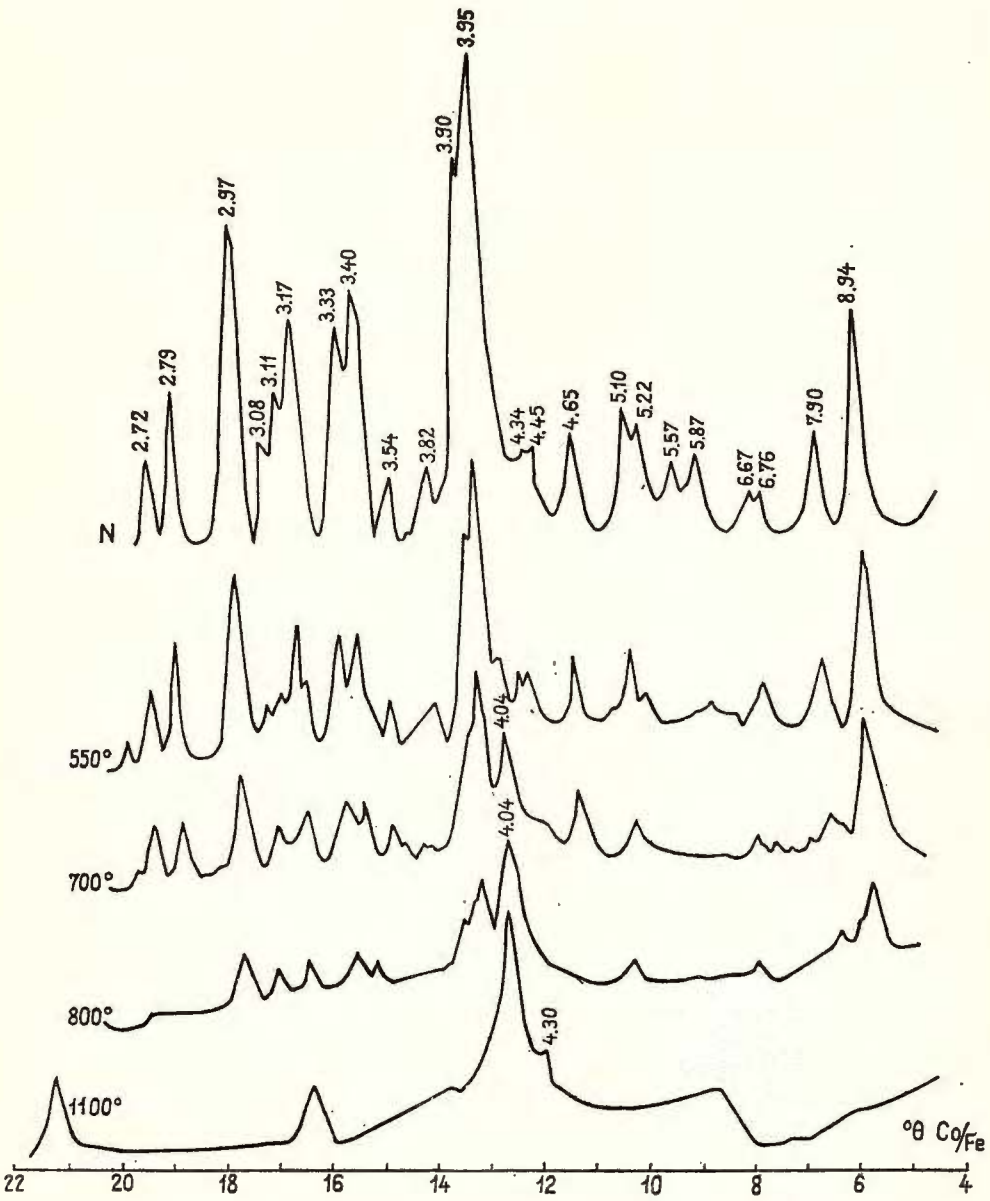

Fig. 1. — Comportement thermique, poursuivi par diffraction *R.X.*, d'une clinoptilolite des tufs de Perşani.

L'analyse thermique différentielle a confirmé à son tour l'existence de la clinoptilolite par l'endotherme dû à la perte en eau de constitution, même au dessous de 200°C ; la différence par rapport à l'heulandite, qui présente un endotherme accentué à 300°C, est évidente (fig. 2).

TABLEAU 1

Liste des indices, équidistances et intensités des principales raies des diagrammes R.X., des poudres de clinoptilolite

hkl	Perşani 100—120 cm		Cuştiui 100—120 cm		Bîrsana 800—820 cm		Mirşid-47 30—50 cm	
	d(Å)	I	d(Å)	I	d(Å)	I	d(Å)	I
020	8,94	40	9,00	80	9,00	70	9,00	40
002	7,90	25	7,90	25	7,90	25	7,95	20
110	6,76	20	6,70	20	6,67	20	6,75	15
111	6,67	10	6,64	10	6,56	10	6,67	15
	5,87	20	5,91	10	5,95	10	5,95	10
112	5,57	20	5,56	10				
	5,22	25	5,22	20	5,20	15	5,18	25
	5,10	25	5,10	25	5,07	25	5,10	20
130	4,65	25	4,62	25	4,61	25	4,67	20
	4,45	10			4,45	15	4,38	25
113	4,34	15	4,35	15	4,33	20	4,30	25
004	3,95	100	3,96	100	3,96	100	3,96	100
132	3,90	70	3,92	85	3,92	90	3,92	80
	3,82	20			3,83	20	3,80	20
200	3,73	15	3,73	15	3,70	15	3,70	15
133	3,54	20	3,55	20	3,53	20	3,56	15
202, 220	3,40	40	3,42	25	3,42	40	3,42	40
222	3,17	40	3,14	35	3,14	35	3,17	35
	3,11	25	3,10	30	3,11	30	3,10	25
203	3,08	10			3,07	30		
	3,08	10	3,04	20			3,06	20
060, 152	2,97	70	2,97	60	2,95	60	2,97	60
					2,88	10	2,88	10
	2,97	45	2,77	30	2,78	40	2,80	30
204	2,72	30	2,72	25	2,72	20	2,73	20
	2,68	10	2,66	15	2,66	10		
	2,55		2,55		2,55		2,54	15
	2,50	10	2,50	10	2,51	10	2,51	25
	2,44	20	2,44	20	2,43	20	2,43	20

La teneur en clinoptilolite, dans les échantillons analysés (tab. 2) a été appréciée ainsi :

— entre 5—15% dans les dépôts plus altérés, à porosité plus élevée, pauvres en matériel tuffacé ;

TABLEAU 2

Distribution sémi-quantitative des composants minéralogiques (%) — estimée par diffraction R.X.

Localité	Profondeur m	Clinoptilolite		Minéraux argileux	Quartz	Feldspath	V_K	K_2O accéssible mg
		K	Ca					
a) Dépots tuffacés								
Mirşid-18	0,15—0,25	85		13	2		32,8	1 680
Tărpia	0,15—0,25	15		70	5	2	11,8	250
Jichiş	0—0,18	10		75	5	2	12,0	108
Bădeşti	0—0,15	15		70	5	2	12,9	192
Cuştiui	0,18—0,28	50		15	16	4	39,8	936
Slătioara	0,09—0,17	85			12		39,8	1 056
Perşani	0—0,20	5		50	35	6	10,9	102
Şinca Veche	0—0,20	10		45	35	8	10,3	90
b) Roches compactes								
Mirşid-17		95			3		45,6	1 420
Şinca Veche	1—1,2	40		40	10		22,3	384
	3—3,2	55		30	10			576
	5—5,2	65		20	10		28,9	744
	8—8,2	75		10	5			624
Perşani	1—1,5	96			4		44,8	1 014
	5—5,2	90			5			624
Cuştiui	1—1,2	80		5	11		35,1	605
	8—8,2	84		5	8		38,5	533
Birsana	1—1,2		80	10	8		19,9	187
	8—8,2		78	10	10		16,4	108
Viile Dej	0,5—0,7		85		10			

Note: la différence jusqu, à 100% est représentée par le matériel amorphe.

— entre 40—95% et avec de faibles variations de la proportion en sens vertical, dans les roches compactes.

Les dépôts à teneur réduite en clinoptilolite contiennent jusqu'à 70% matériaux argileux, comme par exemple:

a) la montmorillonite prédominante;

b) l'illite et les minéraux interstratifiés illite-montmorillonite auxquels s'associent le quartz et parfois le feldspath.

Dans le cas des échantillons qui contiennent des quantités importantes de minéraux argileux le contenu en clinoptilolite est plus important dans la fraction < 10 μ que dans le fraction < 2 μ (fig. 3); d'ailleurs la clinoptilolite est mentionnée fréquemment dans la fraction < 4 μ ou entre 5 et 1 μ (d'après Butuzova, 1964, cité par Travnicova et al., 1973).

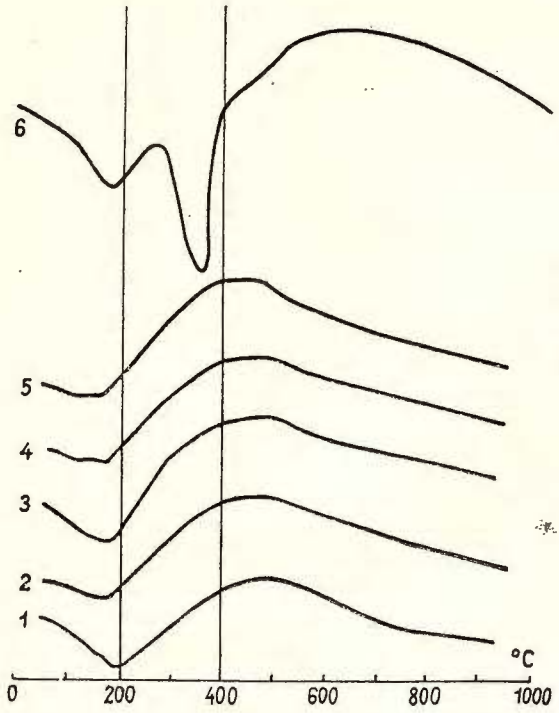

Fig. 2. — Courbes de l'analyse thermique différentielle, des échantillons de clinoptilolite provenant de: (1) Hector — Californie, (2) Mirşid, (3) Bîrsana, (4) Perşani, (5) Cuştiui — Transylvanie et (6) l'heulandite de Prospect Park — New Jersey.

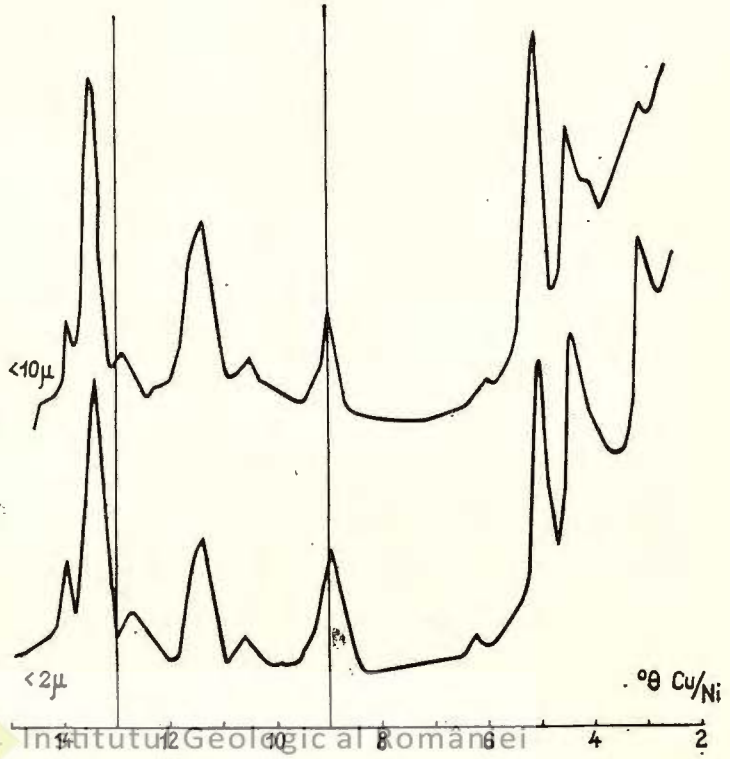

Fig. 3. — Diffractogrammes *R.X.* des fraction $< 2\ \mu$ et $< 10\ \mu$ séparés de la suspension aqueuse de quelques dépôts tuffacés.

Dans les diffractogrammes du même échantillon on a observé une orientation préférentielle d'après le plan (0k0) sur les lames orientées par rapport aux poudres, exemple Mirşid (fig. 4) :

a) pour l'équidistance d correspondant à (020) les intensités des raies sont de 100 pour les lames orientées et seulement de 50 pour les poudres ;

b) pour l'équidistance *d* correspondant à (060) les intensités des raies sont respectivement de 75 et de 65.

La clinoptilolite (96%) Perşani, chauffée en étapes jusqu'à 1100°C indique à 550° C l'apparition de la cristobalite ($d = 4{,}04$ Å) qui à partir de 700° C augmente en contenu, tandis que celui de la clinoptilolite diminue (fig. 1). À 1100° C on observe la formation de la trydimite ($d = 4{,}30$ Å).

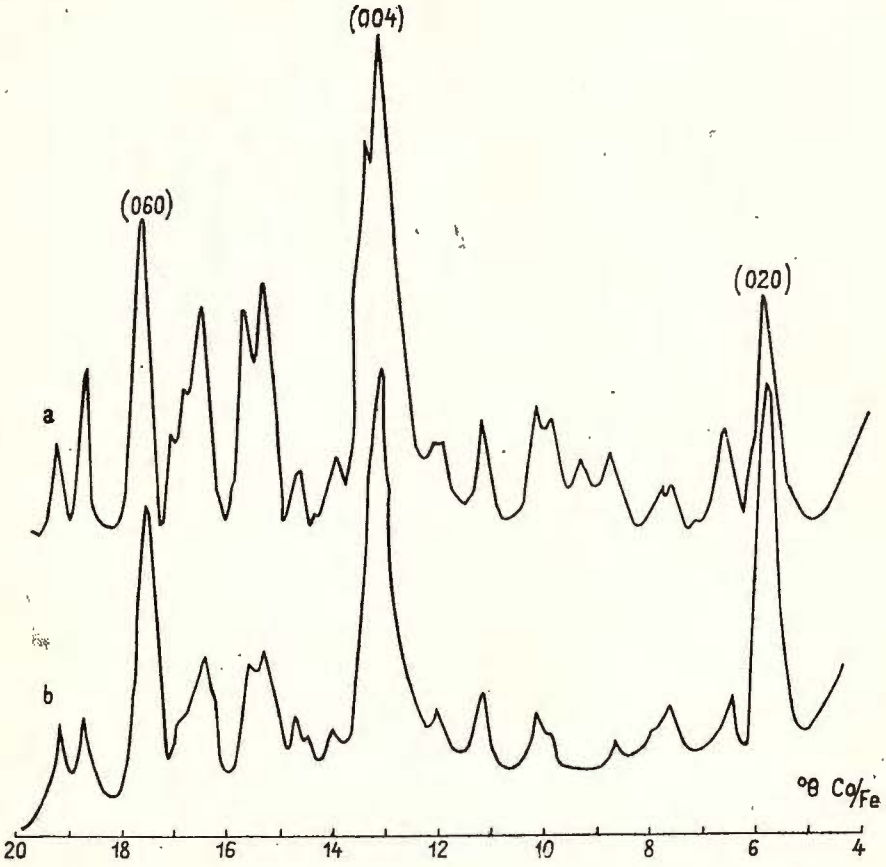

Fig. 4. — Diffractogrammes *R.X.* de la clinoptilolite des tufs de Mirşid-47, (*a*) en poudre, (*b*) lame orientée.

Analyse chimique des roches

Les caractéristiques chimiqo-minéralogiques de la clinoptilolite et de quelques tufs sont indiquées dans le tableau 3.

En général il est difficile de faire des appréciations sur la composition originele des tufs excessivement altérés comme ceux analysés dans notre étude (remarque faite aussi par Surdam, Parker, 1972; Iijima et al., 1968; Bradley, Eugster, 1969).

TABLEAU 3

L'analyse chimique des tufs à clinoptilolite (g % matériel séché à 105°C)

Oxydes	Şinca V. 8—8,2 m	Perşani 1—1,2 m	Perşani + 1—1,2 m	Bîrsana 8—8,2 m	Mirşid-47 0,3—0,5m	Mirşid-47 ++ 0,3—0,5 m
SiO_2	66,90	68,10	66,77	67,65	69,43	67,62
Al_2O_3	12,10	11,80	12,37	12,37	11,00	11,56
Fe_2O_3	1,03	0,95	0,99	1,50	1,03	1,09
TiO_2	0,11	0,15	0,16	0,28	0,11	0,12
MnO	0,04	0,04	0,04	0,04	0,04	0,04
CaO	3,50	2,44	2,54	2,74	2,66	2,81
MgO	1,10	1,34	1,40	1,71	0,91	0,97
Na_2O	0,28	0,39	0,41	0,57	0,29	0,31
K_2O	2,51	3,35	3,49	1,10	3,25	3,46
$H_2O^{-105°}$	8,49	7,46	7,77	8,00	7,62	8,01
$H_2O^{+105°}$	4,06	3,90	4,06	3,48	3,80	4,01
Total	100,12	99,92	100,00	99,44	100,14	100,00
			Rapports moléculaires			
$\frac{Si}{Al + Fe}$	4,11		4,37	4,15		4,69
$\frac{Na+K}{Na+K+Ca+Mg}$	0,42		0,53	0,31		0,53

Analyste: Erna Călinescu, I.G.G.

\+ Valeurs recalculées après l'extraction de 4% SiO_2 (quartz dét. *R.X.*)

++ „ „ „ „ 5% SiO_2 „ „ „

Néanmoins d'après la teneur en SiO_2 de 67—68% (tab. 3), qui correspond à 71,8—72,7% pour le matériel séché à 100°C, ces roches sont plus proches des rhyolites, qui contiennent 72,8% SiO_2, que des dacites avec 65,68% SiO_2 (Codarcea, 1951).

De même le rapport Si/Al + Fe pour les roches à clinoptilolite est de 4,37 ou 4,69 et pour les rhyolites de 4,10. Un approchement entre les tufs à clinoptilolite et les rhyolites a été fait aussi par Hay (1966).

Pour les échantillons de Perşani (100—120) et de Mirşid-47 qui se sont différenciés comme des clinoptilolites presque pures (96% et 95%) nous avons calculé les suivantes formules chimiques :

Perşani-47.

$Na_{0,35}\ K_{1,95}\ Ca_{1,19}\ Mg_{0,91}\ Al_{6,39}\ Fe_{0,32}\ Si_{29,33}\ O_{72}.\ 18H_2O^4$

Mirşid-47

$Na_{0,26}\ K_{1,93}\ Ca_{1,32}\ Mg_{0,63}\ Al_{5,97}\ Fe_{0,36}\ Si_{29,71}\ O_{72}\ .18H_2O^4$

Les rapports Na + K/Na + K + Ca + Mg (~0,57) et ceux Si/Al+F (4—5) caractéristiques de la clinoptilolite (S h e p p a r d, 1971) se véri-

TABLEAU 4

Analyse des cations échangeables de quelques dépôts tuffacés (a) et roches compactes (b) avec clinoptilolite

Localité	Profondeur m	Cations échangeables T méq.	% du T Ca^{2+}	Mg^+	K^+ (Vk)	Na^+	H^+	V %	*pH*	K accessible mg
a) Dépôts tuffacés (sols)										
Mirşid-48	0,2—0,35	137,3	55,6	5,9	32,8	1,0	4,7	95,3	6,5	1 394
Tărpia	0—0,15	113,8	76,5	6,9	11,8	0,9	3,9	96,1	7,1	206
Jichiş	0—0,18	29,7	57,5	17,5	12,0	1,2	11,8	88,2	6,7	103
Bădeşti	0—0,15	61,4	72,3	6,8	12,9	0,9	7,2	92,8	6,5	159
Cuştiui	0—0,20	60,3	42,3	4,9	39,8	0,9	12,1	87,9	5,5	777
Slătioara	0,9—0,17	79,4	41,9	3,4	39,8	0,5	14,4	85,6	5,0	877
Perşani	0—0,20	26,1	55,0	11,5	10,9	1,8	20,8	79,2	5,6	84
Şinca Veche	0—0,20	25,8	53,9	12,8	10,3	2,7	20,3	79,7	5,6	74
b) Roches compactes										
Mirşid-47	0,3—0,5	131,6	40,5	3,8	45,6	5,8	4,3	95,7	5,6	1 179
Şinca Veche	1—1,2	104,5	54,1	18,9	22,3	1,6	3,1	96,9	5,4	319
	5—5,2	154,6	59,0	9,7	28,9	1,7	0,7	98,3	7,2	617
Perşani	1—1,2	151,5	46,8	5,8	44,8	1,8	0,8	99,2	6,5	841
Cuştiui	1—1,2	138,8	54,4	7,8	35,1	1,2	1,5	98,5	6,5	502
	8—8,2	138,9	52,9	5,5	38,5	2,2	0,9	99,1	6,4	442
Bîrsana	1—1,2	130,4	62,6	10,4	19,9	6,4	0,7	99,3	7,6	153
	8—8,2	144,3	56,2	4,7	16,4	22,2	0,5	99,5	—	—

Analyste: Maria Constantinescu, I.C.P.A.

fient dans le cas des échantillons de Perşani et de Mirşid ; les valeurs calculées pour les autres échantillons ne sont pas représentatives parce qu'ils contiennent d'autres minéraux.

L'échantillon de Bîrsana avec une tendance (MgO + CaO) de 4,45% et seulement de 1,65% ($Na_2O + K_2O$) confirme l'existence de la clino-

ptilolite à Ca. Le même échantillon se fait remarquer aussi par l'instabilité thermique (après chauffage à 550° C pendant 4 heures).

Le contenu en K_2O de 1,52—3,49% comparé à celui en Na_2O (0,28—0,36%) pour plusieurs échantillons nous indique une clinoptilolite plus riche en potassium qu'en sodium (à Şinca, Perşani et Mirşid).

Généralement la teneur en K_2O de 1,3—3,48% ne justifie pas la remarquable quantité de potassium échangeable dans les échantillons analysés; ce phénomène est dû à la structure du réseau spécifique aux zéolites, qui dans ce cas peut éliberer facilement les ions de K^+.

Analyse des cations échangeables et du contenu en K_2O accessible aux plantes

Entre le contenu en clinoptilolite et celui en potassium échangeable et accessible aux plantes on remarque plusieurs relations importantes (tab. 4).

La capacité d'échange cationique (T) élevée et le contenu en K échangeable (V_K) très grand surtout dans le cas des roches (T compris entre 100 et 156,4 méq. et V_K compris entre 22 et 45%) sont des propriétés dues à leur nature zéolitique.

Les roches qui contiennent de la clinoptilolite potassique présentent des valeurs du K_2O accessible remarquables (comprises entre 384 et 1420 mg pour 100 g).

Sans pouvoir affirmer l'existence d'une relation directe entre la proportion en clinoptilolite et les valeurs V_K ou K_2O accessible, on observe tout de même un accroissement de ces valeurs à mesure que la teneur du minéral dans le tuf augmente.

Le taux de saturation élevé (V = 85 — 95%) ne correspond pas aux valeurs basses du *pH* (5,2—6,5); probablement les valeurs du *pH* sont influencées par les gels de silice dérivant de l'altération du verre volcanique.

Conclusions

1. La présence de la clinoptilolite dans tous les tufs provenant de différentes régions de Transylvanie suggère la possibilité de son existence aussi dans d'autres tufs de Roumanie; le minéral respectif peut être considéré comme caractéristique des tufs badéniens [4].

2. L'analyse chimique de quelques roches et de la clinoptilolite indique leur relation avec des éruptions rhyolitiques plutôt qu'avec celles dacitiques.

3. Les roches compactes sont en général les plus riches en clinoptilolite (ex. à Mirşid-47 et Perşani) fait établi par l'analyse de diffraction *R.X.* et vérifié par l'ATD.

4. La clinoptilolite la plus fréquemment rencontrée est celle potassique, fait qui explique les grandes valeurs de la capacité d'échange V_K et K_2O accessible.

[4] En 1974 nous avons identifié aussi des zéolites comme la clinoptilolite calcique dans les tufs de Pietrari et de Rîmnicul Vîlcea (district de Vîlcea).

5. L'apparition de la cristobalite et de la trydimite, à la suite du traitement thermique, peut être utilisée dans l'interprétation de la genèse et dans les relations de paragenèse des roches tuffacées.

6. La capacité d'échange élevée et la grande possibilité d'élibérer le potassium suggère l'expérimentation de ces tufs dans l'amélioration et la fertilisation des sols.

Aussi considérons-nous que bon nombre de nos tufs sont des roches zéolitiques et nous espérons que les résultats des recherches géologiques et minéralogiques prochaines confirmeront l'importance économique de ces roches et établiront leur distribution dans les différentes régions de notre pays.

BIBLIOGRAPHIE

Asvadurov H., Codarcea Venera, Conescu A. (1974) Soluri formate pe unele tufuri din Podișul Someșan, *I.S.C.P., A.S.A.S.*, 40, București.

Bradley W. H., Eugster H. P. (1969) Geochemistry and paleolimnology of the trona deposits and associated authigenie minerals of the Green River Formation of Wyoming. *U.S. Geol. Survey Prof. Paper*, 496-B, p. 71, Washington.

Codarcea A. (1951) Manualul inginerului de mine, Secția I-a, Geologie și petrografie, Edit. tehn., p. 280—281, București.

Deer W. A., Howie R. A., Zussman J. (1965) Rock Forming Minerals. *Framework Silicates*, 4, Edit. Longmans, London.

Hay R. L. (1966) Zeolites and zeolitic reactions in sedimentary rocks. *Geol. Soc. Amer. Spec. Paper* 85, p. 130, Washington.

Hey M. H., Bannister F. A. (1934) „Clinoptilolite'' a silica rich variety of heulandite, Part 7 of Studies on the zoolites. *Mineralog. Mag.* 23, 145, p. 556—559, London.

Iijima A., Hay R. L. (1969) Analcime composition in tuffs of the Green River Formation of Wyoming. *Amer. Min.* 53, p. 184—200, Menasha — Wisconsin.

Mason B. H., Sand L. B. (1960) Clinoptilolite from Patagonia — The relation-ship between clinoptilolite and heulandite, *Amer. Min.* 45, p. 341—350, Menasha — Wisconsin.

Mumpton F. A. (1960) Clinoptilolite redifined, *Amer. Min.* 45, no 3—4, p. 351—369 Menasha—Wisconsin.

Popescu Florica, Codarcea Venera, Asvadurov H. (1973) Mineralogical composition of some tuffaceous deposits rich in exchangeable potasium. *Proc. of the first National Clay Conference — Bucharest* 1973, *Stud. tehn. econ.*, I 13, *Inst. Geol. Geof.*, București.

Schaller W. T. (1932) The mordenite-ptilolite group, clinoptilolite, a new species. *Amer. Min.* 17, 4, p. 128—134, Menasha — Wisconsin.

Sheppard R. A. (1971) Clinoptilolite of Possible Economic Value in Sedimentary Deposits of the Conterminous United States. *U.S. Geol. Survey Bull.* 1332-B, Washington.

— Gude A. J. (1971) Sodic Harmotome in Lacustrine Pliocene Tuffs near Wikieup, Mohave Country, Arizona. *U.S. Geol. Survey Prof. Paper* 750-D, p. 50—55, Washington.

Steven T. A., Van Loenen R. E. (1971) Clinoptilolite-bearing tuffs beds in the creede formations, San Juan Mountains, Colorado. *U.S. Geol. Survey Prof. Paper* 750-C, p. 98—103, Washington.

Surdam R. C., Parker R. D. (1972) Authigenic Aluminosilicate Minerals in the Tuffaceous Rocks of the Green River Formation, Wyoming. *Geol. Soc. of Amer. Bull.* 83, p. 689—700, Colorado.

Travnicova L. S., Gradusov B. P., Cijicov N. P. (1973) Zeoliți în unele soluri, Pocivovedenie, 3, Edit. „Știința", Moscova.

MINERALOGY AND GENESIS OF CLAYS IN THE MIOCENE MOLASSE OF THE EAST CARPATHIANS [1]

BY

SILVIU RĂDAN[2]

Sommaire

Minéralogie et genèse des argiles de la molasse miocène des Carpates Orientales. La distribution des minéraux argileux dans les dépôts miocènes est tributaire de deux sources : (1) à l'est une chaîne appartenant à l'avant-pays (caractérisée par illite + chlorite + kaolinite) ; (2) à l'ouest les zones exondées de l'arc carpatique (caractérisées par illite + montmorillonite + chlorite ± kaolinite). Dans le secteur moldave du bassin molassique l'avant-pays a joué un rôle important au cours de la sédimentation de la *formation salifère inférieure*, de la *formation rouge* et du *complexe du gypse de Perchiu*. À la partie supérieure du Miocène inférieur la montmorillonite s'exprime de manière explosive dans les dépôts de la *formation grise*, surjacente au gypse, marquant l'intervention de la source occidentale ainsi que le début de l'activité volcanique dans les Carpates Orientales. En Munténie la chaîne carpatique a constitué une source permanente pendant l'accumulation des dépôts miocènes, de sorte que la montmorillonite y est toujours présente. Dans la genèse des argiles miocènes l'héritage mécanique est le phénomène majeur, les néoformations caractérisent surtout les niveaux tuffacés et les transformations sont plus marquées dans le sel miocène inférieur, où les interstratifiés tendent à une régularisation vers l'allevardite.

Introduction

The clay mineral assemblages yielded by the land to the modern seas and oceans depend mainly upon the composition of the exposed bedrock and the intensity of the weathering process (the latter controlled by climate) in the adjacent continental source areas. The clay minerals transported to the sedimentary basins by rivers and, to a lesser degree, by winds are subsequently redistributed by marine currents, and become

[1] Paper presented at the 2nd National Clay Conference, April 11—12, 1975, Bucharest.

[2] Institutul de geologie și geofizică, str. Caransebeș 1, București.

subject to diagenetic processes. So, the clay minerals occur both as a clastic material and a diagenetic product.

The ancient sediments can preserve the initial distribution patterns of clay minerals if the shallow-burial stage of the diagenesis was not exceeded. As pointed out by Dunoyer (1969), in the deep-burial stage all the clay mineral assemblages tend to be replaced by a binary assemblage : illite + chlorite, which screens in this way the initial pattern of distribution.

On the other hand, the flysch deposits, even if they did not reach the anchizone conditions, are generally devoid of kaolinite and montmorillonite, showing the "classic" assemblage illite — (mica) — chlorite. However, this mineralogical peculiarity is not common as to the molasse deposits, which cover a wide lithofacies range and contain rich and varied clay mineral assemblages (Kubler, 1970).

A first informative study on clay mineralogy of Oligocene (flysch) and Miocene (molasse) deposits in the Romanian East Carpathians (Rădan, Mîndroiu, 1971) [3], pointed out the presence of montmorillonite and kaolinite, together with illite and chlorite, both in Oligocene and in Miocene samples. The investigations focused subsequently on Miocene provided the image of the clay mineral distribution as a whole, and demonstrated the possibility to utilize the clay minerals for sedimentological purposes in the East Carpathians Molasse (Rădan, Bratosin, 1975) [4].

The present paper is a concise summary of mineralogical data solely. All the Miocene lithostratigrafic horizons exposed in different tectonic units of the East Carpathians were sampled. Clay fractions ($< 2\ \mu$) separated from 249 samples, systematically collected from varied localities, were *X*-rayed, and a semiquantitative evaluation of the clay mineral contents was performed by Biscaye's (1965) method. It was not possible to make a distinction between kaolinite and chlorite using the 3.54 Å and 3.57 Å peaks (004 for chlorite and 002 for kaolinite, respectively).

Acknowledgements. The author would like to thank Prof. P. Bourguignon and Prof. J. Thorez for their aid and encouragements during his laboratory works carried out at the Liège University (Belgium), in 1970. Thanks are also due to Mr. I. Vanghelie and Mrs. Florica Popescu of the Institute of Geology and Geophysics, Bucharest, for help with *X*-ray analytical techniques.

Historical summary

Detailed geological studies on Miocene formations in some large areas of the East Carpathians have been carried out mainly by Filipescu (1940), Popescu (1951), Dumitrescu (1952), Joja (1952), Săndulescu (1962), Mirăuţă (1965, 1969), Saulea (1965),

[3] I.G.G. Archives.

[4] I.G.G. Archives.

Polonic, Gabriela Polonic (1967), Macarovici et al. (1967). The most essential data were synthetized in the explanatory notes annexed to the geological map of Romania (1 : 200,000) edited by the Geological Institute (1968—1970) [5]. In this respect, the lithofacial atlas of Romanian Neogene deposits is also of interest (Saulea, 1969).

Some of the above-mentioned authors paid special attention to sedimentary processes, that were operating during the Miocene time, in order to gain a better understanding of the environmental conditions under which the East Carpathians Molasse was deposited. Hence, a particular importance present some sedimentological investigations performed by Panin (1964), Dimian, Elena Dimian (1964), Dumitriu, Cristina Dumitriu (1964), Panin, Ştefana Panin (1967), Polonic, Gabriela Polonic (1968) and Grujinschi (1972) [6].

No references can be quoted on the clay mineralogy of the East Carpathians Molasse since this topic has not been so far studied.

Regional geology

The Miocene and Pliocene Molasse deposits are mainly included in the inner folded limb of the Foredeep (the so-called Subcarpathian Unit or Neogene Zone), and also extend over the areas of several more internal Flysch units (Marginal, Tarcău and Macla Nappes) (Fig. 1).

In the southern (Muntenian) part of the East Carpathians Bend (west of the Buzău Valley), the Neogene Zone is also called the Zone of the Diapir Folds. Northwards to the Diapir Folds Zone, the Miocen e formations of two important synclines are obliquely intersecting the Flysch Zone : Drajna Syncline is covering a part of the Tarcău Unit, and the Slănic Syncline (the northernmost one) covers partially the Tarcău, Macla, Teleajen and Ceahlău Units. Also, in Moldavia, Upper Miocene-Lower Pliocene deposits of the intramontane Comăneşti Depression are overlying the Tarcău and Marginal Nappes.

The stratigraphic features of the Miocene deposits within all the above-mentioned areas are very complex, and it is quite difficult to achieve in brief a coherent and complete correlation scheme.

The Lowermost Miocene sequence starts with an evaporitic horizon represented by the *Lower Gypsum Horizon* (part of the so-called *Cornu Beds*), especially developed within Slănic and Drajna Synclines, and the *Lower Salt Formation*, well represented in the Diapir Folds Zone and in the Moldavian Subcarpathians. The *Salt Formation* occurs either bedded or brecciated contains lenticular gypsum, salt and potassium salts and is replaced in the North Moldavia by a thick conglomeratic horizon (*Lower Almaşu Conglomerates*).

In Mutenia, the Lower Miocene continues with the *Upper Horizon of the Cornu Beds* (sedimentary clayey-marly breccia, conglomerates, sandstones, black shales) followed by the *Brebu Conglomerates* (red and grey polymictic conglomerates and sandstones). In Moldavia, the *Salt Formation* is overlain by the *Condor Sandstone* (feldspathic sandstones and marls) and/or a variegated (*Red*) formation (red, green and grey sandstones, marls and microconglomerates) The latter contains in some areas of South Moldavia a basal red conglomeratic horizon (*Bîrseşti*

[5] An up-to-date synthesis on the East Carpathians Miocene deposits is just in preparation under the guidance of Dr. M. Săndulescu.

[6] Thesis of Doctor's Degree, University of Bucharest Archives.

Conglomerates) which can reach a large vertical extent in Central and North Moldavia (*Pietricica* and *Pleşu Conglomerates*). The *Red Formation* (so-called especially in the southern segment of the Subcarpathian Unit) is more or less isofacial and synchronal with the *Hîrja Beds, Măgieşti Beds, Borzeşti Beds, Tescani Beds, Solca Beds* and *Moişa Sandstone* (green sansdtones and shales) within various structural units or geographical areas. In North Moldavia, the *Lower Almaşu Conglomerates* are overlain by *Almaşu Sandstone* (green and reddish shales and sandstones), *Upper Almaşu Conglomerates* and *Moişa Sandstone*.

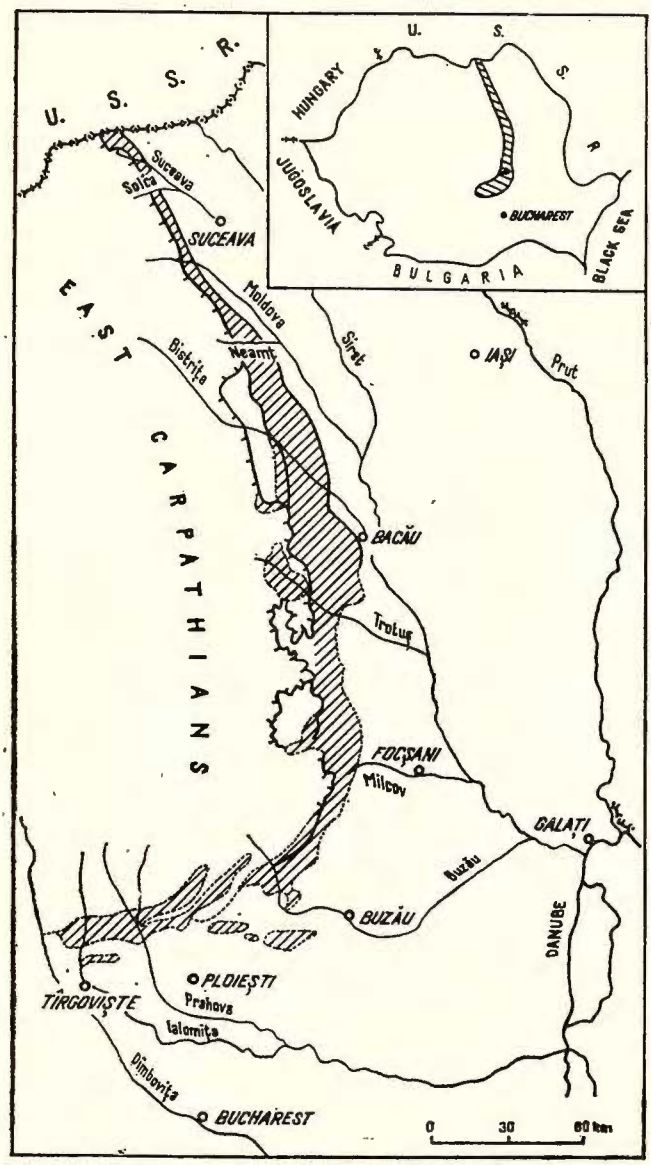

Fig. 1. — Location of Miocene Molasse deposits in the East Carpathians.

The upper part of the Lower Miocene consists of thick „Schlier" and/or flysch-like deposits, red and grey in Muntenia (*Upper Gypsum Horizon*) and predominantly grey in Moldavia (*Perchiu Gypsum Horizon* and *Grey Formation*). Gypsum beds, tuffs and thin laminated dolomites and/or limestones are intercalated at certain levels, but represent, rather seldom, regional stratigraphic guide horizons (except *Perchiu Gypsum Complex*).

The Middle Miocene sequence comprises four lithological units (in ascending order) : *Slănic Tuff* (tuffs and Globigerina marls), *Upper Salt Formation*, also called *Salt Breccia* (sedimentary breccia, shales, salt, gypsum), *Radiolarian Shales* (shales, sands, tuffs and gypsum beds) and *Spirialis Marls* (grey marls, sandstones, tuffs). In some areas of Central and South Moldavia there are two main lithological complexes : *Răchitaşu Sandstone* (sandstones, tuffs, Globigerina marls) and *Haloş-Sărăţelu Beds* (sands, grey marls, Radiolarian shales, Spirialis marls, tuffs, gypsum beds).

The Upper Miocene formations are developed only in Muntenia (oolitic and shelly limestones, marls, clays, sands, conglomerates), in South Moldavia and southern part of Central Moldavia (clays, marls, sandstones, conglomerates, andesitic sandstones, limestones), and also in the Comăneşti Depression (conglomerates, sandstones, sands, clays and coal).

The sedimentological data concerning source area activity and paleocurrent directions indicate that during the Miocene, the Carpathians were a permanent source area for the southern segment (Muntenia) of the molasse basin. In the central segment (Moldavia), the Foreland represented the main source area for *Lower Salt Formation*, *Condor Sandstone*, *Red Formation* and their equivalents, and the Carpathian Bend, for *Grey Formation* deposits. A brief reactivation of supplies from the Foreland source area took probably place at the beginning of the Middle Miocene, followed by the definitive setting up of the sedimentary supplies from the Carpathians.

Results

The semiquantitative distribution of clay minerals in the Miocene formations of the East Carpathians is presented in the Figures 2—7. *X*-ray diffraction analyses performed on 249 samples indicate that illite is ubiquitous in these deposits (except bentonite layers), montmorillonite and chlorite are important clay mineral constituents (showing sometimes preferential occurrences), and kaolinite (in this paper included in chlorite percentages) is generally present in small amounts. Variable contents of vermiculite, mixed-layer clay minerals and clinoptilolite (?) have been also identified.

Lower Miocene. The main lowermost formations of the Miocene Molasse show quite distinct clay mineral assemblages, as it can be seen in Figure 2. So, in Moldavia, the *Lower Salt Formation* and *Lower Almaşu Conglomerates* are characterized by a binary assemblage (55—90% illite + + 10—45% chlorite), or even a monomineral one (illite only), occasionally accompanied by random mixed-layer structures of the 10—14 V, 10—14 M and 14 C—14 M type. The *Lower Gypsum Horizon* cropping out in Muntenia only, contains instead of the above-mentioned assemblage a ternary one, including variable amounts of montmorillonite (5—25%, exceptionally 70%) together with illite (55—70%) and chlorite (10—35%); 10—14 M mixed-layers are constantly present.

A quite peculiar clay mineral suite is provided by the salt deposits from Tîrgu Ocna (Central Moldavia) included in the *Lower Salt Formation* (samples 82—86). The thin clayey interbeds occasionally occurring within the salt deposits do certainly contain, besides illite and chlorite, small amounts (10—20%) of random mixed-layer clay minerals approaching

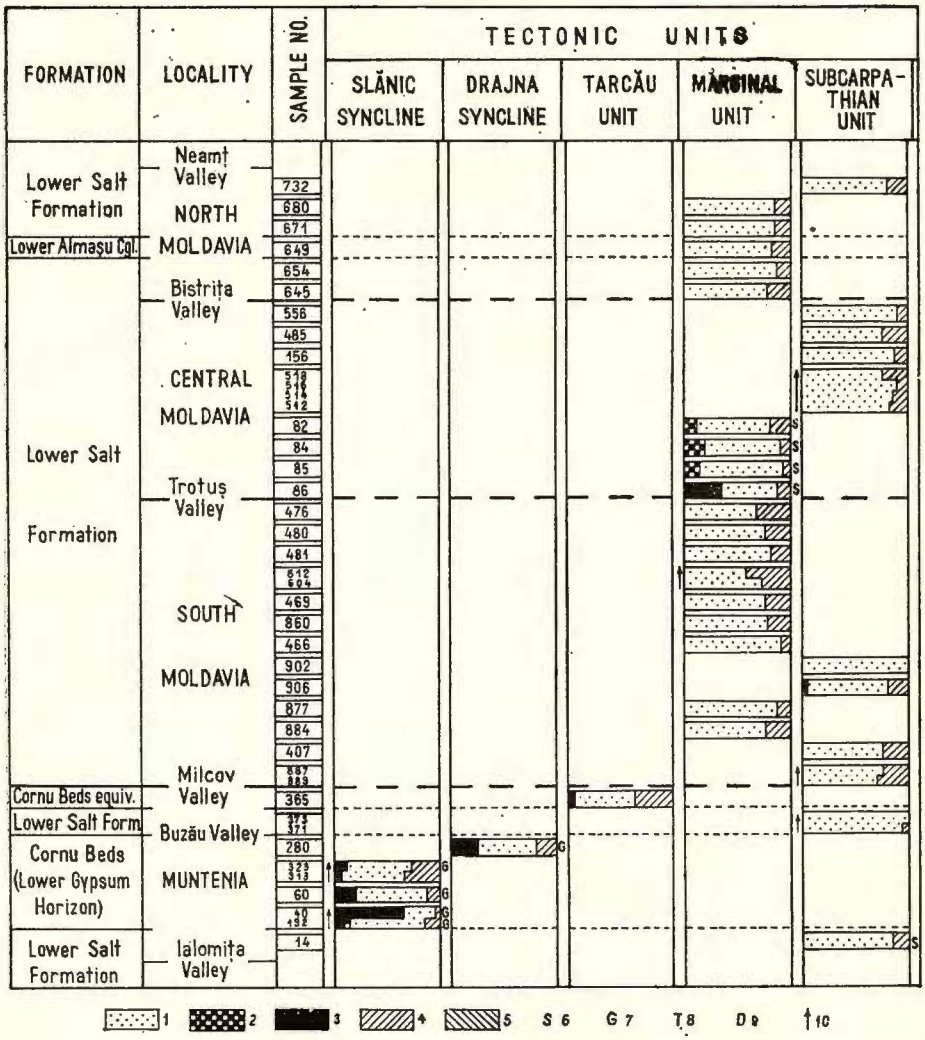

Fig. 2. — Distribution of clay mineral assemblages in the Lower Miocene formations (Cornu Beds — Lower Gypsum Horizon, Lower Salt Formation and Lower Almaşu Conglomerates). Clay minerals : 1, illite ; 2, I-M (allevardite-like) ; 3, montmorillonite ; 4, chlorite (± kaolinite) ; 5, vermiculite. Associated rocks : 6, salt ; 7, gypsum ; 8, tuff ; 9, thin laminated dolomites and/or limestones. 10, samples collected in normal stratigraphic order.

regular interlayering of allevardite type. A clay "pebble" containing montmorillonite (35%) is also to be noted in salt. In contrast with the salt deposits of Tîrgu Ocna, the clays intercalated in the Ocniţa salt massif (Muntenia) do not contain any montmorillonite (sample 14). Few per cent of montmorillonite were identified in *Salt Breccia* of the Valea Sării area (sample 906); taking into account that the age of this "breccia" is controversial, the occurrence of montmorillonite would be in agreement with the opinion of those authors who consider the *Salt Formation* of Valea Sării as Middle Miocene in age.

The next formation succeeding in the Lower Miocene sequence, shows similar pattern of clay mineral distribution as the lowermost ones (Fig. 3). In Moldavia, the *Red Formation* and its equivalents preserve the same binary assemblage as their underlying deposits: illite (55—90%) and chlorite (10—45%) with subsidiary random mixed-layers of the 10—14 M, 10—14 V and 14 C—14 M type. Some samples (5 of 47) collected from *Moişa Sandstone* (3), *Condor Sandstone* (1) and *Red Formation* (1) contain 5—10% montmorillonite. In the Putna Valley area (South Moldavia) small amounts of vermiculite (5—30%) were also identified in the *Bîrseşti Conglomerates* and *Red Formation*.

In Muntenia the *Upper Horizon of Cornu Beds* and *Brebu Conglomerates* resemble the *Lower Gypsum Horizon* in clay mineral composition: 55—75% illite, 15—40% chlorite and 5—30% montmorillonite; the latter is missing in one sample. A gradual change of clay mineralogy was observed along the Slănic Syncline: for both horizons of *Cornu Beds* chlorite becomes scarcer from east (35% in average) to west (15% in average), concomitantly with an increase of montmorillonite proportion (from 5 to 35% in average).

The upper part of the Lower Miocene sequence reveals a marked difference in mineralogy of clay fractions for almost all its constitutive formations (Fig. 4). In Moldavia, the *Perchiu Gypsum Complex* is still generally characterized by illite (50—80%) and chlorite (20—40%) with various random mixed-layers; in the Bistriţa Valley area (Ciritei quarry and Iapa Valley) some clayey intercalations within gypsum complex contain, however, 5—10% montmorillonite. The *Grey Formation* well developed over the *Perchiu Gypsum*, and largely widespread in Moldavia shows, for the first time in this area, a clear-cut ternary assemblage: illite (35—90%), chlorite (5—35%) and montmorillonite (5—50%). The latter becomes more important than chlorite and occasionally comes to be the single component of the clay fraction (in bentonitized tuffs). The random mixed-layers, always present, are almost invariably of the 10—14 M type (in few cases even allevardite-like).

In Muntenia, the *Upper Gypsum Horizon* continues the underlying *Cornu Beds* as regards clay mineralogy, but even in this case the increasing importance of montmorillonite is to be noticed (as it may also reach 100% in bentonitized layers). Illite, still prevailing (10—90%), and chlorite, subordinated (5—35%), complete the common ternary assemblage; the random mixed-layers of 10—14 M type remain, also, ubiquitous

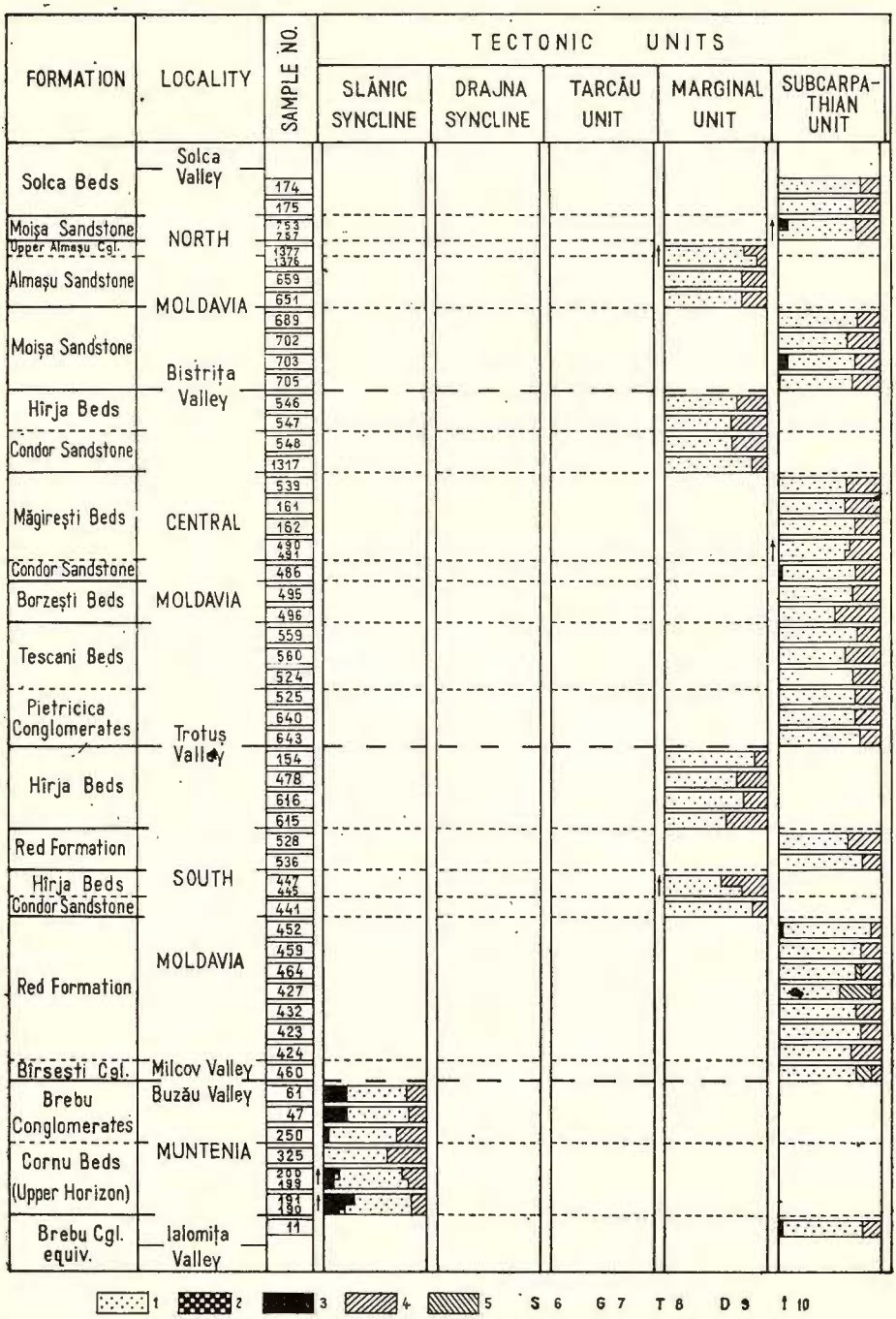

Fig. 3. — Distribution of clay mineral assemblages in the Lower Miocene formations (Cornu Beds — Upper Horizon, Brebu Conglomerates, Red Formation and its equivalents).

See explanation Fig. 2.

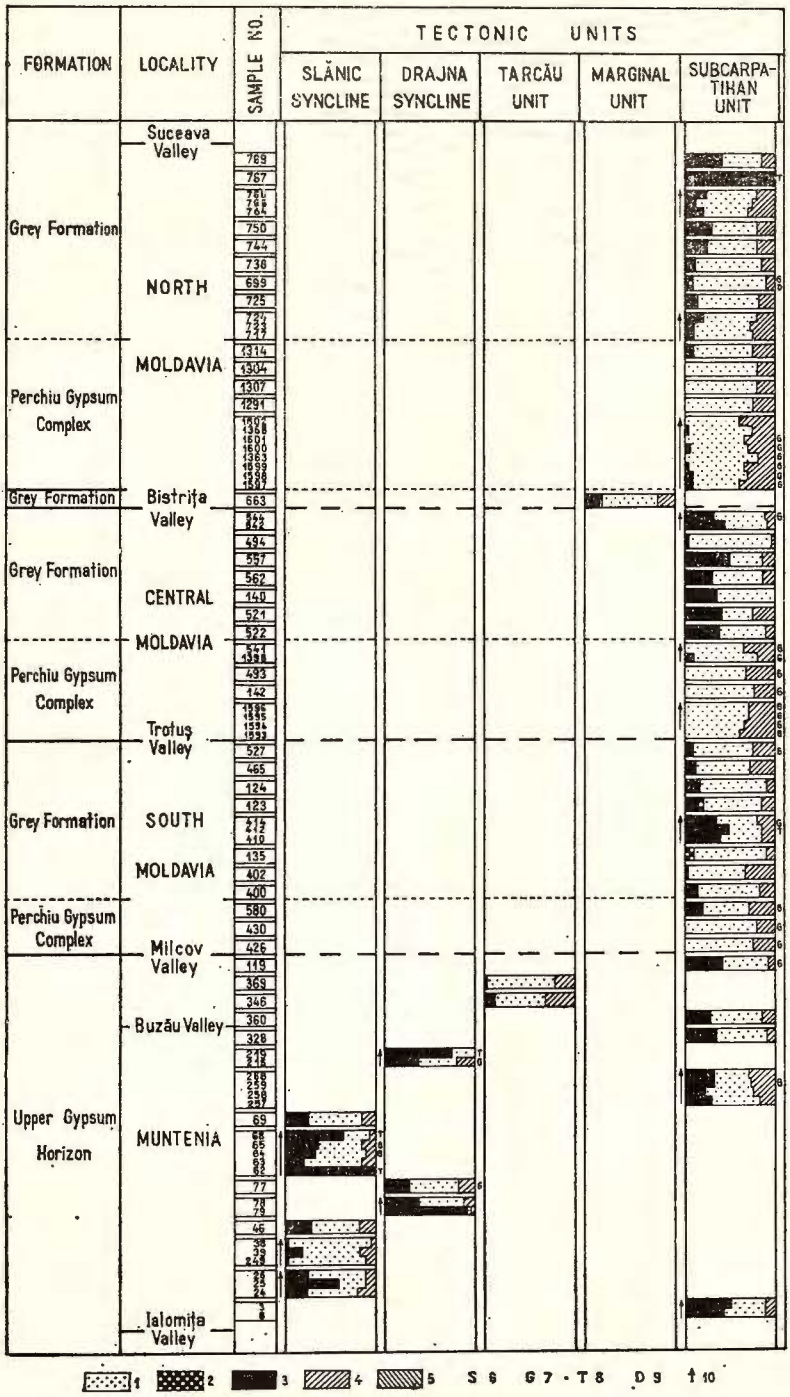

Fig. 4. — Distribution of clay mineral assemblages in the Lower Miocene formations (Upper Gypsum Horizon, Perchiu Gypsum Complex and Grey Formation). See explanation Fig. 2.

Middle Miocene. The clay mineralogy of the Middle Miocene formations is qualitatively unchanged, showing the same three mineral suite that became generalized at the level of the *Grey Formation* within the whole East Carpathians molasse basin (Fig. 5). Argillaceous fractions of *Globigerina Marls*, *Slănic Tuff*, *Răchitaşu Sandstone* and *Haloş-Sărăţelu Beds*

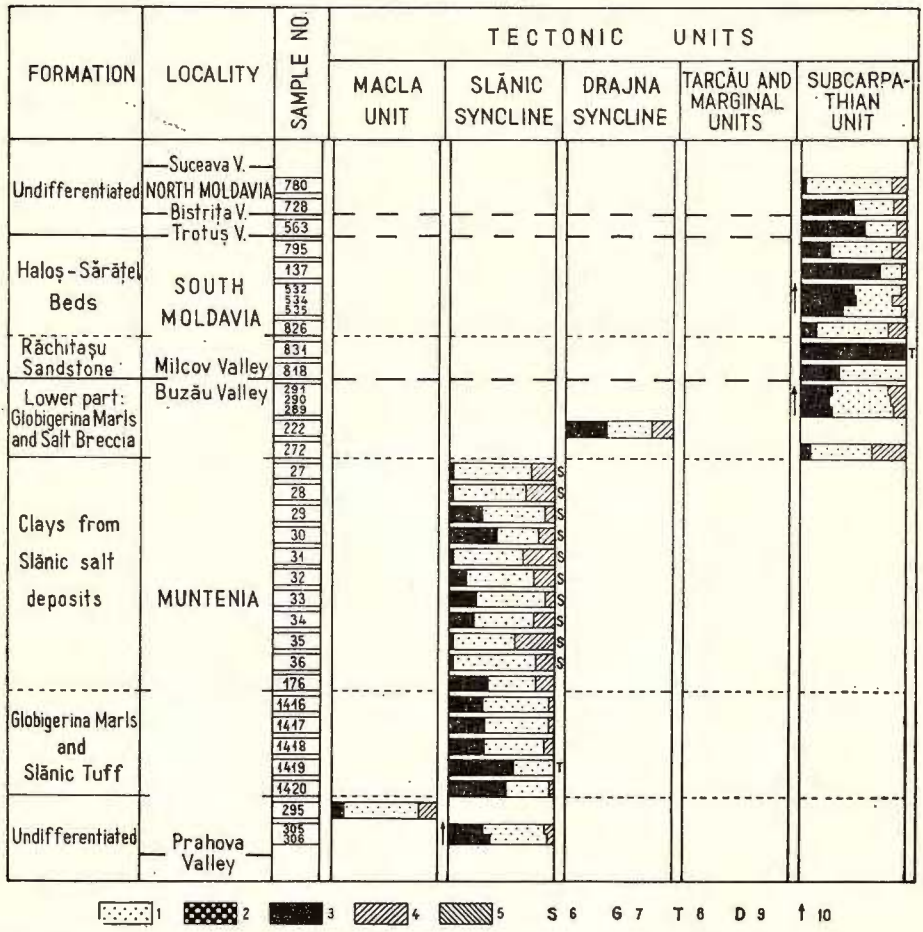

Fig. 5. — Distribution of clay mineral assemblages in the Middle Miocene formations. See explanation Fig. 2.

contain usually significant amounts of montmorillonite (30—75%) because of the disseminated or intercalated pyroclastic material. (As within the underlying formations including cinerites, some tuff intercalations reach to be wholly bentonitized, containing up to 100% montmorillonite, eventually some illite and/or clinoptilolite but no chlorite). Illite contents are

approximately equal as the montmorillonite ones (25—70%), and chlorite is as usually subordinated (5—20%).

Salt Breccia and some stratigraphically undifferentiated deposits (in this paper), encompassing *Radiolarian Shales*, and/or *Spirialis Marls* are characterized by a more restricted occurrence of montmorillonite (5—60%), which is dominated by illite (30—80%) but prevails over

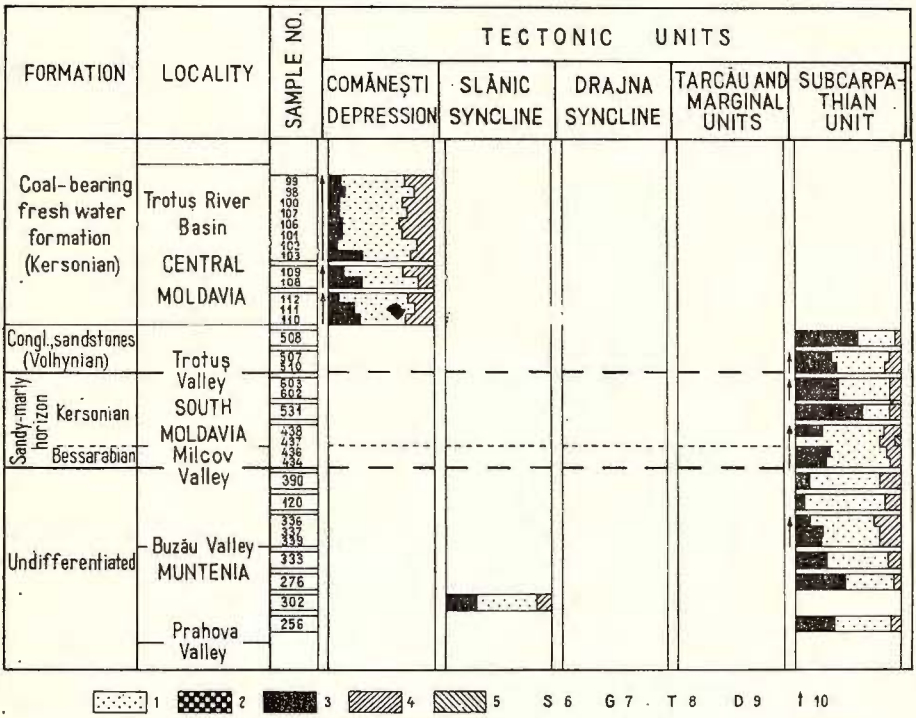

Fig. 6. — Distribution of clay mineral assemblages in the Upper Miocene formations. See explanation Fig. 2.

chlorite (10—20%). As concerns clays finely disseminated or intercalated in the Middle Miocene salt deposits, these contain besides illite (40—80%) and chlorite (10—35%), montmorillonite (5—45%) as well.

The 10—14 M random mixed-layered minerals have been practically found in all clay fractions of the Middle Miocene deposits.

Upper Miocene. No important changes are recorded in clay mineralogy of Upper Miocene deposits as compared to the Middle Miocene sequence (Fig. 6). The pattern of distribution seems to outline some areas characterized by quantitatively differing ternary clay mineral assemblages. So, between Buzău Valley (East Muntenia) and Putna Valley (South Moldavia) and also, in the Comănești Depression, Upper Miocene deposits are rich in illite (45—75%), and contain approximately

equal amounts of montmorillonite (10—35%) and chlorite (10—25% for the first area and 15—35% for the second one). One sample (no. 437) contains 5% vermiculite, and is devoid of montmorillonite.

Within the Trotuș Valley area and Diapir Fold Zone, the clay fractions of Upper Miocene deposits show decreased contents of illite (25—55% and 45—60% respectively), augmented percentages of montmorillonite (35—65% and 30—50%) which can even dominate illite contents, and scarce chlorite (5—15% in both areas).

The random mixed-layer clay minerals are represented by the 10—14 M type in the whole Upper Miocene sequence, except Comănești Depression deposits, where the 14 C—14 M type is also frequently identified.

Discussion and conclusions

A general survey on clay mineral distribution within Miocene Molasse deposits of the East Carpathians reveals two main patterns of evolution for the mineralogy of argillaceous fractions (Fig. 7). In Moldavia, the lower part of the Lower Miocene sequence is characterized by a clay mineral assemblage practically devoid of montmorillonite, this one becoming a permanent constituent only beginning with the *Grey Formation* deposition. In Muntenia, the whole Miocene column of deposits shows an abundance of montmorillonite, even if it does not exceed illite. These facts, correlated with sedimentological data concerning source area activity during the Miocene, are leading to the following concluding remarks :

1. Clay mineralogy of sedimentary material derived from the East Carpathians source area is characterized by a rather complex mineral assemblage : degraded illite (dominant), montmorillonite, chlorite (± kaolinite), and random mixed-layer clay minerals of the 10—14 M type.

2. Clay mineral suite provided by the Foreland source area is devoid of montmorillonite, consisting mostly of a binary assemblage : not degraded illite (dominant) and chlorite (± kaolinite). The random mixed-layers show habitually a wider ranged variety (10—14 M, 10—14 V, 14 C—14 M), but frequently they may be missing.

The decrease of chlorite contents concomitantly with the augmentation of montmorillonite proportion, revealed along the Slănic Syncline (from east to west), points out only a slight influence of the Foreland source area in this region but its increasing importance westwards (to Moldavia).

3. Illite and chlorite (± kaolinite) are detrital. The different degree of illite crystallinity does not seem to be determined by salinity variations within the Miocene Molasse basin. The Lower Miocene conglomerates and *Red formations* which represent, to a large extent, subaerial or shallow water alluvial fans and plains (with footprints of birds, paricopitates, proboscidians, etc.) contain commonly a well crystallized illite, whereas marine sequences as the *Grey Formation* or Middle and Upper Miocene sequences are characterized by degraded illite.

4. Montmorillonite shows a double origin : detrital and authigenic. As detrital mineral, montmorillonite is provided by the Carpathian source area, resulting from the weathered bedrock, within the partially emerged areas of the Flysch and Mesozoic carbonate zones. In this respect, Oligocene Flysch deposits, rich in montmorillonite (Rădan, Mîndroiu,

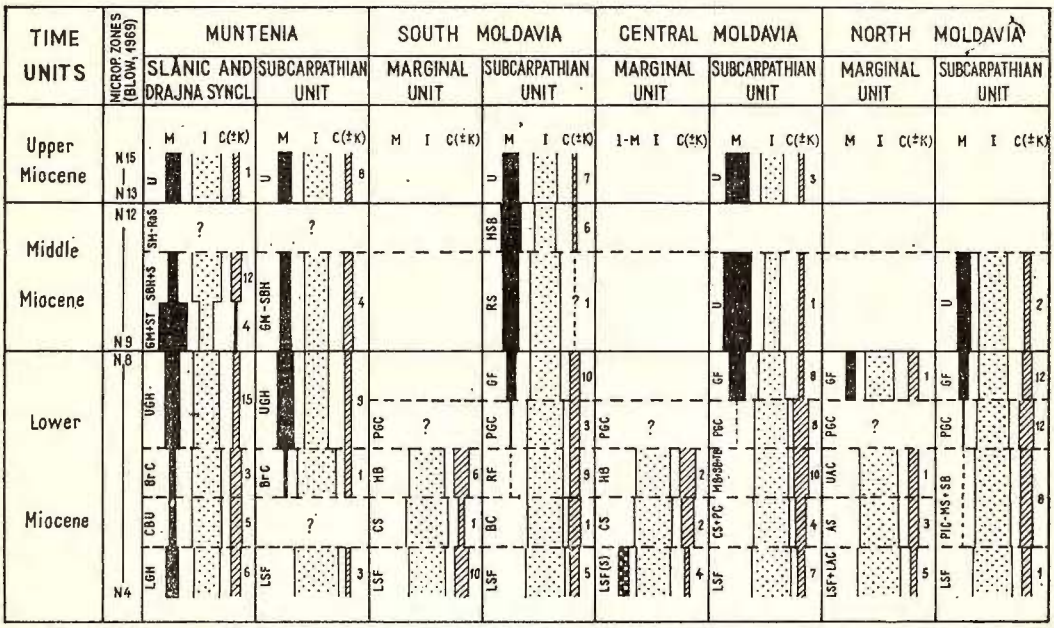

Fig. 7. — Clay mineralogy of East Carpathians Miocene Molasse deposits. LGH, Cornu Beds — Lower Gypsum Horizon ; LSF, Lower Salt Formation ; S, Salt ; LAC, Lower Almaşu Conglomerates ; CBU, Cornu Beds — Upper Horizon ; BrC, Brebu Conglomerates ; CS, Condor Sandstone ; BC, Bîrseşti Conglomerates ; PC, Pietricica Conglomerates ; PlC, Pleşu Conglomerates ; AS, Almaşu Sandstone ; HB, Hîrja Beds ; RF, Red Formation ; MB, Măgireşti Beds ; BB, Borzeşti Beds ; TB , Tescani Beds ; UAC, Uper Almaşu Conglomerates ; MS, Moişa Sandstone ; SB, Solca Beds ; UGH, Upper Gypsum Horizon ; PGC, Perchiu Gypsum Complex ; GF, Grey Formation ; GM, Globigerina Marls ; ST, Slănic Tuff ; SBH, Salt Breccia Horizon ; RS, Răchitaşu Sandstone ; SM, Spirialis Marls ; RaS, Radiolarian Shales ; HSB, Haloş-Sărăţelu Beds ; U, Undifferentiated deposits. The number of samples used to average calculation are noted on the right sides of the columns.

1971) [7], might represent the main source for this mineral. Our data agree with the general patterns of clay mineral distribution and evolution established by Kraus, Šamajová (1973) in some Neogene basins of the West Carpathians (Czechoslovakia).

[7] Op. cit. pt. 3.

Consequently, the preferential clay mineral distribution outlined within the Upper Miocene sequence indicates a stronger influence of the metamorphic bedrock and eventually Flysch deposits (except Oligocene flysch) for those deposits enriched in illite and chlorite (Comăneşti Depression and Buzău-Putna area); on the other hand there is to be admitted a higher importance of the Mesozoic carbonate complexes and/or Oligocene formations as source areas for montmorillonite-rich deposits (Trotuş Valley area and Diapir Folds Zone).

5. Vermiculite, identified in some Lower Miocene deposits, seems to be characteristic especially of the Putna Valley area (South Moldavia). This fact points out a mineralogical peculiarity of the weathering crust in the South Moldavian segment of the Foreland, probably controlled by the bedrock petrography or by the stopping of mica-montmorillonite transformation in the vermiculitic phase.

6. The mineralogy of clay material contained within evaporitic deposits generally follows the distribution pattern of the detrital sequences encompassing them. In this manner it is possible, for instance, to distinguish (in small-sized outcrops) the *Perchiu gypsum* (devoid of montmorillonite) from gypsum beds included within the *Grey Formation* (rich in montmorillonite).

Montmorillonite contents in the *Perchiu Gypsum Complex* of Bistriţa Valley area point out either an earlier beginning of the western source area activity, or only some "pulsations" of Carpathian supplies in this region.

As regards the salt deposits, their clay fractions inherited from the land do not seem to be much transformed by the sedimentary environment. Within the Lower Miocene sequence, Ocniţa salt deposits (Muntenia) are devoid of montmorillonite, showing the typical binary assemblage for evaporites (illite + chlorite), presumably provided by the Foreland. The isochronous *Lower Gypsum Horizon* developed northwards (within Slănic and Drajna Synclines) contains montmorillonite clays. These features might suggest the existence of a rise south of these synclines which protected the Diapir Folds Zone from the Carpathian supplies. Higher up, the Middle Miocene salt deposits, well developed within the Slănic Syncline (not protected), support this evidence, showing a clay fraction rather rich in montmorillonite provided by the Carpathian source area.

However, the Lower Miocene salt deposits of Tîrgu Ocna (Moldavia) are different from the above-mentioned evaporitic rocks as concerns relation of clay minerals to diagenetic changes. In this respect, the random mixed-layer clay minerals approaching regular interlayering of allevardite type are a good indicator of mineral transformation controlled by saline environment. As proved D r o s t e (1963), evaporite sequences containing salts of potassium and magnesium have abundant regular mixed-layer clay minerals formed by diagenesis from chlorite, vermiculite and montmorillonite through transitional random mixed-layer structure. Tîrgu

Ocna evaporite deposits contain potassium salts, so allevardite-like minerals might be produced diagenetically by high K activity.

REFERENCES

Biscaye P. E. (1965) Mineralogy and Sedimentation of Recent Deep-sea Clays in the Atlantic and Adjacent Seas and Oceans. *Geol. Soc. Am. Bull.*, 76, 7, New York.

Dimian M., Dimian Elena (1964) Cercetări sedimentologice privind zona flișului cretacic superior — paleogen și a molasei miocene dintre văile Zăbalei și Buzăului. *D.S. Com. Geol.* XLIX/1, 1961—1962, București.

Droste J. (1963) Clay Mineral Composition of Evaporite Sequences. In A. C. Bersticker Ed.: *Symposium on Salt, Cleveland, Ohio,* 1962. *The Northern Ohio Geol. Soc.*, Inc., Cleveland.

Dumitrescu I. (1952) Studiul geologic al regiunii dintre Oituz și Coza. *An. Com. Geol.*, XXIV. București.

Dumitriu M., Dumitriu Cristina (1964) Notă asupra imbricației conglomeratelor de Brebu. *Acad. R.S.R., Stud. cerc. geol.*, IX/1. București.

Dunoyer de Segonzac G. (1969) Les minéraux argileux dans la diagenèse. Passage au métamorphisme. *Mém. Serv. Carte géol. Als. Lorr.*, 29. Strasbourg.

Filipescu G. M. (1940) Étude géologique de la région comprise entre les vallées du Teleajen et du Slănic-Bîsca Mare (Buzău). *C.R. Inst. Géol. Roum.*, XXIII. București.

Joja T. (1952) Cercetări geologice între valea Rîscei și valea Agapiei. *An. Com. Geol.*, XXIV. București.

Kraus I., Šamajová Eva (1973) Importance of the Clay Minerals for the Determination of Source Areas in the Neogene Basins in the West Carpathians (Summary of the Slovak Text). *Geol. práce,* 16, p. 101—122. Bratislava.

Kubler B. (1970) La composition des fractions fines et la distinction flysch-molasse dans le domaine alpin et périalpin. *Bull. Soc. Géol. France,* (7), XII, 4, p. 599—602, Paris.

Macarovici N., Motaș I., Contescu L. (1967) Caractères stratigraphiques et sédimentologiques des dépôts sarmato-pliocènes de la Courbure des Carpathes Orientales. *An. St. Univ. Al. I. Cuza, Iași,* XIII, sect. II *St. Nat., Geol. Geogr.* Iași.

Mirăuță O. (1965) Faciès et téctonique de la molasse miocène subcarpatique de la Moldavie Centrale. *Carp.-Balk. Geol. Ass. VII Congr., Sofia, Reports,* II, 2, Sofia.

— (1969) Stratigrafia și structura Miocenului subcarpatic din regiunea Moinești — Tazlău *D.S. Inst. Geol.*, LIV/3, 1967, București.

Panin N. (1964) Coexistența urmelor de pași de vertebrate cu mecanoglife în molasa miocenă din Carpații Orientali. *Stud. cerc. geol.*, 9/2. București.

— Panin Ștefana (1967) Directions des courants dans les dépôts miocènes molassiques des Soubcarpates Roumaines. *Ass. Géol. Carp.-Balk., VIII-ème Congr., Rapports* Belgrad.

Polonic P., Polonic Gabriela (1967) Miocenul subcarpatic dintre valea Sucevei și valea Cracăului. *D.S. Inst. Geol.*, LII/3, (1966—1965), p. 39—61. București.

— (1968) Direcții de transport în molasa helvețiană dintre valea Sucevei și valea Trotușului. *D.S. Inst. Geol.*, LIV/1, (1966—1967), p. 205—215. București.

Popescu Gr. (1951) Observații asupra „breciei sării" și a unor masive de sare din zona paleogenă-miocenă a jud. Prahova. *D.S. Inst. Geol. Rom.*, XXXII, (1943—1944), București.

Saulea Emilia (1965) Contribuții la stratigrafia Miocenului din Subcarpații Munteniei. *An. Com. Geol.*, XXXIX, București.

— (1969) Text la hărțile litofaciale ale Neogenului. Publ. Inst. Geol., București.

Săndulescu M. (1962) Stratigrafia și tectonica molasei miocene din regiunea Valea Mare — Berzunț — Onești. *D.S. Com. Geol.*, XLVI, (1958—1959). București.

INFLUENCE OF SOME MINERALS AND SALTS ON THE BEHAVIOUR OF KAOLINITE DTA AND DTG CURVES[1]

BY

DUMITRU N. TODOR,[2] GHEORGHE ENACHE[3]

Sommaire

Influence de certains minéraux et sels sur le comportement des courbes ATD et TGD de la kaolinite. En appliquant l'interprétation graphique basée sur la symétrie des tangentes aux effets thermiques, en condition expérimentales standard, on a démontré la possibilité d'établir la présence de minéraux e de sels (sous forme d'impuretés) dans la masse de la kaolinite.

As it is known the minerals of the groups of kaolinite undergo at heating two essential transformations in their structure. The first one occurring between 500—700°C is a chemical transformation during which the OH groups are eliminated, this transformation being accompanied by a mass loss. The second transformation, between 900—1000°C, is a physical one which takes place releasing thermal energy. This transformation has been much discussed as regards its nature and compounds which generated it (Grim, 1962; Todor, 1972); on the one hand it is thought to be determined by $\bar{\gamma}$ alumina, and on the other hand it is possible to have been caused by the coming into formation of mullite and cristobalite. In this paper we do not try to clarify this problem but to explain some aspects linked to the presence in the kaolinite mass of some impurities and their influence on the above-mentioned structural reorganization.

[1] Paper presented at the 2nd National Clay Conference, April 11—12, 1975, Bucharest.

[2] Institutul de cercetări şi proiectări tehnologice în transporturi, Calea Griviţei 393, Bucureşti.

[3] Întreprinderea geologică de prospecţiuni pentru substanţe minerale solide, str. Caransebeş 1, Bucureşti.

Generally speaking not only this transformation is influenced by some minerals subordinate to kaolinite or by some salts, which are formed during its chemically ennobling process, but also the transformation due to dehydroxylation is influenced. Some of the interferences of several minerals have been already studied by the method of thermal differential analysis, and they are conclusively given by Mackenzie (1957). For practical reason we tackled again this study using a complex methodology of analysis that comprises the three techniques which are frequently utilized: the thermal differential analysis (DTA), the thermal gravimetry (TG) and the differential thermogravimetry (DTG) coupled in a unitary apparatus of the "derivatograph type".

The thermoanalytic interpretation of thus obtained curves was made on the basis of the symmetry of thermal effects inferred from tg α and tg β of the effects, a method which was used by Bramao et al. (1952).

The experimental work was carried out so that most of the experimental constant parameters could be maintained as follows: the heat speed 10°C/minute, the system of Pt, Pt-Rh thermocouples and the same quantity of sample (one gram) being used. The analyses were carried out using two types of reaction crucibles one of calcinated alumina and the other one of alloyed platinum, and as standard materials: Zetlitz kaolinite, Cornwall kaolinite and China kaolinite. These samples were analysed either separately or mixed with other minerals in proportion of 80 per cent kaolinite and 20 per cent admixture. To reach a better homogeneity of mixtures, samples of the same grain size were obtained from aqueous suspensions by pipetting and subsequently drying at room temperature.

Results and discussions

The tg α/tg β ratio was graphically determined for both thermal effects on the DTA and DTG curves. As the DTA curve has not always a perfectly straight zero line, the measurements which were carried out for inferring the tangents were performed like in the Figure 1.

To begin with we must point out that the values obtained for tg α are higher than those for tg β, in all cases when dealing with monomineral kaolinite samples including alumina, prepared according to the two before-mentioned laboratory techniques. When the calculation of tangents was performed using the endothermic dehydration effect, the values for tg α/tg β were between 1.2 and 1.5. In the case when that calculation of the two tangents was carried out by means of the structural reorganization effect, tg α was much lower than tg β (when alumina crucible was used) leading to a 0.5 ratio, while utilizing melting pots the values for the two tangents are almost equal (their ratio being about 1). In fact these data are wholly in good agreement with the already known remarks about experimental parameters in relation to the use of different types of constants for tests (Todor, 1972).

When accessory minerals in the kaolinite mass are clay minerals (montmorillonite, illite, chlorite, etc.) the values of tangents relating to dehydroxylation thermic effects are controlled by the temperature range within which these minerals eliminate their own OH groups. Since argillaceous minerals have about the same OH groups removal temperature range, like kaolinite, the tangent ratio is about 1. Concomitantly tg α,

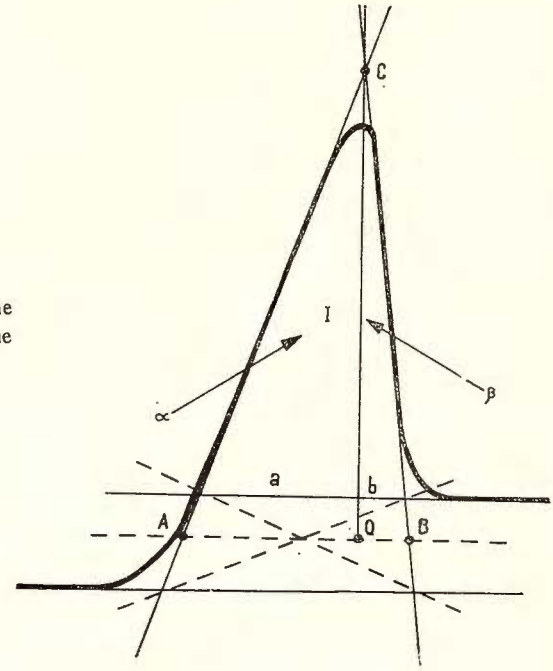

Fig. 1. — Graphic determination of the symmetry of a thermal effect on the basis of the calculus of tangents.

tg β and the ratio between these tangents, measured on the effect of structural reorganization, remain unchanged in the case of these mixtures as in the case of pure kaolinites.

The situation is the same for kaolinite and carbonate mixture: tangents measured on the structural reorganization effect are practically unchanged, but in the case of dehydroxylation effect tg α value marks an essential increase as a function of the nature of carbonate, this determining a strong decrease of the ratio (under 1).

Quartz, feldspar as well as other raw minerals do not have a marked influence on kaolinite effects so that tangent values remain the same.

Sulphides — discussed in detail in a former paper — (T o d o r, E n a c h e, 1975) exert a great influence on kaolinite dehydroxylation effect, making it even unavailable for measurements. The effect of structural reorganization is also influenced increasing sensibly tg β in relation to tg α, and hence the tg α/tg β ratio values decrease even under 0.4—0.3.

The salts which by heating modify melting points, namely NaCl, KCl, Na_2SO_4, $NaCO_3$ etc., do markedly influence the kaolinite thermic behaviour. While the influence on dehydroxylation effect is weak, on structural reorganization effect it is quite strong, leading even to its complete disappearance. In all cases when kaolinite/salt ratio has been 80 per cent to 20 per cent, this effect was completely missing. A mixture of 95 per cent kaolinite and 5 per cent NaCl made the intensity of the

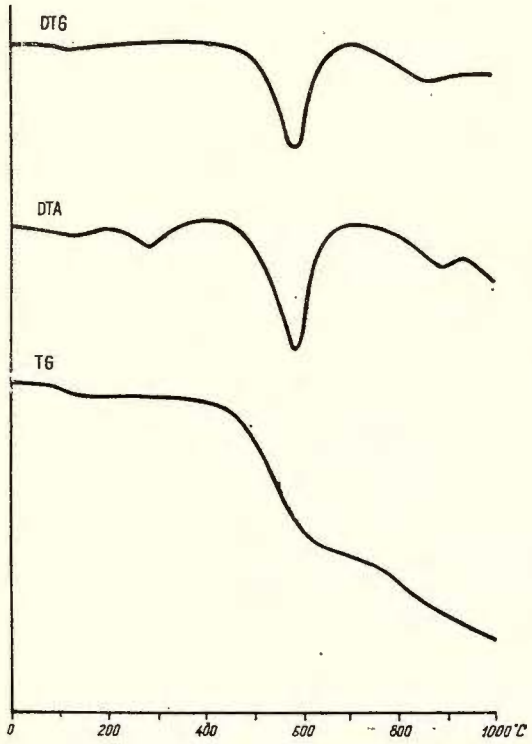

Fig. 2. Thermal curves of the kaolinite mixed with Na_2SO_4.

effect to be about four times lower, but the value of the two tangents has been maintained within the limits of kaolinites without any admixtures.

In the case of kaolinite and alkaline sulphate mixtures another endothermic effect accompanied by a mass loss is occurring between dehydroxylation and structural reorganization effects (Fig. 2). This occurrence of a mass loss effect makes us assume that an interaction between meta-kaolinite and sodium sulphate (resulted from dehydroxylation) does take place, yielding aluminium sulphate in a first phase. The exchange of sodium from sulphate with aluminium from meta-kaolinite would have taken place during kaolinite dehydroxylation reaction; in the course of the increase of temperature SO_3 will be removed. This thermic behaviour

of kaolinite-sodium sulphate mixture is very similar to natural kaolinite-alunitized rock whose endothermic dehydroxylation effect is markedly increased because of the synchronic removal of OH groups of kaolinite and alunite (P o p a, T o d o r, 1971).

When applying the graph interpretation based on tangents of thermic effects symmetry, in standard experimental conditions, to series of mixtures with sufficiently pure kaolinite, one can rather precisely establish the presence of some minerals or accessory salts in the kaolinite mass.

REFERENCES

B r a m a o L., C a d y I. G., H e n d r i c k s G. B., S w e r d l o w M. (1952) Characterization of kaolin minerals. *Soil Sci.* 73, p. 273—287, Baltimore.

G i m R. E. (1962) Applied Clay Mineralogy. Mc. Graw Hill Book Co., New York.

M a c k e n z i e R. C. (1957) The Differential Thermal Investigation of Clays. Mineralog. Soc., London.

P o p a G., T o d o r N. D. (1971) L'étude des alunites à l'aide des méthodes thermiques. *Revue Roum. de Chim.*, 16, p. 381, Bucureşti.

T o d o r N. D. (1972) Analiza termică a mineralelor. Edit. Tehnică, Bucureşti.

— E n a c h e Gh. (1975) The influence of the Sulphides on the determination of the Argillaceous Minerals by Thermal Methods. *Proc. of the first National Clay Conf., Bucharest*, 1973, *Inst. Geol. Geof., Stud. tehn. econ.*, I 13, Bucureşti.

REPORT ON THE TEST OF CLAY MINERAL DETERMINATION BY *X*-RAY DIFFRACTION [1]

The Romanian Group for the Study of Clays organized a test on the clay mineral determination by *X*-ray diffraction with a view to establish whether a standard method in this analytical field is requested in Romania. Four *X*-ray laboratories have participated in this test, namely of the Geological Prospecting Enterprise for Solid Mineral Resources, Bucharest (1); Institute of Geology and Geophysics, Bucharest (2); Research and Design Institute for Cement and Asbestos Cement Industry (3); Research Institute for Soil Science, Bucharest (4).

The following samples from the Research Institute for Soil Science (4) collection were analysed :

1. Aghireş kaolinite—sample 315 — G. Gâţă collection,
2. Gurasada bentonite — sample 1643 — C. Crăciun collection,
3. Glacial Till-Illinois illite — sample 962s — M. Mortland collection, Michigan U.S.A.

The *X*-ray diffraction patterns were recorded using the oriented aggregates prepared by sedimenting and drying the suspensions on glass slides at room temperature. The suspension have been prepared applying the following methods :

— fractions $< 10\ \mu$ — the Neacşu und Urcan (1975) method (without chemical treatments)

— fractions $< 2\ \mu$ — Institute of Geology and Geophysics method

— fractions $< 1\ \mu$ — Gâţă (1972) method)(NaOH dispersion and Ca-saturated fractions).

The equipment and the working conditions are presented in Table 1. There are two types of equipment, the laboratories (1) and (2) using TUR-M 61 type and the laboratories (3) and (4) a URS-50 IM type. As regards the control of alignment the first laboratory utilizes the quartz line at 13.3°-2 θ (3.34 Å), the second laboratory — aluminium lines at 19.24° and 22.36°-2θ (2.3327 and 2.0206 Å respectively), the third and the fourth laboratories do also utilize the aluminium lines at 38.48°

[1] Paper presented at the 2nd National Clay Conference, April 11—12, 1975, Bucharest.

TABLE 1

Working conditions of the X-ray equipments used in the test

Laboratory	1	2	3	4a	4b	4c
Equipment	TUR-M61	TUR-M61	URS-50IM	URS-50 IM		
X-ray radiation	Cu Kα, Ni-filtered					
kV	30	30	35	35	35	35
mA	25	20	6	7	7	6
goniometer type	HZG-3	HZG-3	GUR-4	HZG-3	GUR-4	GUR-4
scanning speed	2°θ/min.	$\frac{1}{2}$°θ/min.	2°θ/min.	1°θ/min.	1°θ/min.	1°θ/min.
detector	VAZ-330	VAZ-330	MSTR-4	MSTR-4	MSTR-4	MSTR-4
detector voltage	1 550	1 550	1 350	1 430	1 440	1 440
paper speed mm/h	600	300	600	600	600	600
recorder scale	60	60	200	18	200	200
analysts	G. Neacşu T. Urcan	Florica Popescu	Stela Ciocănel	Gh. Gâţă C. Schramek		

and 44.72°-2θ; in addition the last one utilizes an illite standard (Illinois) at 6.30—8.82° and 12.5°-2θ or 14.0—10.01 and 7.061 Å. Moreover the intensity ratio of (001) and (002) lines of illite must be of 2.37 ± 0.1 in order to have a good agreement in the quantitative determinations.

The results of the *X*-ray determination test are presented in Tables 2, 3 and 4 for the Aghireş kaolinite, Gurasada bentonite and Illinois illite. Moreover in Tables does also appear the ratio of intensities (001) and (002) lines for kaolinite (Tab. 2) and for illite (Tab. 4) respectively; in Table 3 there is calculated the ratio of intensities of the lines at 13.5 Å (montmorillonite) and 4.04 Å (cristobalite).

The results obtained for the same grain size fraction display some fluctuations in the diffraction line positions but these variations do not change the identification of the mineral components of samples. All the laboratories determined the same mineralogical composition of the analysed specimens: kaolinite with some illite and quartz as impurities in the Aghireş kaolinite, montmorillonite and cristobalite with some oligoclase in the Gurasada bentonite and illite and chlorite-like minerals in the Illinois illite.

As regards the calculated ratios there should be pointed out the wide-ranging variation of these ratio values. For this reason the quantitative determination by means of *X*-ray diffraction patterns may be carried out only with a suitable standard system of transformation factors specific to the working conditions of each equipment.

The change of ratio values also depends on the grain size, possibly because of the shifts of the orientation degree due to other minerals which

TABLE 2

Comparative values obtained for Aghireș kaolinite

Size fraction		Laboratory						Fluctuation interval
		1	2	3	4a	4b	4c	
<10 μ	Å	—	9.74	—	9.91	9.85	9.90	0.170
		7.118	7.129	7.182	7.151	7.121	7.135	0.064
		—	4.328	4.342	4.340	4.349	4.339	0.021
		3.552	3.574	3.573	3.576	3.557	3.560	0.024
		3.319	3.322	3.331	3.321	3.323	3.328	0.012
	(001)/(002)	0.967	1.056	0.967	1.106	0.937	0.938	—
<2 μ	Å	—	—	—	10.01	9.96	9.93	0.080
		7.116	7.118	7.181	7.189	7.146	7.166	0.073
		3.554	3.561	3,556	3.561	3.557	3.356	0.007
		3.317	3.325	3.328	3.328	3.328	3.323	0.011
	(001)/(002)	1.144	1.078	1.344	1.246	1.279	1.062	—
<1 μ	Å	9.89	10.08	10.04	10.02	10.02	10.02	0.190
		7.115	7.164	7.172	7.134	7.112	7.131	0.060
		3.554	3.578	3.568	3.565	3.557	3.559	0.024
		3.315	3.337	3.334	3.328	3.328	3.323	0.022
	(001)/(002)	1.026	1.221	0.955	1.254	0.902	0.932	—

TABLE 3

Comparative values obtained for Gurasada bentonite

Size fraction		Laboratory						Fluctuation interval
		1	2	3	4a	4b	4c	
<10 μ	Å	13.35	12.66	13.26	13.11	12.68	12.77	0.690
		4.414	4.449	4.443	4.438	4.442	4.434	0.035
		4.011	4.036	4.036	4.030	4.030	4.030	4.025
	M/C	1.600	1.148	1.837	2.576	1.782	1.783	—
<2 μ	Å	13.60	13.46	13.22	13.33	13.35	13.27	0.380
		—	4.898	4.988	—	4.991	4.994	0.096
		4.029	4.038	4.062	4.043	4.043	4.054	0.033
	M/C	3.971	2.846	5.332	5.133	8.682	4.091	—
<1 μ	Å	13.87	13.66	13.56	13.60	13.60	13.73	0.210
		4.919	4.914	5.502	4.998	5.045	5.043	0.131
		4.007	4.047	4.021	4.027	4.020	4.037	0.040
	M/C	12.00	5.071	6.132	9.321	5.754	7.550	—

M/C — ratio of intensities of the lines at 13.5 Å (montmorillonite) and 4.04 Å (cristobalite).

TABLE 4

Comparative values obtained for Illinois illite

Size fraction		Laboratory						Fluctuation interval
		1	2	3	4a	4b	4c	
<10 μ	Å	13.73	13.82	13.65	13.97	13.77	13.83	0.320
		9.86	10.02	10.04	10.03	10.02	9.97	0.280
		7.016	7.012	7.089	7.065	7.016	7.011	0.077
		4.958	4.982	4.942	4.980	4.936	4.938	0.046
		4.687	4.687	4.711	4.727	4.721	4.702	0.040
		4.250	4.220	4.224	4.262	4.228	4.224	0.042
		3.577	3.513	3.520	3.534	3.520	3.524	0.027
		3.315	3.323	3.315	3.339	3.317	3.322	0.024
		1.540	1.198	2.313	1.977	2.257	2.255	—
	(001)/(002)	13.77	14.17	13.92	14.01	13.88	13.79	0.400
<2 μ	Å	9.86	10.11	10.02	10.05	9.99	9.99	0.190
		7.005	7.118	7.089	7.078	7.061	7.033	0.084
		4.947	4.960	4.984	4.960	4.955	4.952	0.013
		4.687	4.717	4.721	4.692	4.714	4.709	0.034
		3.507	3.524	3.517	3.531	3.520	3.517	0.024
		3.310	3.313	3.314	3.325	3.311	3.316	0.015
		2.551	2.254	3.475	2.956	3.071	3.667	—
	(001)/(002)	13.86	14.15	13.82	14.05	14.09	13.92	0.270
<1 μ	Å	9.93	10.11	9.93	10.05	9.98	10.01	0.180
		7.039	7.129	7.042	7.095	7.054	7.076	0.090
		4.969	4.997	4.969	4.985	4.972	4.968	0.029
		3.529	3.536	3.522	3.534	3.534	3.535	0.014
		3.324	3.332	3.310	3.324	3.316	3.325	0.022
	(001)/(002)	2.323	1.860	2.728	2.387	2.603	2.622	—

TABLE 5

Variation of basal spacings (in Å) of the Ca-saturated clay fractions as a function of moisture content in the atmosphere of laboratory (temperature 20 ± 2°C)

Clay fraction (< 1μ)	moisture (%)		
	47	65	74
Valea Chioarului montmorillonite	13.68	13.87	14.01
Illinois illite	13.94 10.02	14.05 10.05	14.08 10.03

occur in the samples, the most essential effect belonging to bentonite fractions. The values recorded for the Gurasada bentonite do also present a greater fluctuation of peak position obtained by the four laboratories, presumably due to the temperature and moisture variations of the atmosphere of each laboratory. In order to verify this assumption, in the laboratory no. 4 there was recorded one slide with oriented aggregates from Valea Chioarului montmorillonite ($< 1\ \mu$) at different moisture levels in comparison with another slide with oriented aggregates from Illinois illite ($< 1\ \mu$). The experimental data (Tab. 5) show a fluctuation interval twice greater for montmorillonite than for chlorite-like minerals from the Illinois illite in spite of the same working conditions.

The *X*-ray diffraction patterns obtained by the four laboratories point out the variation of the experimental data as a function of the working conditions and of the fraction separation method. For the identification of minerals from samples in a qualitative method, a standard method of the working conditions does not appear as necessary since in all the laboratories the same mineral components were found.

Many difficulties are met with when one must standardize a quantitative method. Besides the effect of the pretreatments and the grain size of samples some conventional working conditions are to be elaborated too; the latter could favour the achievement of a suitable measurement based on transformation indice system characteristic of each equipment. As the *X*-ray analyses are used nowadays in quite a large number of scientifical and technical fields, namely geology, soil science, ceramics, cement industry, mining industry and so on, it is not recommendable to standardize the quantitative method because of the different features of equipments.

Reported by Gheorghe Gâţă
Institutul pentru ştinţa solului Bd.
Mărăşti 61, Bucureşti.

Redactor : ALEXANDRA MARINESCU
Traduceri : MARIANA SAULEA, MARGARETA HÂRJEU
Ilustrația : V. NIȚU

Dat la cules : martie 1978. Bun de tipar : iunie 1978. Tiraj : 750 ex. Hîrtie scris I A. Format 70×100/49 g. Coli de tipar 10¾. Com. 1595. Pentru biblioteci indicele de clasificare 55(058).

Tiparul executat de Întreprinderea poligrafică „Informația", str. Brezoianu nr. 23—25, București, Republica Socialistă România.

Technical and Economical Studies, the series from A to J, were published in the course of time by the following Institutions:

INSTITUTUL GEOLOGIC AL ROMÂNIEI (1906—1950);
COMITETUL GEOLOGIC (1950—1966);
COMITETUL DE STAT AL GEOLOGIEI (1966—1970);
INSTITUTUL GEOLOGIC (1970—1074);
INSTITUTUL DE GEOLOGIE ŞI GEOFIZICĂ (1974)